

Development of Enantioselective Organocatalytic Hydrogenation Methods  
and  
Progress Toward the Total Synthesis of (+)-Minfiensine

Thesis by  
Jamison Bryce Tuttle

In Partial Fulfillment of the Requirements for the  
degree of

Doctor of Philosophy

California Institute of Technology

Pasadena, California

2008

(Defended 18 April 2008)

© 2008

Jamison Bryce Tuttle

All Rights Reserved

## Acknowledgements

I would like to thank my research advisor Prof. David MacMillan, for providing me with an amazing graduate experience. His unique perspective on chemistry has deeply influenced my own views and will undoubtedly continue on with me during my chemistry endeavours. I am grateful for the faith he put in me to work on my own, his commitment to scientific excellence, and for providing a first-class research environment. I will always be grateful for this opportunity to work in his laboratory and for the support he lent me to establish my future career.

In a similar way I am grateful to my thesis committee for guiding me during the course of my graduate studies. In particular, I would like to thank Prof. Brian Stoltz for serving as the committee chairman. He is a stand-out chemist and teacher in this field and someone whom I will always admire. Additionally, I would like to thank Prof. Mitchio Okumura and Prof. Robert Grubbs for their scientific curiosity and reading of this thesis.

I would also like to thank my MacMillan Group West labmates with whom I've had the privilege of working with during my graduate studies. Joel Austin for being a fantastic baymate and a great friend. His unique perspective on nearly everything was always welcomed. Ian Mangion, for being a "nice person" whose rendition of the Harvard "Crimson Red" song to the spirit was particularly stirring. I will always appreciate his viewpoints on all things life and chemistry. Sean Brown whose intensity in the lab was equally matched by his intensity on the intramural soccer field. Sandra Lee for being a wonderful person whose company was always enjoyed. Catherine Larsen whose energy and cheery outlook brightened up the lab. Mike Brochu, who always saw the lighter side

of things. Nikki Goodwin is an amazing human being and someone whom I enjoyed working with on the West Coast and bumping into on the East Coast. I appreciate Katie Saliba's selflessness and benevolence, and skill as an editor *par excellence*. Joe Carpenter was my second baymate and aside from being an amazing person, is one whose depth of auto knowledge was continually impressive. Phong Pham was baymate #3, and one whose company was always enjoyed. His incredibly unique perspective on life always brought a smile to my face. Thanks to Anthony Mastracchio, whose enthusiasm for chemistry was contagious. Finally, to Casey Jones, for being a wonderful person who brightened my days.

The Caltech post-doc crew was outstanding. In particular, Dr. Stephane Ouellet who really helped me along at the outset and who was always willing to tolerate my cursory attempts at speaking French. Dr. Gerald Lelais, a remarkably thorough chemist who, I believe, took supreme pleasure in dismantling me on the tennis court. Dr. JB Hong, a great friend and confidant whose company I always enjoyed. Dr. Simon Blakey, my favorite Kiwi, for his sharp wit and his soccer ability. Dr. DeMichael Chung for being a good guy with a refreshing perspective on life. I want to thank Dr. Yong Chen for his scientific insights and his legendary late nights during group social events. Dr. Kate Ashton for always smiling. Drs. Masanori Yoshida and Akio Kayano for their inspirational work ethic and friendly dispositions. Last but not least, Dr. Abbas Walji, a talented chemist with whom I enjoyed tapping into for his in-depth knowledge of organic chemistry and for learning some useful Swahili lingo.

I would like to thank my colleagues from MacMillan Lab East. The first-year students, Brian LaForteza, Anna Allen, Anthony Casarez, Mark Vander Wal, Christine



Yang, Hui-Wen Shih for their unbridled enthusiasm. A special thanks to Benji Horning from this class, whose unique personality has been particularly refreshing. The second-years, including Alex Warkentin for bringing in an ISCO expertise and a strange Greek Statue. Jeff Van Humbeck for Pier's catalyst and in-depth knowledge of all things Canadian. Grace Wang for her resourcefulness and benevolence, not to mention her collection of musicals. A special thanks goes out to Nate Jui for being a great soccer tennis competitor and a fantastic friend. He is a good man and was very supportive during a particularly stressful last year.

I would like to thank the Princeton post-docs. Dr. Mark Kerr for expanding my urban dictionary vocabulary and for exciting exchanges of chemistry ideas. Dr. Trevor Rainey, the subtle Englishman whose scientific insights were always welcomed. Dr. David "Nice", for enthusiastically sharing his "cup of Joe" and brightening up the darker days. Dr. Andy McNally, a scouseboy unparalleled, who bravely joined us for our high-impact soccer tennis extravaganzas. Dr. Tom Graham, a great guy whose dry humor was always entertaining. Dr. Hahn Kim, for being a good friend and confidant and whose wisdom I always appreciated. Thanks to Dr. Maud Reiter, the most enthusiastic Luxembourgian I have ever met and whose laugh shook the pillars of the earth. Thanks to Drs. Muriel Amatore and Pilar Garcia Garcia for their unique personalities that I have had the pleasure to know. Dr. Jay Conrad for his insights into metathesis and for being the only person I know who drank from the Stanley Cup. To the others who just recently joined as I was leaving, Drs. Mark Pickworth, Alan Curbishly, Esther Lee, John Wilson, Staffan Torrsell, and Jong-Rock Kong for bringing in their own flair for science to the group.

I would like to thank my friends outside of the group: Mike Krout, Raissa Trend, Dan Caspi, and Mike Meyer from the Stoltz Lab for enriching my graduate experience. Carey Hsu, Ray Doss, David Chenowith, and Julie Poposki from the Dervan Group for teaching me about the biochemistry/organic chemistry interface. Grubbs Group members, Dr. Tobias Ritter, Dr. Greg Beutner and Erin Guidry, for their support and friendship.

I appreciate those with whom I've worked most closely, including Amanda Reider, who courageously entered the fray of imidazolidinone catalyst synthesis. David Nagib, who put forth a noble effort trying to tackle a difficult problem in our project. I would like to thank Spencer Jones and Brian Simmons, two talented chemists who have nobly accepted the responsibility to forge ahead as the newest permutation of team minfiensine.

A special thanks goes out to my classmates. Robert "Rando" Knowles, a great friend, for his continued support during my grad career. His depth of chemistry knowledge is endless and his commitment to the art of synthesis was always impressive. He will undoubtedly continue to do great things in this field as a future professor and is the only rock star I will ever know. I would like to thank Teresa Beeson for bringing in an unbridled intensity and unique viewpoint. She is one of the most interesting people I have ever met. Thanks to Diane Carrera, who should have been my classmate, for her laughter and ability to always lighten my mood.

I would like to thank my thesis and proposal proofreaders, Rob Knowles, Diane Carrera, Dr. David Nicewicz, Dr. Mark Kerr, Dr. Hahn Kim, Dr. Esther Lee, and Dr. Andy McNally. Thanks to Dr. Trevor Rainey for helping me with critical theoretical calculations. I would like to thank Dr. Michael Day and Larry Henling for helping acquire and interpret my crystal structures.

My parents need to be thanked for being my best motivators during the course of my studies. Their endless support during my graduate studies will always be deeply appreciated. For my brothers, Billy and Sean, and their families for continuously improving my mood during some of my more stressful moments. Thanks to my in-laws for their generosity and ability to alleviate the pressure during this whole experience.

Last and foremost I would like to thank my best friend and amazing wife Jessica Fontela for all of her support during the long nights I spent in lab. I can only imagine how difficult it was. I am indebted to her for marrying me and being the mother of my son, as those two events are undoubtedly the brightest occasions that have occurred in my life. She has been there through the good and the bad, and sacrificed her own existence in California to move with me to New Jersey, and for that I am eternally grateful. I am ecstatic that my future is inextricably intertwined with hers.

## ABSTRACT

The development of an enantioselective organocatalytic hydrogenation reaction utilizing the LUMO-lowering activation of  $\alpha,\beta$ -unsaturated aldehydes has been developed. This strategy employs an imidazolidinone catalyst to activate the alkene towards conjugate reduction of the pendant  $\beta,\beta$ -disubstituted alkene by a Hantzsch dihydropyridine. This is the first general methodology that utilizes disubstituted alkenes for iminium activation chemistry and stereoconvergently reduces mixtures of olefin geometric isomers to favor an enantioenriched product. Furthermore, the reagents are air and moisture stable making this new process operationally trivial.

By exploiting the aforementioned mode of reactivity, enones have been successfully reduced utilizing a privileged imidazolidinone catalyst. These studies led to the discovery of a novel Hantzsch dihydropyridine that exhibits a dramatic increase in reactivity. Further comparison of these Hantzsch derivatives provides interesting physical and structural data that may account for the observed differences.

A rapid entry into the tetracyclic framework of minfiensine utilizing our group's organocascade cyclization methodology was undertaken. This strategy demonstrates the first example of a 2,3-dialkyl substituted indole starting material successfully reacting under our pyrroloindoline-forming conditions. Various strategies for introducing an allyl silane moiety for use as a SOMOphile to furnish the final ring of the pentacycle were pursued. Numerous attempts were unsuccessful, and studies for introducing the allylsilane post-cyclization were undertaken. These experiments have led to the construction of a vicinal diol that should be two transformations away from attempting the key SOMO cyclization. If successful, the resulting intermediate will be six steps away from the final natural product.

## Table of Contents

Acknowledgements .....	iii
Abstract .....	viii
Table of Contents .....	ix
List of Figures .....	xi
List of Tables .....	xiv
List of Abbreviations .....	xv

### ***Chapter 1: LUMO-Lowering Enantioselective Organocatalytic***

Introduction.....	1
Development of LUMO-Lowering Iminium Activation .....	2
Summary of Thesis Research .....	5

### ***Chapter 2: Development of an Enantioselective Organocatalytic Hydride Reduction of $\alpha,\beta$ -Unsaturated Aldehydes***

Introduction.....	6
Optimizing the Reaction.....	10
Analysis of the Catalyst: Explaining the <i>t</i> -Butyl Imidazolidinone.....	11
Analysis of the Catalyst: Rationalizing the Decreased Selectivity and Reactivity .....	16
Absolute Sense of Enantioinduction .....	17
Assessing the Effect of Olefin Geometry.....	18
Developing a Facile Use of This Methodology .....	22
Related Work .....	23
Conclusions.....	24
Supporting Information .....	25

### ***Chapter 3: Design and Development of an Organocatalytic Reduction of $\alpha,\beta$ -Unsaturated Enones***

Introduction.....	40
Development of an Organocatalytic Enone Hydrogenation Reaction .....	42
Substrate Scope.....	44
Absolute Sense of Enantioinduction .....	46
Challenges Associated with this Chemistry.....	47
Utilizing <i>t</i> -Butyl Hantzsch Dihydropyridine in the Reduction of Geranial .....	50
Explanation of the Reactivity Differences .....	52
Structural Features That May Further Contribute to Reactivity Differences.....	53
Dynamic Kinetic Resolution .....	57
Recent Developments .....	58

Conclusion .....	59
Supporting Information .....	60

#### ***Chapter 4: Progress Toward the Total Synthesis of (+)-Minfiensine***

Isolation, Structure and Biological Activity.....	97
Synthetic Strategy .....	99
Retrosynthetic Analysis.....	105
Unsuccessful Approaches to the Elaborated Caprylolactam.....	107
Modifying the Strategy.....	111
Future Directions .....	121
Conclusion .....	122
Supporting Information .....	123

## List of Figures

### ***Chapter 1: LUMO-Lowering Enantioselective Organocatalytic***

<i>Number</i>	<i>Page</i>
1. Single Enantiomer Drugs .....	1
2. Examples of Chiral Pool Derived Catalysts .....	2
3. Engineering the Requirements for Enantioselectivity .....	3
4. The First Example of Imidazolidinone Iminum Activation .....	4
5. Organocatalysis Publication Starting in 2000.....	4

### ***Chapter 2: Development of an Enantioselective Organocatalytic Hydride Reduction of $\alpha,\beta$ -Unsaturated Aldehydes***

<i>Number</i>	<i>Page</i>
1. Hydrogen-Bearing Stereocenters and Transition-Metal Catalyzed Hydrogenation.....	6
2. Enzymatic Catalytic Enantioselective Hydrogenation .....	7
3. Utilizing the Concepts of Bio-Reduction for Organocatalytic Reduction .....	8
4. A Proposed Catalytic Cycle for EOHR .....	9
5. Comparing the 2 <sup>nd</sup> Generation Catalyst to the Hydrogenation Catalyst .....	13
6. Enzyme Crystal Structures Support an <i>Endo</i> Transition State.....	14
7. Houk's Theoretical Calculations Support an <i>Endo</i> Transition State.....	15
8. Explaining the <i>Endo</i> Transition using FMO.....	15
9. Rationalizing the Reactivity and Selectivity Differences.....	17
10. Sense of Absolute Enantioinduction of the Tri-Substituted Olefin.....	18
11. Evaluating the Effects of Olefin Mixtures on Enantioselectivity.....	20
12. Results of a VT-NMR Experiment.....	21
13. Proposed Isomerization Mechanism.....	22
14. Mixture of Asymmetric Catalytic Hydrogenation: MacH-( <i>R</i> ).....	22

**Chapter 3: Design and Development of an Organocatalytic Reduction of  $\alpha,\beta$ -Unsaturated Cyclic Ketones**

<i>Number</i>	<i>Page</i>
1. Reactivity Differences Between Unsaturated Aldehydes and Ketones .....	41
2. Challenges for Stereocontrol.....	41
3. Typical Organocatalysts Failed to Catalyze a Reaction.....	42
4. Absolute Sense of Enantioinduction.....	47
5. Challenges Associated with the Reduction Chemistry.....	47
6. Methyl Versus Ethyl Stereodifferentiation: Comparing the Hantzsch Ester Derivatives .....	51
7. Explaining the Increase in Enantioselectivity Demonstrated by the <i>t</i> -Butyl Hantzsch .....	51
8. Explaining the Hantzsch Ester Rate Difference .....	52
9. Comparing Homogeneous Reactions of Both Hantzsch Ester Derivatives.....	53
10. X-Ray Crystallography Analysis of Both Hantzsch Derivatives .....	54
11. Analyzing the Dihydropyridine Rings.....	55
12. Effect of Puckering on Hydride Transfer .....	56
13. Assessing the Puckering Effect on Dihydropyridine Reactivity.....	56
14. An Alternative Approach to Cyclic Enone Stereogenicity .....	57

**Chapter 4: Progress Toward the Total Synthesis (+)-Minfiensine**

<i>Number</i>	<i>Page</i>
1. Structurally Related Members of the Strychnos Alkaloid Family .....	97
2. Overman's Synthetic Strategy.....	98
3. Completion of Overman's Synthesis .....	99
4. Organocatalytic Pyrroloindoline Formation Relies on Interception of Reactive Intermediate ....	101
5. Organocatalytic Cyclization Is a Powerful Entry into Natural Products .....	101
6. Utilizing the Energy Released via the Collapse of a Nine-Membered Ring .....	102
7. Assembling the Tetracyclic Ring System.....	104
8. A Retrosynthetic Analysis of Minfiensine.....	106
9. SOMO Catalysis Can Forge the Final C-C Bond of the Caged Cycle .....	107
10. Attempts to Access the Nine-Membered Lactam using Ring-Closing Metathesis .....	108
11. Van Maarseveen's Intramolecular Staudinger Ligation.....	109
12. A Similar Strategy to Access the Lactam.....	110
13. Issues with Lithiating Substituted Caprylactams.....	111



14. Simplifying the Nine-Membered Lactam Intermediate .....	112
15. Testing the Stability of Electron-Rich Heterocycles Under SOMO Conditions .....	116
16. MM3 Structures of Two Imidazolidinone Catalysts .....	118
17. Increasing the Temperature Increases the Enantioselectivity .....	119
18. Eyring Plot Analysis of the OC Reaction .....	120
19. Plans to Complete the Synthesis .....	122

## List of Tables

### ***Chapter 2: Development of an Enantioselective Organocatalytic Hydride Reduction of $\alpha,\beta$ -Unsaturated Aldehydes***

<i>Number</i>	<i>Page</i>
1. Effect of Catalyst and Co-Catalyst on Hydrogenation .....	10
2. Assessing Various Dihydropyridine NADH Mimics .....	11
3. Substrate Scope for the EOHR .....	12

### ***Chapter 3: Design and Development of an Organocatalytic Reduction of $\alpha,\beta$ -Unsaturated Cyclic Ketones***

<i>Number</i>	<i>Page</i>
1. Optimizing the Enone Hydrogenation .....	43
2. Substrate Scope: Cyclopentenones .....	45
3. Substrate Scope: Larger Rings .....	46
4. Analyzing the Hantzsch Derivatives for Efficacy .....	48
5. Comparison of Ethyl and <i>t</i> -Butyl Hantzsch Reduction Reactions with Larger Rings .....	49
6. Comparison of Ethyl and <i>t</i> -Butyl Hantzsch Reductions of Cyclopentenones .....	50

### ***Chapter 4: Progress Toward the Total Synthesis (+)-Minfiensine***

<i>Number</i>	<i>Page</i>
1. Subjecting the Caprylolactam to a Variety of Deprotection Conditions .....	115
2. Evaluating Co-Catalysts .....	120

## LIST OF ABBREVIATIONS

<b>AcOH</b>	acetic acid
<b>Alloc</b>	allyl carbamate
<b>BINAP</b>	2,2'-bis(diphenylphosphino)-1,1'-binaphthyl
<b>Bn</b>	benzyl
<b>BOC</b>	tert-butyl carbamate
<b>BZ</b>	benzoyl
<b>CAN</b>	ceric (IV) ammonium nitrate
<b>DABCO</b>	1,4-diazabicyclo[2.2.2]octane
<b>DMAP</b>	dimethylamino pyridine
<b>DME</b>	dimethoxyethane
<b>DMF</b>	dimethylformamide
<b>DMP</b>	Dess-Martin periodinane
<b>DNBA</b>	di-nitrobenzoic acid
<b>EOHR</b>	enantioselective organocatalytic hydride reduction
<b>EtOH</b>	ethyl alcohol
<b>FADH</b>	flavin adenine dihydronucleotide
<b>FGI</b>	functional group interconversion
<b>GLC</b>	gas liquid chromatography
<b>HCl</b>	hydrochloric acid

<b>HOMO</b>	highest occupied molecular orbital
<b>I-Mes</b>	1,3-dimesitylimidazol-2-ylidene
<b>Ind</b>	indole
<b>KH</b>	potassium hydride
<b>KHMDS</b>	potassium hexamethyldisilazide
<b>LCMS</b>	liquid chromatography mass spectrometer
<b>LDA</b>	lithium diisopropylamide
<b>LUMO</b>	lowest unoccupied molecular orbital
<b>MacH-R</b>	mixture for asymmetric catalytic hydrogenation-(R)
<b>m-CPBA</b>	meta-chloroperoxybenzoic acid
<b>NADH</b>	nicotinamide adenine dinucleotide
<b>NaOt-Bu</b>	sodium tert-butoxide
<b>NMO</b>	N-methylmorpholine-N-oxide
<b>NMR</b>	nuclear magnetic resonance
<b>Tf</b>	trifluoromethylsulfonate
<b>Pd(OAc)<sub>2</sub></b>	palladium(II)acetate
<b>Phth</b>	phthalimide
<b>PMHS</b>	polymethylhydrosiloxane
<b>PMP</b>	para-methoxyphenyl
<b>RCM</b>	ring-closing metathesis
<b>RT</b>	Room temperature
<b>SFC</b>	supercritical fluid chromatography

<b>SOMO</b>	singly occupied molecular orbital
<b>TBA</b>	tribromoacetic acid
<b>TBS</b>	tert-butyldimethylsilane
<b>TBSCl</b>	tert-butyldimethylsilane chloride
<b>TCA</b>	trichloroacetic acid
<b>TFA</b>	trifluoroacetic acid
<b>THF</b>	tetrahydrofuran
<b>TIPS</b>	triisopropylsilyl
<b>TS</b>	transition state
<b>TsOH</b>	Para-toluenesulfonic acid
<b>Uwave</b>	microwave
<b>VT-NMR</b>	variable-temperature nuclear magnetic resonance

*To Jessica*

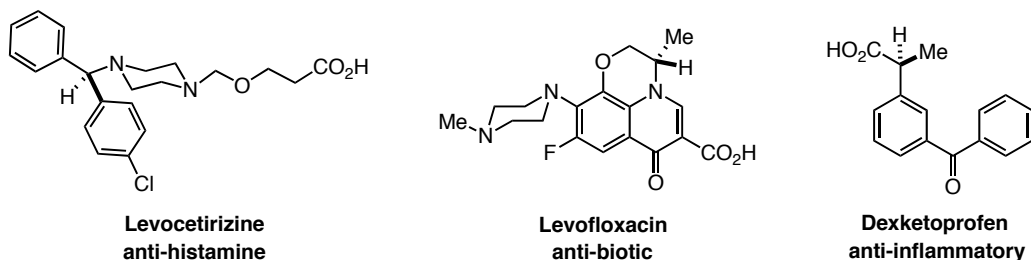
# Chapter 1

## LUMO-Lowering Enantioselective Organcatalysis

### Introduction

During the last 30 years, the field of organic chemistry has responded to the challenges of developing new methods to access single-enantiomer products.<sup>1</sup> Underlying this challenge is the emphasis placed on atom economical processes,<sup>2</sup> the need for alternative chiral building blocks, and the desire of fine chemical and pharmaceutical industries to utilize enantiopure materials (Fig. 1).<sup>3</sup> Accordingly, the field of asymmetric catalysis has grown dramatically and has culminated with rewarding the pioneers of this vast body of chemistry—Sharpless, Noyori, and Knowles—with the 2001 Nobel Prize in Chemistry.<sup>4</sup>

**Figure 1. Single Enantiomer Drugs**



While the majority of these powerful transformations utilize transition metals and chiral-ligands, recent advancements into the readily available chiral pool employ organic molecules, such as amino acids and sugars (Fig. 2). In an early example, the Hajos-Parrish group reported a desymmetrizing intramolecular aldol cyclization using the amino

(1) Jacobsen, E. N. P., A., Yamamoto, H. *Comprehensive Asymmetric Catalysis*; Springer: Heidelberg, 1999.

(2) (a) Trost, B. M. *Angew. Chem. Int. Ed. Eng.* **1995**, *34*, 259-281. (b) Trost, B. M. *Science* **1991**, *254*, 1471-1477.

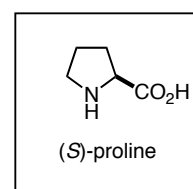
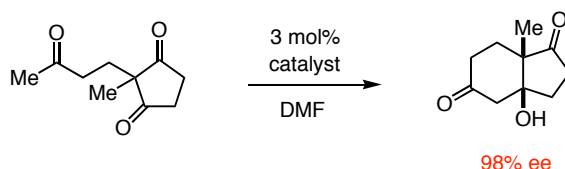
(3) <http://www.fda.gov/cder/guidance/stereo.htm>

(4) (a) Sharpless, K. B. *Angew. Chem. Int. Ed.* **2002**, *41*, 2024-2032. (b) Noyori, R. *Adv. Synth. Cat.* **2003**, *345*, 15-32. (c) Knowles, W. S. *Angew. Chem. Int. Ed.* **2002**, *41*, 1999-2007.

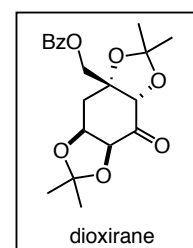
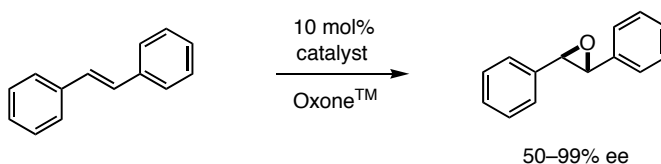
acid proline.<sup>5</sup> Furthermore, the groups of Shi, Yang, and Denmark have utilized chiral ketones, in this case derived from fructose, to catalyze enantioselective epoxidations.<sup>6</sup> This seminal work has laid the foundation for the burgeoning field of organocatalysis, by influencing the development of a broad range of new reaction methods and inspiring the creation of new catalyst architectures.

**Figure 2. Examples of Chiral Pool Derived Catalysts**

■ Intramolecular aldol: Hajos–Parrish *J. Org. Chem.* **1974**, *39*, 1615



■ Enantioselective catalytic epoxidations: Shi, Yang, Denmark



### ***Development of LUMO-Lowering Iminium Activation***

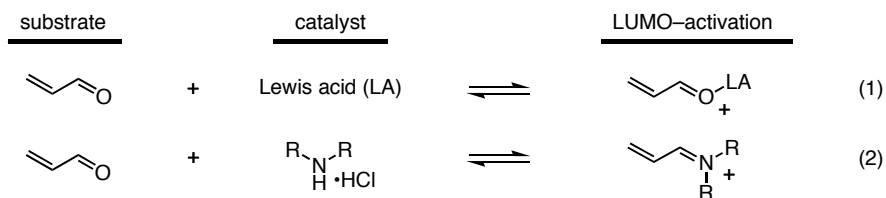
The idea for iminium activation of  $\alpha,\beta$ -unsaturated carbonyl was influenced by related transition-metal induced methods of alkene activation (eq. 1). Specifically, we planned to mimic the LUMO-lowering activation of an olefin by reversible coordination of a Lewis acid to a carbonyl lone pair (eq. 1). It was envisioned that the equilibrium condensation between a secondary amine and an aldehyde to produce an electron-

(5) Hajos, Z. G.; Parrish, D. R. *J. Org. Chem.* **1974**, *39*, 1612-1615.

(6) (a) Frohn, M.; Shi, Y. *Synthesis* **2000**, 1979-2000. (b) Yang, D.; Wang, X. C.; Wong, M. K.; Yip, Y. C.; Tang, M. W. *J. Am. Chem. Soc.* **1996**, *118*, 11311-11312. (c) Denmark, S. E.; Wu, Z. C. *Synlett* **1999**, 847-859.

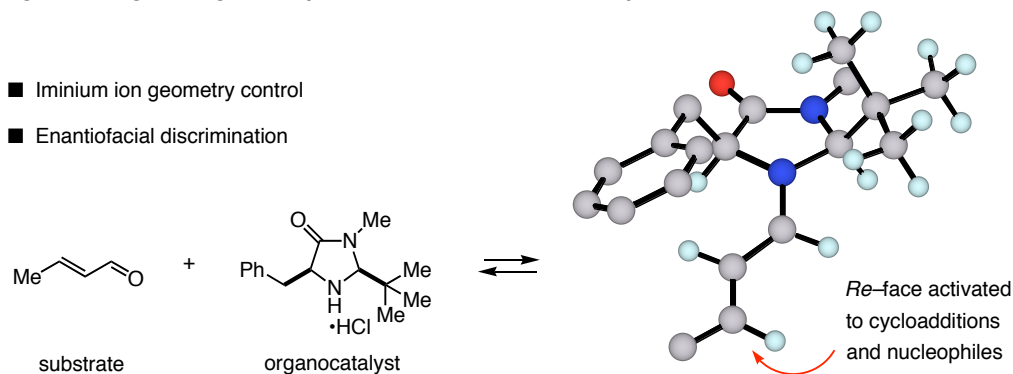


deficient intermediate would similarly activate the conjugated  $\pi$ -system towards nucleophilic additions (eq. 2).



In order to make this process enantioselective, two structural requirements need to be fulfilled (Fig. 3). The first is to control iminium ion geometry and, the second, to influence the trajectory of the incoming nucleophile to one enantioface of the  $\pi$ -system.

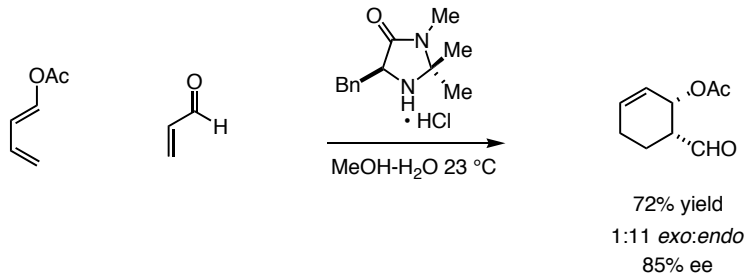
**Figure 3. Engineering the Requirements for Enantioselectivity**



In order to fulfill these necessities, imidazolidinone catalysts were developed bearing the requisite chiral functionality. These organocatalysts are readily assembled from the chiral pool and are typically air and moisture stable allowing for straightforward storage and implementation. In the event of a condensation reaction with an  $\alpha,\beta$ -unsaturated carbonyl compound, the activated intermediate favors the *s-trans* geometry about the iminium by selectively partitioning the bulkier alkyl group under the benzyl group while orienting the smaller hydrogen beneath the sterically more demanding *t*-butyl moiety. In 2000, our group reported the first successful demonstration of this

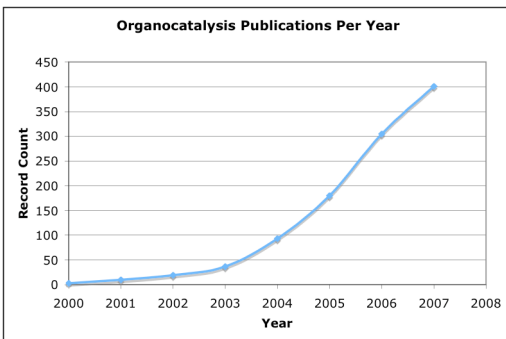
concept in the context of a Diels-Alder cycloaddition utilizing  $\alpha,\beta$ -unsaturated aldehydes as dienophiles in conjunction with a variety of dienes (Fig. 4).<sup>7</sup>

**Figure 4. The First Example of Imidazolidinone Iminium Activation**



Indeed, this mode of activation has revitalized the field of organocatalysis and has led to the development of many powerful catalytic asymmetric transformations (Fig. 5).<sup>8</sup> These new methods include cycloadditions, heteroconjugate additions, cyclopropanations, Mukaiyama-Michael additions, Friedel-Crafts alkylations, cascade reactions, and conjugate addition of boron reagents.<sup>9</sup>

**Figure 5. Organocatalysis Publication Trend Starting in 2000**



(7) Ahrendt, K. A.; Borths, C. J.; MacMillan, D. W. C. *J. Am. Chem. Soc.* **2000**, *122*, 4243-4244.

(8) Web of Knowledge search, "organocatalysis" or "organocatalytic" in topic.

(9) (a) Lelais, G.; MacMillan, D. W. C. *Aldrichim Acta* **2006**, *39*, 79-87. (b) Lee, S.; MacMillan, D. W. C. *J. Am. Chem. Soc.* **2007**, *129*, 15438.

### ***Summary of Thesis Research***

The following chapters detail research efforts that focus on further establishing iminium activation as a powerful mode of activation. Chapter 2 discusses the development of a novel mode of catalytic asymmetric hydrogenation of  $\alpha,\beta$ -unsaturated aldehydes utilizing Hantzsch dihydropyridines.<sup>10</sup> Chapter 3 focuses on the extension of this technology toward  $\alpha,\beta$ -unsaturated ketones utilizing a different imidazolidinone catalyst in conjunction with a novel Hantzsch analogue.<sup>11</sup> Finally, Chapter 4 details the efforts made towards the total synthesis of (+)-minfiensine utilizing an organocatalytic cascade cyclization reaction for rapid entry into the pyrroloindoline core of this natural product.

---

(9) Ouellet, S. G.; Tuttle, J. B.; MacMillan, D. W. C. *J. Am. Chem. Soc.* **2005**, *127*, 32-33.

(10) Tuttle, J. B.; Ouellet, S. G.; MacMillan, D. W. C. *J. Am. Chem. Soc.* **2006**, *128*, 12662-12663.

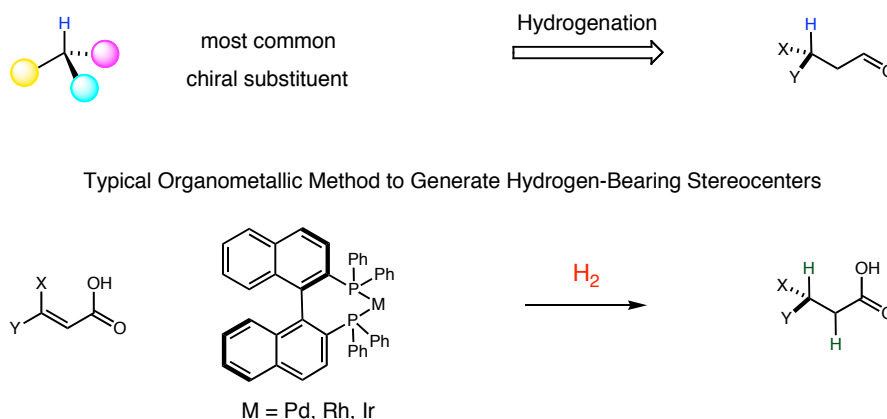
## Chapter 2

### Development of an Enantioselective Organocatalytic Hydride Reduction Reaction of $\alpha,\beta$ -Unsaturated Aldehydes

#### Introduction

Within the vast chemical architecture known as stereogenicity, hydrogen is the most common, discrete substituent. Not surprisingly, therefore, the field of enantioselective catalysis has focused great attention on the invention of hydrogenation technologies over the last 50 years,<sup>1</sup> the importance of which has culminated in the Nobel Prize for the pioneers of this important transformation (Fig. 1).<sup>2</sup>

**Figure 1. Hydrogen-Bearing Stereocenters and Transition-Metal Catalyzed Hydrogenation**

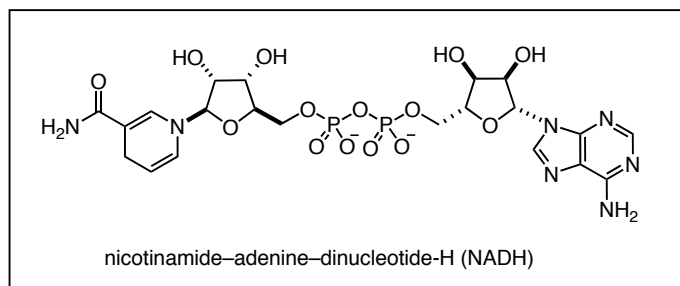
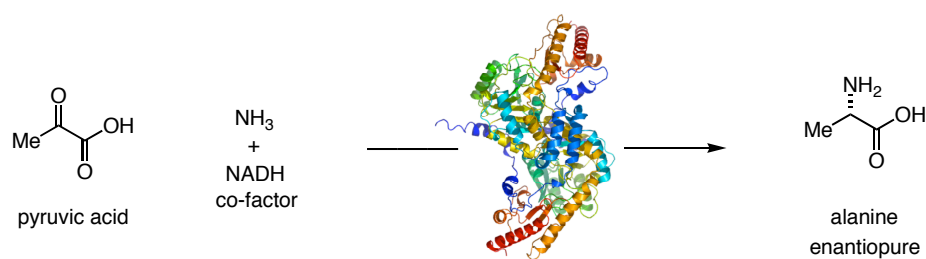


While the field of hydrogenation chemistry has matured as an integral methodology in the realms of industrial and academic chemistry,<sup>3</sup> this reaction platform is not the most common method for asymmetric hydrogenation. Indeed, biological systems have

- (1) (a) Akabori, S.; Sakurai, S.; Izumi, Y.; Fujii, Y. *Nature* **1956**, *178*, 323-324. (b) Okhuma, T. K., M.; Noyori, R. *Catalytic Asymmetric Synthesis*; Wiley-VCH: New York, 2000. (c) Noyori, R.; Ohkuma, T. *Angew. Chem. Int. Ed.* **2001**, *40*, 40-73.
- (2) (a) Knowles, W. S. *Angew. Chem. Int. Ed.* **2002**, *41*, 1999-2007. (b) Noyori, R. *Angew. Chem. Int. Ed.* **2002**, *41*, 2008-2022.
- (3) (a) Shimizu, H.; Nagasaki, I.; Matsumura, K.; Sayo, N.; Saito, T. *Acc. Chem. Res.* **2007**, *40*, 1385-1393. (b) Genet, J. P. *Acc. Chem. Res.* **2003**, *36*, 908-918.

developed highly efficient tools for performing enantioselective hydrogenation.<sup>4</sup> Specifically, substrates are reduced in the enzymatic active site in the presence of co-factors such as NAD(P)H and FADH (Fig. 2).<sup>5</sup> For example, the enzyme alanine dehydrogenase utilizes a series of hydrogen bonds to both activate and sequester pyruvate imine for an enantiospecific hydride delivery to the iminium carbon.<sup>6</sup>

**Figure 2. Enzymatic Catalytic Enantioselective Hydrogenation**



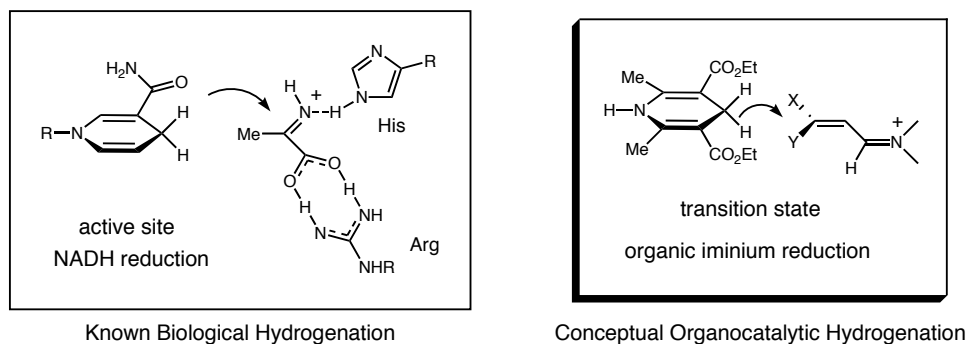
From these conceptual blueprints, a related alternative strategy was envisioned utilizing our iminium activation technology and an alternative dihydropyridine that functions as an NADH mimic (Fig. 3).

(4) Alberts, B. B., D.; Lewis, J.; Raff, M.; Roberts, K.; Watson, J. D. *Molecular Biology of the Cell*; Garland: New York & London, 2002.

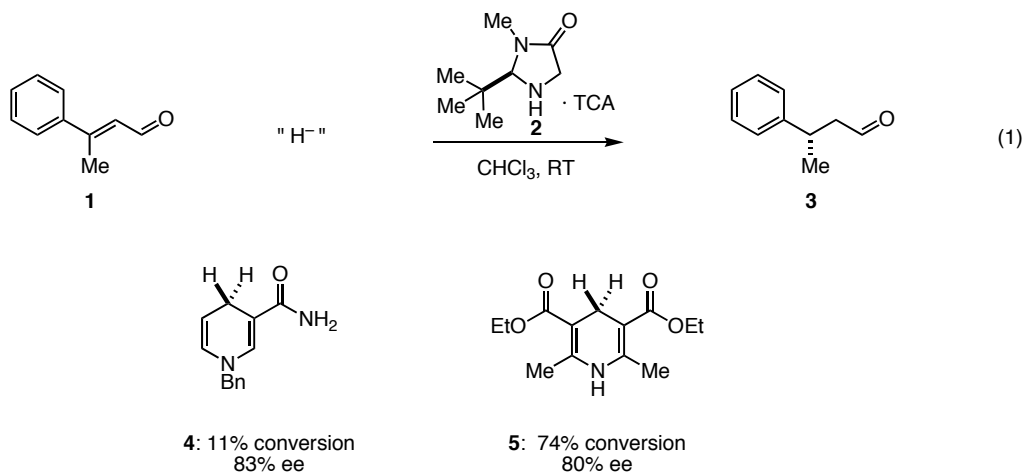
(5) You, K.-S.; Oppenheimer, N. J. *Crit. Rev. Biochem. Mol. Bio.* **1985**, *17*, 313 - 451.

(6) (a) Alizade, M. A.; Bressler, R.; Brendel, K. *Biochim. Biophys. Acta* **1975**, *397*, 5-8. (b) Sedelnikova, S.; Rice, D. W.; Shibata, H.; Sawa, Y.; Baker, P. J. *Acta Crystallogr., Sect. D: Biol. Crystallogr.* **1998**, *54*, 407-408. (c) Matsui, K.; Tamegai, Y.; Miyano, A.; Kameda, Y. *Chem. Pharm. Bull.* **1977**, *25*, 2061-2066.

Figure 3. Utilizing the Concepts of Bio-Reduction for Organocatalytic Reduction



Dr. Stephane Ouellet performed the preliminary investigations into developing an analogous reaction (eq. 1). Initial use of N-benzylnicotinamide **1** gave a low conversion and a good ee. We were pleased to find the ethyl Hantzsch dihydropyridine **2**<sup>7</sup> provided the desired product with an improved yield and comparable ee.<sup>8</sup> The increased yield is attributed to the ability of the dihydropyridine to provide a proton to the intermediate enamine to complete the catalytic cycle (*vide infra*).

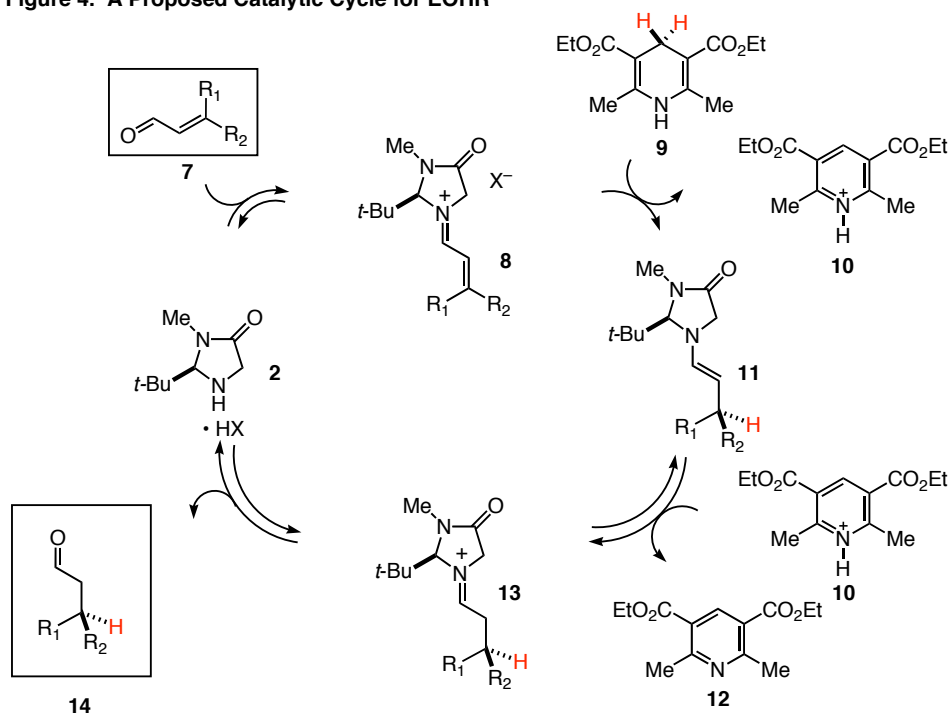


(7) Hantzsch, A. Hantzsch, A. *Liebigs Ann. Chem.* **1882**, 215.

(8) (a) Pandit, U. K.; Mascabre, F. R.; Gase, R. A.; Deniesarink, M. J. *J. Chem. Soc., Chem. Commun.* **1974**, 627-628. (b) Niesarink, M. J. D.; Pandit, U. K. *Tetrahedron Lett.* **1978**, 1335-1338. (c) Pandit, U. K.; Gase, R. A.; Mascabre, F. R.; Deniesarink, J. *J. Chem. Soc., Chem. Commun.* **1975**, 211-212.

The proposed catalytic cycle begins with condensation of imidazolidinone catalyst salt **2** onto  $\alpha,\beta$ -unsaturated aldehyde **7** to provide iminium intermediate **8** (Fig. 4). Conjugate reduction by dihydropyridine **9** forms both pyridinium **10** and enamine **11**. Importantly, this step is irreversible due to the aromatization of Hantzsch **9** and is the proposed driving force for this reaction. Protonation of **11** by either pyridinium **6** or acid co-catalyst (formed via re-protonated conjugate base) gives iminium **13** that undergoes hydrolysis to provide the desired aldehyde **14** and releases catalyst **2** back into the cycle. In this chemistry, the enal substrates are reduced with high 1,4 chemoselectivity whereas 1,2 alcohol products are never observed. This suggests the dihydropyridine is a soft hydride donor, preferentially reacting at the softer site on the iminium acceptor. Fortuitously, pyridine by-product **12** does not interfere with the catalytic cycle.

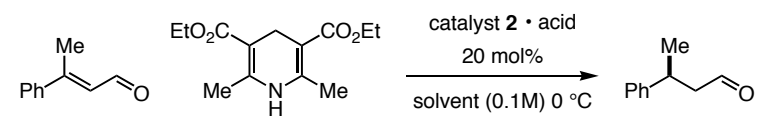
**Figure 4. A Proposed Catalytic Cycle for EOHR**



### Optimizing the Reaction

A range of solvents and co-catalysts were surveyed for their effects on this transformation (Table 1). Solvents having lower dielectric constants provided the desired product with optimal conversion and enantioexcess (Table 1, entries 1–4). A survey of acids indicated less acidic co-catalysts increased the conversion and ee (Table 1, entries 5-8). This is attributed to a greater propensity for the weaker conjugate base to function as a better hydrogen shuttle, facilitating faster catalytic turnover.

**Table 1. Effect of Catalyst and Co-Catalyst on Hydrogenation**

					
entry	acid co-catalyst	solvent	time (h)	% conversion <sup>a</sup>	%ee <sup>b</sup>
1	TFA	toluene	6.5	85	89
2	TFA	Et <sub>2</sub> O	1	39	86
3	TFA	CH <sub>2</sub> Cl <sub>2</sub>	1	95	83
4	TFA	THF	1	54	87
5	TFA	CHCl <sub>3</sub>	1	85	85
6	<i>p</i> -TsOH	CHCl <sub>3</sub>	7	61	90
7	TBA	CHCl <sub>3</sub>	2	96	85
8	TCA	CHCl <sub>3</sub>	2	94	84

<sup>a</sup>Conversion determined by GC analysis comparison to an internal standard.

<sup>b</sup>Enantiomeric excess determined by chiral GC analysis.

Next, a variety of hydride sources were subjected to these optimal conditions (Table 2). Surprisingly, NADH did not react under standard conditions (Table 2, entry 1). Nicotinamide, the “business-end” of NADH, gave similar conversion but an increased ee compared to the original conditions (Table 2, entry 2, 15% conversion, 88% ee). In general, improved reactivity was achieved in the Hantzsch dihydropyridine series (Table 2, entries 3-6). Interestingly, the reactivity is strongly influenced by the electronics of the substituents found on the dihydropyridine 3,5-positions. For instance, ketone functionality provided the desired product in low yields but good



enantioselectivity (Table 2, entries 3-4). The problem of low conversion was solved by introducing less electronegative ester moieties, as shown by an increased yield with good levels of enantioexcess (Table 2, entries 5-6). The ethyl ester analogue provided the highest ee with good conversion and was used to expand the substrate scope (Table 2, entry 6).

**Table 2. Assessing Various Dihydropyridine NADH Mimics**

Reaction scheme: (E)-3-methyl-3-phenylprop-2-enal + catalyst **2** • TCA (20 mol%) in CHCl<sub>3</sub> at -30 °C yields (S)-3-methyl-3-phenylpropanal.

entry	hydrogen component	time (h)	% conversion <sup>a</sup>	%ee <sup>b</sup>
1	NADH	24	---	---
2	N-Bn-Nicotinamide	26	15	88
3	R = COMe	26	45	86
4	R = CPh	24	54	80
5	R = CO <sub>2</sub> Bn	7	94	88
6	R = CO <sub>2</sub> Et	7	92	92

<sup>a</sup>Conversion determined by GC analysis comparison to an internal standard.

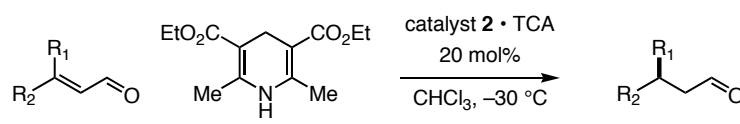
<sup>b</sup>Enantiomeric excess determined by chiral GC analysis.

### Substrate Scope

Having identified the optimal reductant for this transformation, we next examined the scope of  $\alpha,\beta$ -unsaturated aldehydes amenable to this new methodology (Table 3). A broad range of compounds was reduced in high yield and with good enantioselectivity. The catalyst can distinguish between subtle steric differences between methyl and ethyl substituents found on the  $\beta$ -center (Table 3, entries 1, 2 and 3, 4). Sterically dense side-chains increase substrate reactivity as indicated by lower catalyst loading and reduced reaction time (Table 3, entry 7). Moreover, iminium stabilizing aldehydes (Table 3, entries 1, 2, 8) as well as enals that do not readily participate in iminium formation (Table 3, entry 5) are readily reduced under these conditions. Importantly, this mild hydride

delivery system is compatible with substrates that are susceptible to over-reduction (Table 3, entries 5, 8).<sup>9</sup>

**Table 3. Substrate Scope for the EOHR**



entry	<i>E</i> / <i>Z</i> ratio	R <sub>1</sub>	R <sub>2</sub>	time (h)	% yield	%ee <sup>a</sup>
1	> 20 / 1	Me	Ph	23	91	93 <sup>b</sup>
2	> 20 / 1	Et	Ph	16	74	94
3	5 / 1	Me	<i>c</i> -hex	10	91	96 <sup>b</sup>
4	3 / 1	Et	<i>c</i> -hex	23	95	91 <sup>c</sup>
5	> 20 / 1	Me	CO <sub>2</sub> Me	26	83 <sup>d</sup>	91 <sup>e</sup>
6	> 20 / 1	Me	CH <sub>2</sub> OTIPS	72	74	87
7	> 20 / 1	Me	<i>t</i> -Bu	0.5	95 <sup>d</sup>	97 <sup>f</sup>
8	> 20 / 1	Me	3,4-Cl <sub>2</sub> Ph	16	92	97

<sup>a</sup>Enantiomeric excess determined by chiral GC analysis. <sup>b</sup>Performed at -45 °C.

<sup>c</sup>Using 10 mol % catalyst. <sup>d</sup>Yield determined by NMR. <sup>e</sup>Performed at -50 °C.

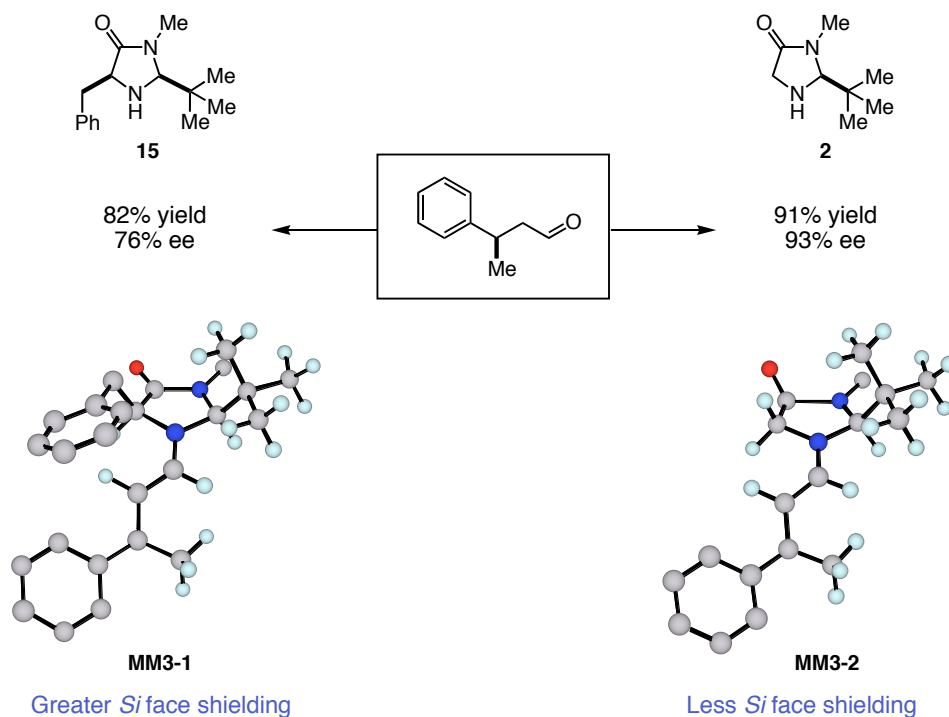
<sup>f</sup>Using 5 mol % catalyst at 23 °C.

### ***Analysis of the Catalyst: Explaining the *t*-Butyl Imidazolidinone***

A unique aspect to this chemistry is the nature of the organocatalyst. The majority of imidazolidinone-mediated iminium activation publications utilize catalysts that are functionalized on the 2,5-carbons.<sup>10</sup> For example, a broad-range of enantioselective transformations has been discovered utilizing our second-generation catalyst **15** bearing *t*-butyl and benzyl moieties, respectively, in these positions. Intriguingly, in this methodology, we discovered the *t*-butyl catalyst **2** exhibited a clear difference in reactivity and selectivity compared to the second-generation catalyst **15**. (Fig. 5, 2<sup>nd</sup> generation gives 82% yield, 76% ee; *t*-butyl gives 91% yield, 93% ee). This effect is non-intuitive considering less *Si*-face shielding occurs in iminium **MM3-2** formed with the *t*-butyl imidazolidinone catalyst compared to that of **MM3-1**.

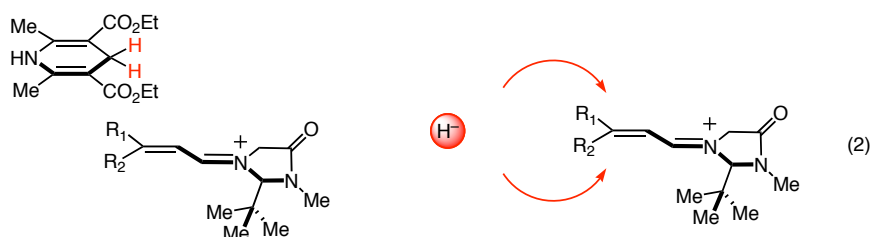
(9) Keinan, E.; Greenspoon, N. J. *Am. Chem. Soc.* **1986**, *108*, 7314. (b) Cortese, N. A.; Heck, R. F. *J. Org. Chem.* **1978**, *43*, 3985.

(10) Lelais, G.; MacMillan, D. W. C. *Aldrichimica Acta* **2006**, *39*, 79-87.

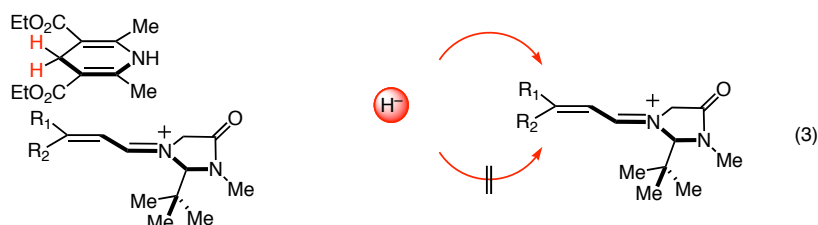
Figure 5. Comparing the 2<sup>nd</sup>-Generation Catalyst to the Hydrogenation Catalyst

Transition state analysis provides insight into the nature of this effect. The dihydropyridine can approach the activated iminium species by two pathways. One possibility is in an *exo*-orientation. In this transition state, the nitrogen of the Hantzsch ester is oriented distal from the stereodefining *t*-butyl moiety of the imidazolidinone and hydride is delivered with minimal substrate-catalyst interaction (eq. 2). In this case, the hydride could be delivered to either face of the  $\pi$ -system, resulting in a decreased enantioselectivity. Alternatively, the dihydropyridine could approach in an *endo*-orientation where interaction with the catalyst is now enhanced (eq. 3). In this stacked transition state, one  $\pi$ -face is favored because now the catalyst has greater control over the approaching dihydropyridine, and directs the hydride delivery to one stereoface, providing higher levels of enantiocontrol.

### Hantzsch dihydropyridine reduction *Exo* transition state



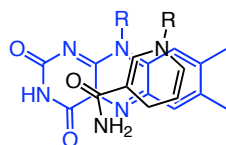
### Hantzsch dihydropyridine *endo* transition state



Indeed, we believe the *endo*-transition state (eq. 3) operates in this chemistry for two reasons. The first supporting evidence is found in biological systems. Crystal structures of enzyme active sites containing substrates and NAD(P)H co-factors show the nicotinamide moiety prefers an *endo*-orientation (Fig. 6).<sup>11</sup>

**Figure 6. Enzyme Crystal Structures Support an *Endo* Transition State**

Ferredoxin NADP reductase



NADPH Glutathione reductase

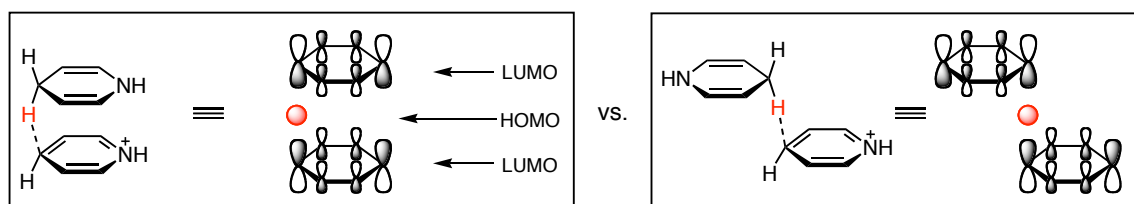


The second piece of evidence derives from theoretical modeling.<sup>12</sup> The Houk group performed calculations on both *exo*- and *endo*-transition states of dihydropyridine reduction of a pyridinium cation (Fig. 7). In this simple system, the *endo* approach was favored over the *exo* by 2.7 kcal/mol.

(11) (a) Karplus, P. A.; Daniels, M. J.; Herriott, J. R. *Science* **1991**, 251, 60-66. (b) Karplus, P. A.; Schulz, G. E. *J. Mol. Biol.* **1989**, 210, 163-180. (c) Pai, E. F.; Karplus, P. A.; Schulz, G. E. *Biochemistry* **1988**, 27, 4465-4474. (d) Abadzapatero, C.; Griffith, J. P.; Sussman, J. L.; Rossmann, M. G. *J. Mol. Biol.* **1987**, 198, 445-467.

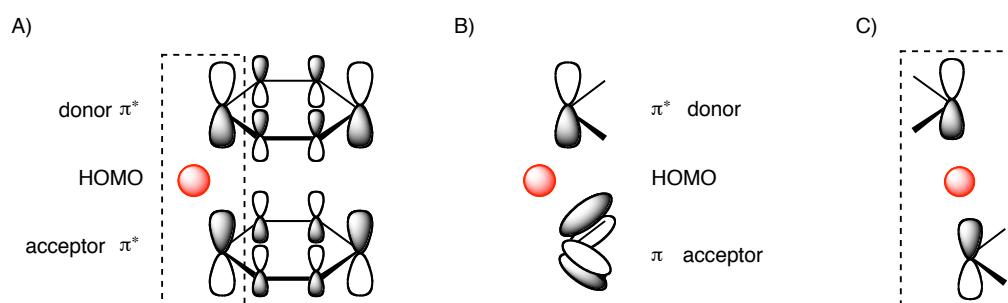
(12) Wu, Y. D.; Lai, D. K. W.; Houk, K. N. *J. Am. Chem. Soc.* **1995**, 117, 4100-4108.

Figure 7. Houk's Theoretical Calculations Support an *Endo* Transition State



Further analysis of these transition states helps to explain the impact FMOs have on stabilizing the *endo* orientation (Fig. 8). The Houk group's theoretical modeling supports a favorable  $\pi^*$ -HOMO- $\pi^*$  overlap between the hydride donor/hydride/hydride acceptor, respectively.<sup>13</sup> In particular, the LUMO-LUMO interaction at the C-4 frontier orbitals is the largest contribution to this effect (Fig. 8, A, dashed box). It is calculated that the composite LUMO created in this overlap, despite being unfilled, is lower in energy than in the non-interacting case. Importantly, this overlap is more significant in the *endo*-transition state due to an energetically favorable bent delivery of the hydride. Calculations indicate an obtuse delivery angle is favored over a linear approach by 1.7

Figure 8. Explaining the *Endo* TS using FMO



■ A and B correlate to the *endo* transition state

■ C correlates to the *exo* transition state

kcal/mol for two reasons. The first is that the hydride HOMO and pyridinium LUMO interaction is maximized. The second reason is that the hydride HOMO interaction with the pyridinium HOMO is, at the same time, minimized (Fig. 8, B). In the linear approach

(13) (a) Wu, Y. D.; Lai, D. K. W.; Houk, K. N. *J. Am. Chem. Soc.* **1995**, *117*, 4100-4108. (b) Houk, K. N.; Paddonrow, M. N.; Rondan, N. G.; Wu, Y. D.; Brown, F. K.; Spellmeyer, D. C.; Metz, J. T.; Li, Y.; Loncharich, R. J. *Science* **1986**, *231*, 1108-1117. (24) Wu, Y. D.; Houk, K. N. *J. Am. Chem. Soc.* **1987**, *109*, 2226-2227.

this HOMO-HOMO destabilizing interaction is increased, disfavoring this transition state geometry. For the *exo* transition state this LUMO-LUMO stabilizing interaction is absent (Fig. 8, compare A to C) and therefore is not as stabilized as the *endo*-conformation.

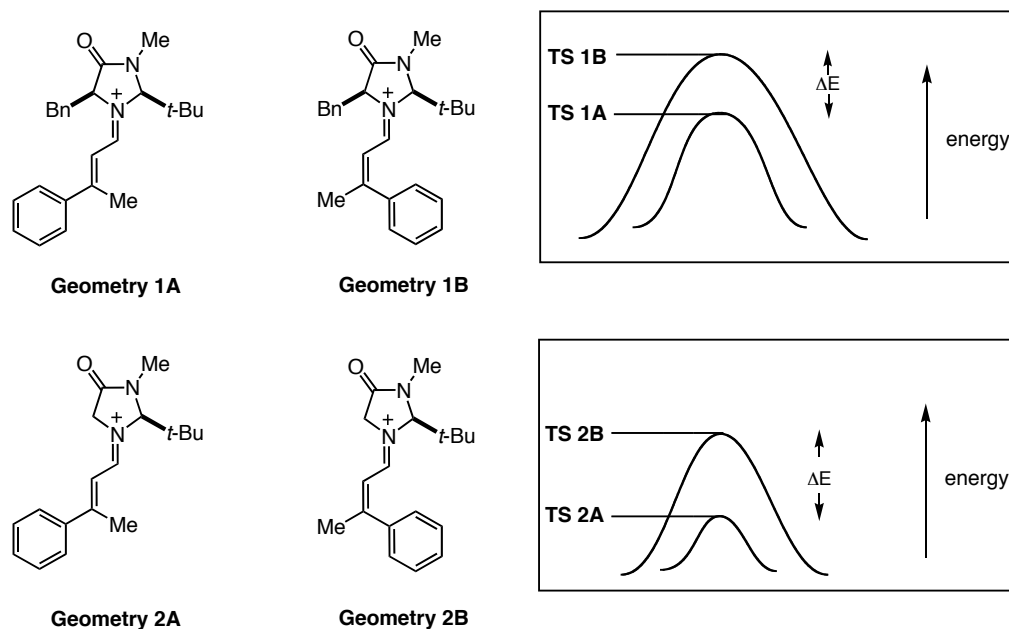
### ***Analysis of the Catalyst: Rationalizing the Decreased Reactivity and Selectivity***

While the effectiveness of catalyst **2** has been discussed, the decreased efficiency of catalyst **15** needs to be explained. We postulate that, in the transition state, interactions of the  $\beta$ -substituents on the substrate with the imidazolidinone may decrease the reactivity and selectivity for bis-substituted catalysts. The reason for this is based upon relative energies of the iminium intermediates and the forming sp<sup>3</sup> center created by hydride delivery in the transition state (Fig. 9). In the event, and if isomerization of the olefin occurs (*vide infra*), then two possible iminium intermediates can form using catalyst **15**, **1A/1B**—or in the case of catalyst **2**, **2A/2B**. For catalyst **15**, the overall energy of both iminium transition states are higher than catalyst **2** due to the possibility for the substrate to interact with both the benzyl and the *t*-butyl group. As a result, this increased energy may favor a competing pathway leading to a decreased yield of reduced product (Fig. 5, 82% yield). Conversely, the transition states for catalyst **2** are overall lower in energy due to the minimal catalyst/substrate interaction during sp<sup>3</sup> bond formation. In this case, the decrease in energy favors the desired reaction pathway resulting in an increased overall yield of reduced product (Fig. 5, 91% yield).

The observed selectivity difference can also be described in terms of transition state energies. For catalyst **15**, the interaction of both geometrical isomers with the benzyl and *t*-butyl moieties may only have a small  $\Delta E$  between the two transition states

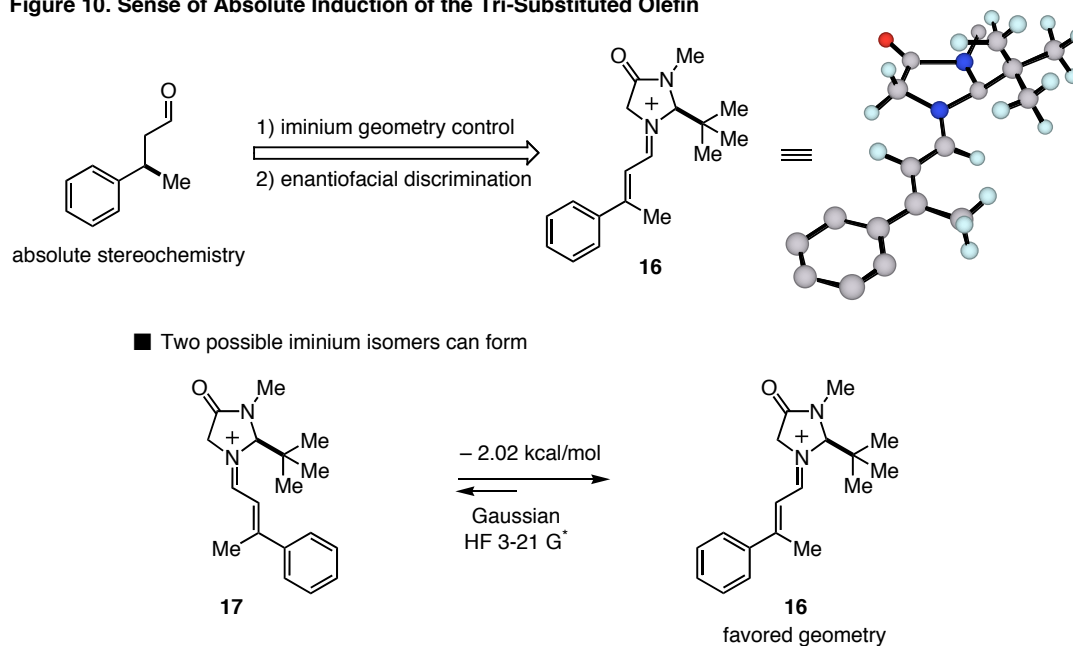
**1A** and **1B**, causing the decrease in enantioselectivity (Fig. 5, 76% ee). Conversely, for catalyst **2**, the  $\Delta E$  difference between transition state **2B** and **2A** may be large, favoring the reduction of isomer **2A**, resulting in an increased ee (Fig. 5, 93% ee)

**Figure 9. Rationalizing the Reactivity and Selectivity Differences**



### ***Absolute Sense of Enantioinduction***

By comparison to a known compound, we assigned our absolute stereochemistry as the (*R*)-enantiomer. The sense of enantio-induction is consistent with the proposed requirements for stereocontrol, namely, iminium ion geometry control and enantiofacial discrimination (Fig. 10). Gaussian modeling of these two iminium intermediates indicated a 2.02 kcal/mol energy difference in favor of iminium **16**, providing further support that imidazolidinone catalysts effectively favor the *s-trans* geometry.

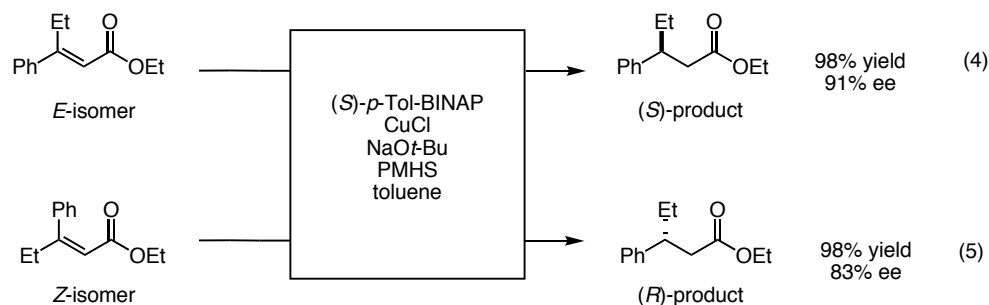
**Figure 10. Sense of Absolute Induction of the Tri-Substituted Olefin**

### *Assessing the Effect of Olefin Geometry*

Most hydrogenation technologies used in conjunction with tri-substituted olefins are dependent on the distribution of geometrical isomers. For example, subjecting pure *E*-olefin to Buchwald's enantioselective catalytic copper hydride conditions provides the (*S*)-product in high yield and good ee (eq. 4).<sup>14</sup> Conversely, reacting pure *Z*-olefin to the exact conditions provides the (*R*)-product (eq. 5). Taken together, a 1:1 mixture of geometrical isomers will produce nearly racemic product. These results indicate transition-metal hydrogenation technologies are limited to using pure olefin isomers to access highly enantioenriched products. In this context, we sought to understand how olefin geometry would impact organocatalytic hydrogenation.

(14) Appella, D. H.; Moritani, Y.; Shintani, R.; Ferreira, E. M.; Buchwald, S. L. *J. Am. Chem. Soc.* **1999**, *121*, 9473-9474.

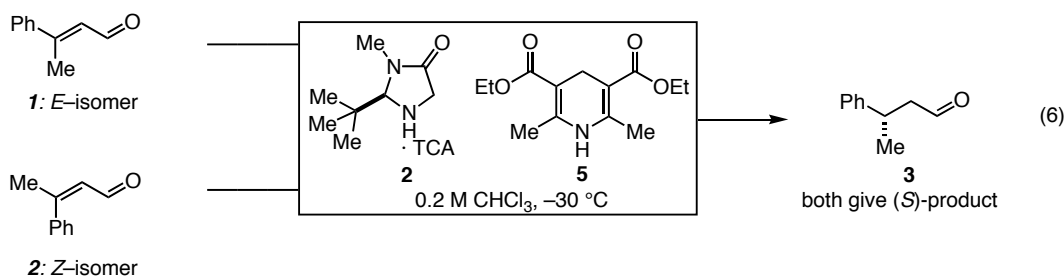




■ 1:1 Mixtures of *E* and *Z*-isomers provide racemic product

To assess this effect, pure *Z*-olefin **18** and pure *E*-olefin **1** were subjected to the same organocatalytic conditions (eq. 6). To our great delight both reactions produced the *same* (*S*)-enantiomer of product **3**.

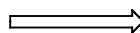
■ Pure *E* and pure *Z*-isomers provide the *same* enantiomer



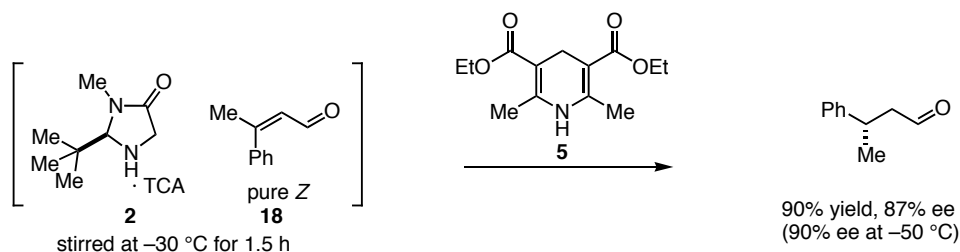
Furthermore, subjecting mixtures of geometrical isomers to EOHR produced a trend of higher ee's as the ratio of *E*-isomer to *Z*-isomer increases (Fig. 11). These results show the organocatalytic reduction is more stereoselective and not *stereospecific* like transition-metal mediated reactions. Interestingly, the product ee is increased after “aging” a solution of *Z*-isomer **18** with catalyst **2**•TCA for 1.5 hours, followed by addition of dihydropyridine **5**, and is further improved by cooling down the solution to  $-50^\circ\text{C}$ .

**Figure 11. Evaluating the Effects of Olefin Mixtures on Enantioselectivity**

ratio ( <i>E/Z</i> )	( <i>S</i> )
100 / 0	93% ee
80 / 20	91% ee
50 / 50	89% ee
20 / 80	86% ee
0 / 100	84% ee

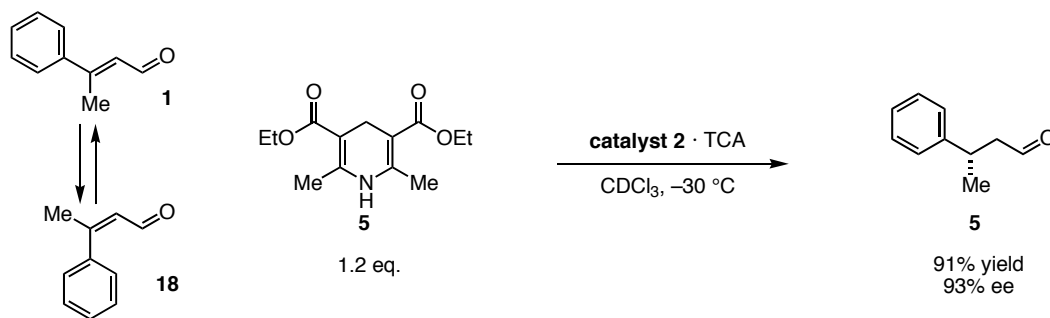
*Enantioselective not Enantiospecific*

■ Pre-equilibrating the amine catalyst and the *Z* aldehyde

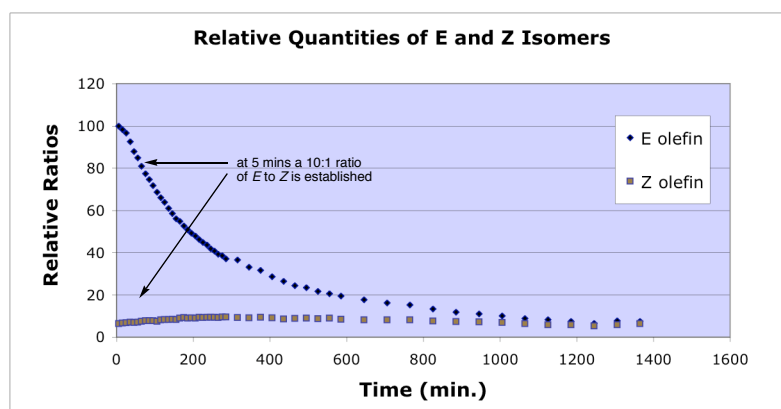


A VT-NMR experiment was utilized to probe this phenomenon. *E*-isomer **1** was added to a homogeneous solution of catalyst **2**•TCA salt in  $\text{CDCl}_3$  cooled to  $-30\text{ }^{\circ}\text{C}$  and monitored over time (Fig. 12). Interestingly, a rapid isomerization event produced a 10:1 mixture of *E*-isomer **1** to *Z*-isomer **18** in 5 minutes. This is significant because as the reaction proceeds, the relative concentration of *Z*-olefin **18** remains steady, while *E*-olefin **1** is selectively consumed, producing (*S*)-enantiomer **3**. Importantly, as the reaction proceeds and **1** is reduced, more **18** is isomerized to **1** in order to maintain this equilibrium. This dynamic kinetic resolution is the basis for the high ee and, to our delight, indicates this hydrogenation method can accommodate mixtures of geometrical isomers. It is a powerful complement to many of the current methods that access tri-substituted alkenes, such as Horner-Wadsworth-Emmons reactions and olefin metathesis, because the resulting mixtures of geometrical isomers will only have a small impact on product enantioselectivity.

Figure 12. Results of a VT-NMR Experiment



■ *E* olefin reacts more rapidly than the *Z* olefin

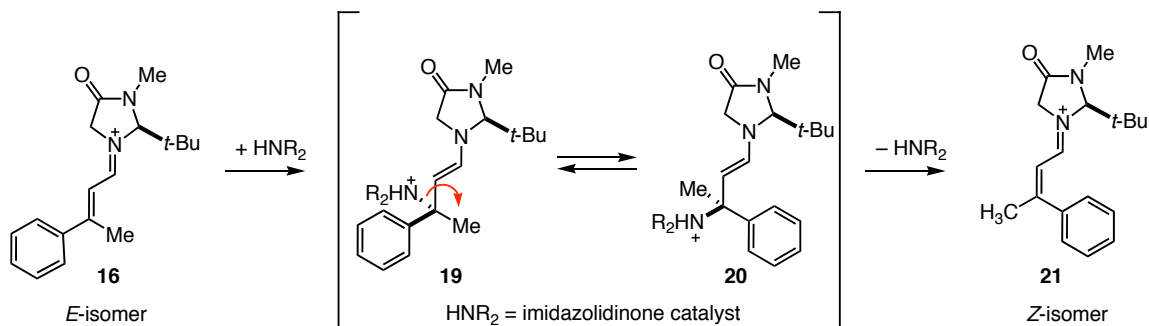


Experimental observations provide insight into the cause of isomerization. This event is most likely caused by the imidazolidinone catalyst as it occurs in the absence of acid co-catalyst. Two plausible mechanisms may be at work (Fig. 13). One may be a Bayliss-Hillman-type addition elimination mediated isomerization. In the event, conjugate addition of catalyst to iminium **16** provides intermediate **19** that undergoes sigma bond rotation leading to **20**. Species **20** eliminates the amine to provide *Z*-isomer **21**. The second possible mechanism may be attributed to Brønsted acid-base chemistry. Iminium **16** could be deprotonated to provide diene **22**, which undergoes sigma-bond rotation to form diene **23**. Finally, diene **23** is re-protonated to furnish *Z*-isomer **21**.

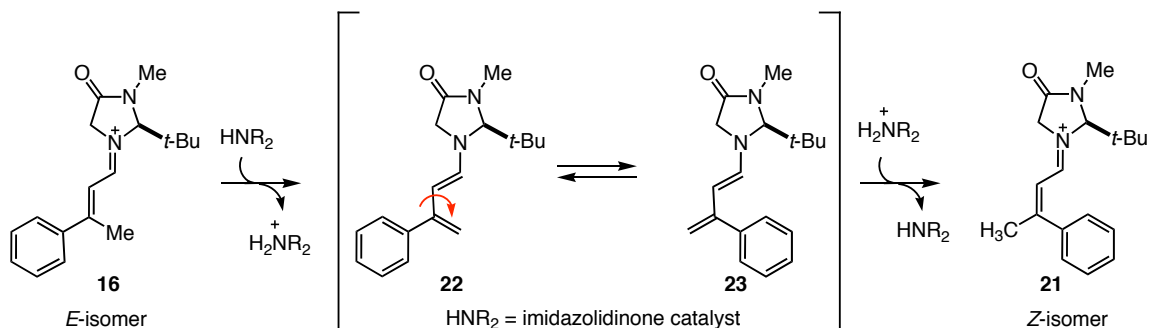
Mechanistic work to discriminate between these two modes of isomerization has yet to be performed.

**Figure 13. Proposed Isomerization Mechanisms**

■ Bayliss-Hillman type addition/elimination



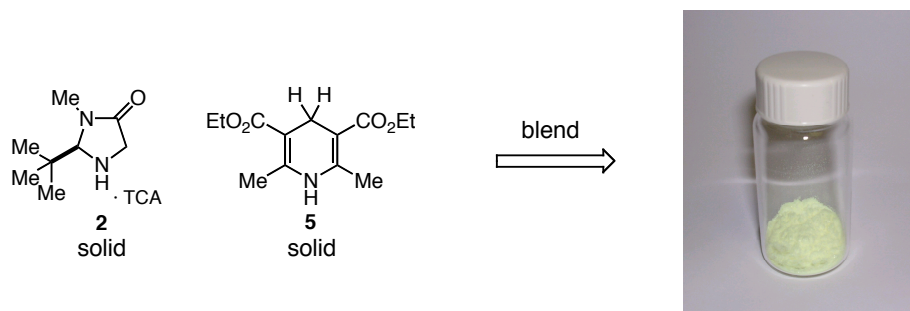
■ A deprotonation/reprotonation event



### *Developing a Facile Use of This Methodology*

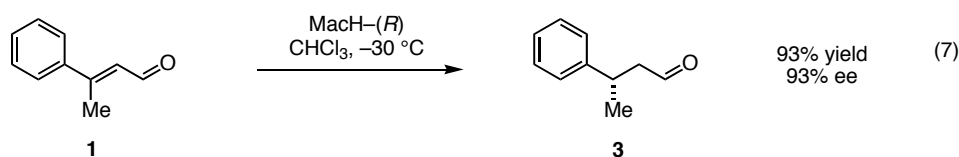
Our next goal was to develop this methodology into a single reagent to facilitate a greater ease-of-use reaction platform. This was achieved by milling together the Hantzsch dihydropyridine **5** (solid) with catalyst **2**•TCA salt (solid) in a 6:1 ratio (Fig. 14). The resulting reagent was termed Mixture for Asymmetric Catalytic Hydrogenation

**Figure 14. Mixture for Asymmetric Catalytic Hydrogenation: Mach-(R)**



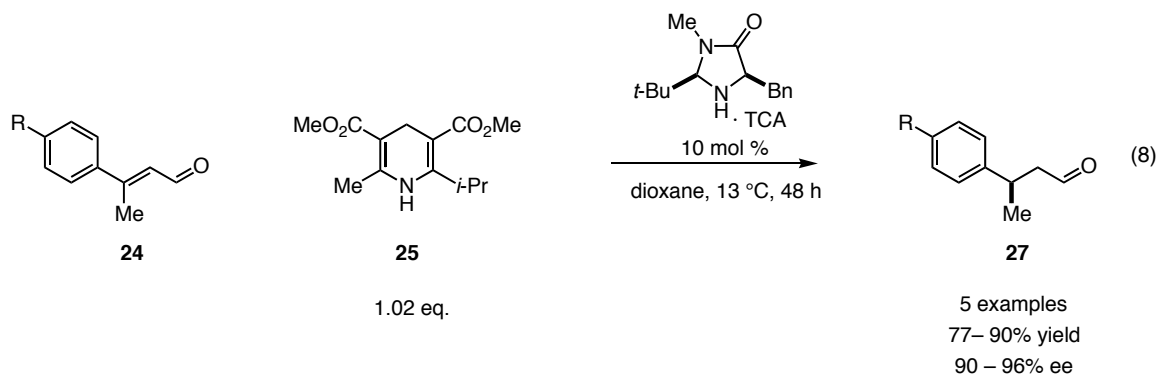
and is commercially available as the mnemonic MacH-(*R*). Gratifyingly, even after 16 months of storage at 0 °C, MacH-(*R*) reduced substrate **1** to provide **3** in good yield and good ee (eq. 7). This stability study indicates the reagent can be stored for long periods of time without any noticeable degradation.

■ Asymmetric transfer hydrogenation using MacH (after 16 months storage at 0 °C)



### Related Work

Around the time we reported our enantioselective catalytic hydrogenation technology, the List Group reported a similar methodology (eq. 8).<sup>15</sup> In this work, a range



(15) Yang, J. W.; Fonseca, M. T. H.; Vignola, N.; List, B. *Angew. Chem. Int. Ed.* **2005**, *44*, 108-110.

of para-substituted  $\alpha,\beta$ -unsaturated aldehydes **24** are reduced using non-symmetrical Hantzsch **25** and the MacMillan 2<sup>nd</sup> generation imidazolidinone catalyst to provide general product **27** in good yields and good ee's. Other extensions of this reduction platform include tandem catalysis<sup>16</sup> and total synthesis.<sup>17</sup>

### Conclusions

In summary we have documented the development of a new hydrogenation technology applied to the LUMO-lowering activation of  $\alpha,\beta$ -unsaturated aldehydes. This work demonstrates the generality of the organocatalytic approach to LUMO-lowering catalysis. Future extension of this work will focus on broadening both the substrate and reaction scope of this new process, as well as its extension into new tandem catalysis processes.

---

(16) (a) Huang, Y.; Walji, A. M.; Larsen, C. H.; MacMillan, D. W. C. *J. Am. Chem. Soc.* **2005**, *127*, 15051-15053. (b) Walji, A. M.; MacMillan, D. W. C. *Synlett* **2007**, 1477-1489.

(17) de Figueiredo, R. M.; Berner, R.; Julis, J.; Liu, T.; Tuerp, D.; Christmann, M. *J. Org. Chem.* **2007**, *72*, 640-642.

## Supporting Information

**General Information.** Commercial reagents were purified prior to use following the guidelines of Perrin and Armarego.<sup>1</sup> Non-aqueous reagents were transferred under nitrogen via syringe or cannula and purified according to the method of Grubbs.<sup>2</sup> Organic solutions were concentrated under reduced pressure on a Büchi rotary evaporator. Chromatographic purification of products was accomplished using forced-flow chromatography on ICN 60 32-64 mesh silica gel and Iatrobeads<sup>®</sup> according to the method of Still.<sup>3</sup> Thin-layer chromatography (TLC) was performed on EM Reagents 0.25 mm silica gel 60-F plates. Chromatograms were visualized by fluorescence quenching or by staining using either potassium permanganate or anisaldehyde stain.

<sup>1</sup>H and <sup>13</sup>C NMR spectra were recorded on a Varian Mercury 300 Spectrometer, and are internally referenced to residual solvent signals. Data for <sup>1</sup>H NMR are reported as follows: chemical shift (δ ppm), multiplicity (s = singlet, d = doublet, t = triplet, q = quartet, m = multiplet), integration, coupling constant (Hz) and assignment. Data for <sup>13</sup>C NMR are reported in terms of chemical shift. IR spectra were recorded on a Perkin Elmer Paragon 1000 spectrometer and are reported in terms of frequency of absorption (cm<sup>-1</sup>). Mass spectra were obtained from the Caltech Mass Spectroscopy Facility by electron ionization, chemical ionization, or fast atom/ion bombardment techniques. Gas liquid chromatography (GLC) was performed on Hewlett-Packard 6850 and 6890 Series gas chromatographs equipped with a split-mode capillary injection system and flame ionization detectors using a Bodman Chiraldex b-DM (30 m × 0.25 mm), a Bodman

---

(1) Perrin, D. D. A., W. L. F. *Purification of Laboratory Chemicals*, 3rd ed.; Pergamon Press: Of, 1988.

(2) Pangborn, A. B.; Giardello, M. A.; Grubbs, R. H.; Rosen, R. K.; Timmers, F. J. *Organometallics* **1996**, *15*, 1518-1520.

(3) Still, W. C.; Kahn, M.; Mitra, A. *J. Org. Chem.* **1978**, *43*, 2923-2925.

Chiraldex  $\Gamma$ -TA (30 m  $\times$  0.25 mm), or a Hydrodex-B-TBDAC (50 m  $\times$  0.25 mm) column as noted. High-performance liquid chromatography (HPLC) was performed on Hewlett-Packard 1100 Series chromatographs using a Chiralcel OD-H column (25 cm) and OD-H guard (5 cm). Optical rotations were measured on a Jasco P-1010 polarimeter, and  $[\alpha]_D$  values are reported in  $10^{-1} \text{ dg cm}^2 \text{ g}^{-1}$ ; concentration (c) is in g/100 mL.

### Preparation of the starting materials

The following  $\alpha,\beta$ -unsaturated aldehydes have already been described in the literature:

(*E*)-3-phenylbut-2-enal,<sup>4</sup> (*E*)-3-phenylpent-2-enal,<sup>5</sup> (*E*)-methyl 3-formyl-2-methylacrylate.<sup>6</sup>

**Diethyl-1,4-dihydro-2,6dimethylpyridine-3,5-dicarboxylate:** A modified procedure from a reported method.<sup>7</sup> In a beaker, a solid suspension of neat ammonium acetate (20.7 g, 268 mmol, 1.25 eq.), hexamethylenetetramine (30 g, 214 mmol, 1.0 eq.), and ethyl acetoacetate (69.6 g, 535 mmol, 2.5 eq.) was heated in a conventional microwave on “high” power 2 x 35 seconds, with gentle swirling in between cycles. After the second heating phase and, upon cooling, a solid rapidly forms. After cooling, the solid was triturated with absolute ethanol (4 x 150 mL) and 5% water ethanol solution (2 x 100 mL) and dried on high vacuum to provide a light green solid that matched the reported characterization data.

---

(4) Gandhi, R. P. W., J. S.; Mukherji, S. M. *J. Ind. Chem. Soc.* **1957**, *34*, 509.

(5) Schreiber, W. L.; Pittet, A. O.; Vock, M. H. *J. Agr. Food Chem.* **1974**, *22*, 269.

(6) Ishida, A.; Mukaiyama, T. *Bull. Chem. Soc. Jap.* **1978**, *51*, 2077.

(7) Eynde, J. J. V.; Mayence, A. *Molecules* **2003**, *8*, 381-391.



**Resolution of 2-*tert*-butyl-3-methylimidazolidin-4-one:** The imidazolidinone was synthesized according to a Seebach method.<sup>8</sup> Dissolve 30 g of racemic imidazolidinone and 15 g of *R*-mandelic acid into ~25 mL of reagent grade acetone and GENTLY heat until homogenous (do not boil as ee will drop). The resulting solution was cooled to room-temperature and then placed in a freezer for 12 hours to produce a light yellow solid. Afterwards, wash the solid three times with ice-cold acetone (35 mL) and two times with room temperature ether (30 mL) to isolate 15 g of a white solid. Depending on the scale, another re-crystallization/wash sequence may be necessary. The resulting white solid (6 g) was free based with 3 N NaOH (100 mL), and the aqueous layer was extracted three times with methylene chloride (100 mL). The organic layer was dried over Na<sub>2</sub>SO<sub>4</sub>, filtered, and concentrated to produce a clear oil (5.0 g). A small portion (10 mg) was put aside. The rest of the batch was dissolved in a 2:1 Et<sub>2</sub>O:pentane solution (50 mL). To this was added dropwise, with swirling, a solution of TCA (5.2 g) dissolved in a 2:1 Et<sub>2</sub>O:pentane solution (20 mL). Crystallization begins at room temperature and is continued at 0 °C for 2–3 hours. The crystals were filtered off and washed three times in ice cold 2:1 Et<sub>2</sub>O:pentane solution then dried on high vacuum to produce a white solid (6.2 g). The solid should be stored at 4 °C as it seems to oil out after 6 months at room temperature.

**Determining ee:** The 10 mg aliquot was BOC protected with 1 eq. triethylamine and 1 eq. di-*tert*-butyldicarbonate by shaking the components in a vial with ethylacetate for about 5–10 minutes, quenching in water, and then injecting a small aliquot of the organic phase onto an achiral GC.

---

(8) Fitzi, R.; Seebach, D. *Angew. Chem. Int. Ed. Eng.* **1986**, 25, 345-346.

The enantiomeric ratio was determined by GLC using a B-DM ChiralDEX (50 m  $\times$  0.25 mm) column (155 °C isotherm, 1 mL/min.); (*R*) isomer  $t_r$  = 19.2 min. and (*S*) isomer  $t_r$  = 20.1 min. (Here, the *S* isomer is the major enantiomer because the BOC group changes the Cahn-Ingold-Prelog prioritization.)

**(*E*)-3-(3,4-dichlorophenyl)-*N*-methoxy-*N*-methylbut-2-enamide:** To a solution of sodium metal (1.05 g, 45.9 mmol), dissolved in EtOH (32 mL) and cooled to 0 °C, was added diethyl (*N*-methoxy-*N*-methylcarbamoylmethyl)-phosphonate (10 g, 41.8 mmol). The resulting light yellow solution was stirred for 10 minutes. To this was added 3,4-dichloroacetophenone (7.11 g, 37.6 mmol) and the resulting solution stirred at 60 °C for approximately 2.5 hours until judged complete by TLC. The reaction mixture was concentrated *in vacuo*. The resulting residue was purified by flash chromatography (30% EtOAc/hexanes) to provide a clear oil (4.34 g, 42% yield).

IR (film) 3064, 2965, 2937, 1651, 1623, 1551, 1471, 1441, 1411, 1371, 1323, 1179, 1138, 1028, 981, 868, 821, 662, 474  $\text{cm}^{-1}$ ;  $^1\text{H}$  NMR (300 MHz,  $\text{CDCl}_3$ )  $\delta$  7.57 (d, 1H,  $J$  = 2.1 Hz,  $\text{ClC}=\text{CH}=\text{CH}$ ), 7.47 (d, 1H,  $J$  = 8.51 Hz,  $\text{ClC}=\text{CH}=\text{C}$ ), 7.33 (dd, 1H,  $J$  = 2.1, 8.24 Hz,  $\text{ClC}=\text{CH}=\text{CH}$ ), 6.56 (bs, 1H,  $\text{CH}_3\text{C}=\text{CH}$ ), 3.74 (s, 3H,  $\text{NOCH}_3$ ), 3.30 (s, 3H,  $\text{NCH}_3$ ), 2.50 (d, 3H,  $J$  = 1.33 Hz,  $\text{CH}_3$ );  $^{13}\text{C}$  NMR (75 MHz,  $\text{CDCl}_3$ )  $\delta$  171.1, 167.3, 132.9, 132.6, 130.4, 128.3, 125.6, 117.3, 61.7, 60.4, 21.1, 17.8; HRMS ( $\text{EI}^+$ ) exact mass calculated for  $[\text{M}]^+$  ( $\text{C}_{10}\text{H}_{16}\text{OCl}_2$ ) requires  $m/z$  273.0323, found  $m/z$  273.0317.

**(*E*)-3-(3,4-dichlorophenyl)but-2-enal:** To a solution of (*E*)-3-(3,4-dichlorophenyl)-*N*-methoxy-*N*-methylbut-2-enamide (800 mg, 2.92 mmol) in  $\text{CH}_2\text{Cl}_2$  (15 mL), cooled to  $-78$

°C in a dry ice/acetone bath, was added DIBALH (3.07 mmol, 0.547 mL). After 3.5 hours, THF was added and the reaction mixture was warmed to room temperature. The viscous solution was poured into 100 mL of a saturated solution of potassium sodium tartrate and stirred for 15 minutes. The organic layer was separated and the aqueous layer was extracted with 100 mL of CH<sub>2</sub>Cl<sub>2</sub> (3×). The organic layers were dried over Na<sub>2</sub>SO<sub>4</sub>, filtered, and concentrated *in vacuo*. The residue was purified by flash chromatography (5% EtOAc/hexanes) and triturated with pentanes to afford the title compound as a colorless oil (160 mg, 25% yield).

IR (film) 3285, 3089, 2963, 2886, 1653, 1616, 1548, 1474, 1444, 1389, 1324, 1279, 1242, 1148, 1137, 1071, 1028, 954, 898, 865, 828, 698, 536 cm<sup>-1</sup>; <sup>1</sup>H NMR (300 MHz, CDCl<sub>3</sub>)  $\delta$  11.9 (d, 1H, *J* = 7.71 Hz CHO), 7.65 (d, 1H, *J* = 2.13 Hz, ClC=CH=CH), 7.52 (d, 1H, *J* = 8.51 Hz, ClC=CH=C), 7.40 (dd, 1H, *J* = 2.13, 8.24 Hz, ClC=CH=CH), 6.38 (dd, 1H, *J* = 1.06, 7.74 Hz CHCHO), 2.57 (d, 3H, *J* = 1.06, CH<sub>3</sub>); <sup>13</sup>C NMR (75 MHz, CDCl<sub>3</sub>)  $\delta$  190.8, 154.5, 140.5, 134.2, 130.8, 128.2, 128.0, 125.4, 65.9, 16.3; HRMS (EI<sup>+</sup>) exact mass calculated for [M]<sup>+</sup> (C<sub>10</sub>H<sub>8</sub>OCl<sub>2</sub>) requires *m/z* 213.9952, found *m/z* 213.9950.

**(*E*)-3-cyclohexylbut-2-en-1-ol:** To a 0 °C solution of (*E*)-ethyl 3-cyclohexylbut-2-enoate<sup>9</sup> (1 g, 5.09 mmol) in dry Et<sub>2</sub>O (10 mL) was added a solution of lithium aluminum hydride (5.10 mL, 5.10 mmol, 1 M in Et<sub>2</sub>O). After 5 minutes, the reaction mixture was neutralized by dropwise addition of THF solution followed by addition of a saturated solution of potassium sodium tartrate. The reaction mixture was stirred for 25 minutes, then diluted with Et<sub>2</sub>O. The organic layer was separated and washed with water, dried

(9) Appella, D. H. Y., M.; Shantini, R.; Ferreira, E. M.; Buchwald, S. M. *J. Am. Chem. Soc.* **1999**, *121*, 9473.

over Na<sub>2</sub>SO<sub>4</sub>, and concentrated *in vacuo* to afford (*E*)-3-cyclohexylbut-2-en-1-ol as a colorless oil which was used directly in the following reaction.

**(*E*)-3-cyclohexylbut-2-enal:** To a solution of (*E*)-3-cyclohexylbut-2-enol (700 mg, 4.54 mmol) in dichloromethane (11 mL), cooled to 0 °C, was added Dess-Martin periodinane (2.11 g, 4.99 mmol). The resulting suspension was warmed to 23 °C and stirred for approximately 30 minutes until the reaction was judged to be complete by TLC. The reaction mixture was poured into 50 mL of saturated aqueous NaHCO<sub>3</sub> containing Na<sub>2</sub>S<sub>2</sub>O<sub>3</sub> (1 g). This mixture was stirred vigorously until both layers became clear. The aqueous layer was extracted with 50 mL of CH<sub>2</sub>Cl<sub>2</sub> (2×) and the combined organic layers were dried over MgSO<sub>4</sub>, filtered, and concentrated *in vacuo*. The residue was purified by flash chromatography (25% EtOAc/hexanes) to afford the title compound as a colorless oil (350 mg, 51% yield) that was a 5.2:1 mixture of *E*:*Z* isomers. Major isomer: IR (film) 2929, 2854, 1729, 1674, 1640, 1450, 1383, 1198, 1164, 894, 850, 522 cm<sup>-1</sup>; <sup>1</sup>H NMR (300 MHz, CDCl<sub>3</sub>)  $\delta$  10.5 (d, 1H, *J* = 7.9 Hz CHO), 5.90 (dq, 1H, *J* = 1.1, 7.9 Hz, C=CH), 2.18 (d, 3H, *J* = 1.3 Hz, CH<sub>3</sub>), 2.09 – 2.02 (m, 1H, CH<sub>2</sub>CHCH<sub>2</sub>), 1.87 – 1.70 (m, 5H), 1.40 (m, 5H); <sup>13</sup>C NMR (75 MHz, CDCl<sub>3</sub>)  $\delta$  191.9, 168.8, 125.8, 48.4, 31.4, 31.2, 26.3, 26.1, 26.0, 16.1; HRMS (EI<sup>+</sup>) exact mass calculated for [M]<sup>+</sup> (C<sub>10</sub>H<sub>16</sub>O) requires *m/z* 152.1201, found *m/z* 152.1205.

**(*E*)-ethyl 3-cyclohexylpent-2-enoate:** To 90 mL of EtOH, cooled to 0 °C in an ice bath, was added sodium metal (1.64 g, 71.3 mmol). Once the metal had completely dissolved, triethyl phosphonoacetate (15.9 g, 14.1 mL, 71.3 mmol) was added via syringe. The

resulting solution was warmed to room temperature and stirred for 10 minutes. Cyclohexyl ethyl ketone (9.44 g, 9.20 mL, 67.3 mmol) was added and the solution stirred for 15 hours at room temperature. The reaction was quenched in 100 mL ice water slurry. The aqueous layer was extracted with 200 mL of Et<sub>2</sub>O (3×). The combined organic layers were washed with 400 mL of brine, dried over Na<sub>2</sub>SO<sub>4</sub>, filtered, and concentrated *in vacuo*. The product was purified by flash chromatography (1% Et<sub>2</sub>O/pentane) to provide a clear oil (2.5 g, 18% yield) that was a 3:1 mixture of *E*:*Z* isomers. Major isomer: IR (film) 2977, 2929, 2854, 2360, 2341, 1716, 1638, 1448, 1203, 1147, 1042, 862, 750 cm<sup>-1</sup>; <sup>1</sup>H NMR (300 MHz, CDCl<sub>3</sub>)  $\delta$  5.58 (s, 1H, C=CH), 4.15 (q, 2H, *J* = 4.1 Hz, OCH<sub>2</sub>CH<sub>3</sub>), 2.58 (q, 2H, *J* = 7.4 Hz, CH<sub>2</sub>CH<sub>3</sub>), 1.81 – 1.62 (m, 5H), 1.35 – 1.11 (m, 9H), 1.06 (t, 3H, *J* = 2.2 Hz, CH<sub>2</sub>CH<sub>3</sub>); <sup>13</sup>C NMR (75 MHz, CDCl<sub>3</sub>)  $\delta$  171.3, 113.4, 59.6, 46.8, 32.3, 31.2, 26.9, 26.8, 26.6, 26.3, 25.3, 14.5, 13.8; HRMS (EI<sup>+</sup>) exact mass calculated for [M]<sup>+</sup> (C<sub>13</sub>H<sub>22</sub>O<sub>2</sub>) requires *m/z* 210.1620, found *m/z* 210.1628.

**(*E*)-3-cyclohexylpent-2-enol:** To a solution of (*E*)-ethyl 3-cyclohexylpent-2-enoate (2.3 g, 10.9 mmol) in Et<sub>2</sub>O (22 mL), was added lithium aluminum hydride (1.0 M in Et<sub>2</sub>O, 10.9 mL, 10.9 mmol) dropwise. After 5 minutes, the reaction mixture was slowly quenched with 1 mL of MeOH and poured into 100 mL of a saturated solution of potassium sodium tartrate. The aqueous layer was extracted with 100 mL of Et<sub>2</sub>O (3×). The combined organics were dried over Na<sub>2</sub>SO<sub>4</sub>, filtered, and concentrated. The product was purified by flash chromatography (10% EtOAc/hexanes) to provide a clear oil (1.59 g, 87% yield) that was a 3:1 mixture of *E*:*Z* isomers. Major isomer: IR (film) 3421,

2929, 2854, 1732, 1684, 1635, 1449, 1235, 1164, 864, 749  $\text{cm}^{-1}$ ;  $^1\text{H}$  NMR (300 MHz,  $\text{CDCl}_3$ )  $\delta$  5.33 (t, 1H,  $J = 6.7$  Hz,  $\text{CHCH}_2\text{OH}$ ), 4.17 (d, 2H,  $J = 6.9$  Hz,  $\text{CH}_2\text{OH}$ ), 2.07 (q, 2H,  $J = 7.4$  Hz,  $\text{CH}_2\text{CH}_3$ ), 1.99 – 1.63 (m, 6H), 1.48 – 1.08 (m, 6H), 0.97 (t, 3H,  $J = 7.4$  Hz,  $\text{CH}_2\text{CH}_3$ );  $^{13}\text{C}$  NMR (75 MHz,  $\text{CDCl}_3$ )  $\delta$  151.1, 121.2, 59.4, 44.8, 32.6, 31.6, 26.9, 26.7, 26.4, 23.1, 14.7; HRMS ( $\text{EI}^+$ ) exact mass calculated for  $[\text{M}]^+$  ( $\text{C}_{11}\text{H}_{20}\text{O}$ ) requires  $m/z$  168.1514, found  $m/z$  168.1520.

**(*E*)-3-cyclohexylpent-2-enal:** To a solution of (*E*)-3-cyclohexylpent-2-enol (1.50 g, 8.91 mmol) in dichloromethane (45 mL), cooled to 0 °C, was added Dess-Martin periodinane (9.7 g, 22.9 mmol). The resulting suspension was warmed to room temperature and stirred for approximately 2 hours until the reaction was judged to be complete by TLC. The reaction was poured into 100 mL of saturated aqueous  $\text{NaHCO}_3$  containing  $\text{Na}_2\text{S}_2\text{O}_3$  (3 g). This mixture was stirred vigorously until both layers became clear. The aqueous layer was extracted with  $\text{CH}_2\text{Cl}_2$  (2 $\times$ ) and the combined organic layers were dried over  $\text{MgSO}_4$ , filtered and concentrated *in vacuo*. The residue was purified by flash chromatography (5%  $\text{Et}_2\text{O}$ /pentane) to afford the title compound (1 g, 68% yield) as a colorless oil that was a 3:1 mixture of *E*:*Z* isomers. Major isomer: IR (film) 2927, 2746, 1668, 1622, 1450, 1189, 1124, 860  $\text{cm}^{-1}$ ;  $^1\text{H}$  NMR (300 MHz,  $\text{CDCl}_3$ )  $\delta$  10.04 (d, 1H,  $J = 8.24$  Hz,  $\text{CHO}$ ), 5.83 (d, 1H,  $J = 8.24$  Hz,  $\text{C}=\text{CH}$ ), 2.61 (q, 2H,  $J = 7.4$  Hz,  $\text{CH}_2\text{CH}_3$ ), 2.07 (tt, 1H,  $J = 2.6, 11.0$  Hz,  $\text{CH}_2\text{CHCH}_2$ ), 1.88 – 1.71 (m, 5H), 1.41 – 1.15 (m, 8H);  $^{13}\text{C}$  NMR (75 MHz,  $\text{CDCl}_3$ )  $\delta$  191.8, 175.2, 124.9, 46.2, 31.9, 26.5, 26.3, 26.0, 25.9, 24.2, 15.4; HRMS ( $\text{EI}^+$ ) exact mass calculated for  $[\text{M}]^+$  ( $\text{C}_{11}\text{H}_{18}\text{O}$ ) requires  $m/z$  166.1358, found  $m/z$  166.1355.

**(E)-ethyl-4-[tris-(1-methylethyl)silyloxy]-3-methylbut-2-enoate:** To a suspension of sodium hydride (60% dispersion in mineral oil, 1.58 g, 62.6 mmol) in dry toluene (500 mL) at 0 °C was added, dropwise, triethyl phosphonoacetate (12.4 mL, 62.6 mmol) under an atmosphere of argon. After 30 minutes, 1-[tris-(1-methylethyl)silyloxy]-pentanone (12 g, 52.2 mmol) was diluted into toluene (25 mL) and added to the reaction mixture, which was then allowed to warm to room temperature over a period of 2 hours. The resulting mixture was washed with water, dried over MgSO<sub>4</sub> and concentrated *in vacuo*. The residue was purified by flash chromatography (3% Et<sub>2</sub>O/pentane) to afford (E)-ethyl 4-[tris-(1-methylethyl)silyloxy]-3-methylbut-2-enoate as a colorless oil (10.5 g, 67% yield). Major isomer: IR (film) 2945, 2868, 1716, 1663, 1223, 1154, 1114 cm<sup>-1</sup>; <sup>1</sup>H NMR (300 MHz, CDCl<sub>3</sub>)  $\delta$  6.07 (bs, 1H, CH), 4.21 (s, 2H, CH<sub>2</sub>OTIPS), 4.17 (q, 2H, *J* = 6.9 Hz, CH<sub>3</sub>CH<sub>2</sub>O), 2.06 (s, 3H, CCH<sub>3</sub>), 1.29 (t, 3H, *J* = 7.8 Hz, CH<sub>3</sub>CH<sub>2</sub>O), 1.09 (m, 21H, TIPS); <sup>13</sup>C NMR (75 MHz, CDCl<sub>3</sub>)  $\delta$  167.0, 157.0, 113.2, 67.2, 59.4, 17.9, 15.3, 14.3, 11.9; HRMS (EI<sup>+</sup>) exact mass calculated for [M]<sup>+</sup> (C<sub>16</sub>H<sub>32</sub>O<sub>3</sub>Si) requires *m/z* 300.2121, found *m/z* 300.2125.

**(E)-3-[tris-(1-methylethyl)silyloxy]but-2-en-1-ol:** To a 0 °C solution of (E)-ethyl 4-[tris-(1-methylethyl)silyloxy]-3-methylbut-2-enoate (5 g, 17.6 mmol) in dry Et<sub>2</sub>O was added a solution of lithium aluminum hydride (17.6 mL, 17.6 mmol, 1 M in Et<sub>2</sub>O). After 30 minutes, the reaction mixture was neutralized by dropwise addition of THF followed by addition of a saturated solution of potassium sodium tartrate. The reaction mixture was stirred overnight and then diluted with Et<sub>2</sub>O. The organic layer was separated and

washed with water, dried over  $\text{MgSO}_4$ , and concentrated *in vacuo* to afford (*E*)-3-[tris-(1-methylethyl)silyloxy]but-2-en-1-ol as a colorless oil which was used directly in the next reaction.

**(*E*)-3-[tris-(1-methylethyl)silyloxymethyl]but-2-enal:** To a room-temperature solution of (*E*)-3-[tris-(1-methylethyl)silyloxy]but-2-en-1-ol (crude from the previous step, assumed 17.6 mmol) in dichloromethane (100 mL) was added Dess-Martin periodinane (9.7 g, 22.9 mmol). The resulting suspension was stirred for 60 minutes, until the reaction was judged to be complete by TLC. The reaction mixture was diluted with  $\text{Et}_2\text{O}$  and a saturated aqueous solution of  $\text{NaHCO}_3$  containing  $\text{Na}_2\text{S}_2\text{O}_3$  was added. This mixture was stirred vigorously until both layers became clear. The aqueous layer was extracted with 100 mL of  $\text{CH}_2\text{Cl}_2$  (2 $\times$ ) and the combined organic layers were dried over  $\text{MgSO}_4$ , filtered, and concentrated *in vacuo*. The residue was purified by flash chromatography (5%  $\text{Et}_2\text{O}$ /pentane) to afford the title compound as a colorless oil (3.69 g, 82% yield). IR (film) 2944, 2867, 1681, 1464, 1384, 1123  $\text{cm}^{-1}$ ;  $^1\text{H}$  NMR (300 MHz,  $\text{CDCl}_3$ )  $\delta$  10.09 (d, 1H,  $J$  = 8.3 Hz, CHO), 6.28 (dd, 1H,  $J$  = 1.5, 8.4 Hz, CH), 4.28 (d, 2H,  $J$  = 0.9 Hz,  $\text{CH}_2\text{OTIPS}$ ), 2.09 (d, 3H,  $J$  = 0.6 Hz,  $\text{CH}_3\text{C}$ ), 1.1 – 1.0 (m, 21H, TIPS);  $^{13}\text{C}$  NMR (75 MHz,  $\text{CDCl}_3$ )  $\delta$  191.2, 161.6, 124.1, 67.0, 18.0, 14.1, 11.9; HRMS ( $\text{EI}^+$ ) exact mass calculated for  $[\text{M}]^+$  ( $\text{C}_{14}\text{H}_{28}\text{O}_2\text{Si}$ ) requires  $m/z$  256.1859, found  $m/z$  256.1862.

**General Procedure for the enantioselective hydrogenation of enal:** A colorless solution of (*E*)-3-phenylbut-2-enal (140 mg, 1 mmol) dissolved in 5 mL of chloroform



(0.2 M) was cooled to  $-30\text{ }^{\circ}\text{C}$  in a dry ice/acetone bath. To this solution was added the trichloroacetic acid salt of (*R*)-2-*tert*-butyl-3-methylimidazolidin-4-one (64 mg, 0.2 mmol) and Hantzsch ester (304 mg, 1.2 mmol). The resulting yellow suspension was stirred at  $-30\text{ }^{\circ}\text{C}$  until the reaction was determined to be complete by TLC, by which time the mixture was a light yellow homogeneous solution.

Workup procedure A: The reaction mixture was then diluted with  $\text{Et}_2\text{O}$  and passed through a short pad of silica gel. The resulting solution was concentrated *in vacuo* and purified by flash chromatography (solvent noted) to provide the title compounds.

Workup procedure B: The cold reaction mixture was poured into a 10% HCl solution and diluted with  $\text{Et}_2\text{O}$ . The organic layer was washed 4 times with 10% HCl solution and once with a saturated aqueous solution of  $\text{NaHCO}_3$ . The resulting solution was dried over  $\text{MgSO}_4$  and concentrated *in vacuo*. The residue was purified by flash chromatography (solvent noted) to provide the title compounds.

**(*S*)-3-phenylbutanal:** Prepared according to the general procedure from (*E*)-3-phenylbut-2-enal (140 mg, 1 mmol) for 23 hours, using workup procedure A to provide the title compound as a colorless oil (127 mg, 91% yield, 93% ee) after purification by flash chromatography on Iatrobeads<sup>®</sup> (15 – 20%  $\text{Et}_2\text{O}$ /pentane). The physical data were identical in all respects to those previously reported.<sup>10</sup> The enantiomeric ratio was determined by GLC using a Bodman Chiraldex  $\beta$ -DM (30 m  $\times$  0.25 mm) column (90  $^{\circ}\text{C}$  isotherm, 1 mL/min.); (*R*) isomer  $t_r$  = 38.6 min. and (*S*) isomer  $t_r$  = 39.5 min.  $[\alpha]_D^{22} = +32.9^{\circ}$  ( $c$  = 1.00, EtOH).

---

(10) Bull, S. D. D., S. G.; Nicholson, R. L.; Sanganee, H. J.; Smith, A. D. *Org. Biomol. Chem.* **2003**, *1*, 2886.

**(S)-3-phenylpentanal:** Prepared according to the general procedure from (*E*)-3-phenylpent-2-enal (160 mg, 1 mmol) for 16 hours, using workup procedure A to provide the title compound as a colorless oil (119 mg, 74% yield, 94% ee) after purification by flash chromatography on Iatrobeds® (10% Et<sub>2</sub>O/pentane). The physical data were identical in all respects to those previously reported.<sup>11</sup> The enantiomeric ratio was determined by GLC using a Bodman ChiralDEX  $\beta$ -DM (30 m  $\times$  0.25 mm) column (95 °C isotherm, 1 mL/min.); (*R*) isomer  $t_r$  = 42.8 min. and (*S*) isomer  $t_r$  = 43.9 min.  $[\alpha]_D^{22}$  = +20.1° (c = 1.00, EtOH).

**(S)-3-(3,4-dichlorophenyl)butanal:** Prepared according to the general procedure from (*E*)-3-(3,4-dichlorophenyl)but-2-enal (150 mg, 0.691 mmol) for 19 hours, using workup procedure A to provide the title compound as a colorless oil (133 mg, 89% yield, 92% ee) after purification by flash chromatography on silica gel (50% CH<sub>2</sub>Cl<sub>2</sub>/pentane). The enantiomeric ratio was determined by GLC using a Bodman ChiralDEX  $\Gamma$ -TA (30 m  $\times$  0.25 mm) column (120 °C isotherm, 1 mL/min.); (*S*) isomer  $t_r$  = 42.7 min. and (*R*) isomer  $t_r$  = 44.8 min. IR (film) 2966, 2931, 2825, 2725, 1725, 1564, 1470, 1403, 1277, 1135, 1030, 882, 823, 709, 678, 596 cm<sup>-1</sup>; <sup>1</sup>H NMR (300 MHz, CDCl<sub>3</sub>)  $\delta$  9.74 (t, 1H,  $J$  = 1.09 Hz CHO), 7.40 (d, 1H,  $J$  = 8.21 Hz, ClC=CHCH), 7.34 (d, 1H,  $J$  = 2.35 Hz, ClCCHC), 7.09 (dd, 1H,  $J$  = 2.35, 8.21 Hz ClCCHCH), 3.37 (qdd, 1H,  $J$  = 7.04, 7.04, 7.04 Hz CH<sub>3</sub>CHCH<sub>2</sub>), 2.74 (ddd, 2H, 1.47, 7.04, 17.30 Hz CH<sub>2</sub>CHO), 1.32 (d, 3H,  $J$  = 7.04 Hz, CH<sub>3</sub>); <sup>13</sup>C NMR (75 MHz, CDCl<sub>3</sub>)  $\delta$  200.7, 145.9, 132.6, 130.6, 130.4, 128.9, 126.4,

(11) Berlan, J.; Bersace, Y.; Pourcelot, G.; Cresson, P. *Tetrahedron* **1986**, *42*, 4757. (Reported a rotation of +2.1° for a product that was 15% ee.)

51.5, 33.4, 21.9; HRMS ( $\text{EI}^+$ ) exact mass calculated for  $[\text{M}]^+$  ( $\text{C}_{10}\text{H}_{10}\text{OCl}_2$ ) requires  $m/z$  216.0109, found  $m/z$  216.0103;  $[\alpha]_D^{22} = +27.6^\circ$  ( $c = 1.59$ ,  $\text{CHCl}_3$ ).

**(S)-3-cyclohexylbutanal:** Prepared according to the general procedure from (*E*)-3-cyclohexylbut-2-enal (154 mg, 1 mmol) for 22 hours, using workup procedure A to provide the title compound as a colorless oil (45.1 mg, 91% yield, 96% ee) after purification by flash chromatography on silica gel (10%  $\text{Et}_2\text{O}$ /hexane). The physical data were identical in all respects to those previously reported.<sup>12</sup> The enantiomeric ratio was determined by GLC using a Bodman Chiraldex  $\beta$ -DM (30 m  $\times$  0.25 mm) column (80 °C isotherm, 1 mL/min.); (*R*) isomer  $t_r = 70.6$  min. and (*S*) isomer  $t_r = 71.3$  min.  $[\alpha]_D^{22} = +8.3^\circ$  ( $c = 1.00$ ,  $\text{EtOH}$ ).

**(S)-3-cyclohexylpentanal:** Prepared according to the general procedure from (*E*)-3-cyclohexylpent-2-enal (250 mg, 1.50 mmol) for 24 hours, using workup procedure A to provide the title compound as a colorless oil (240.8 mg, 95% yield, 91% ee) after purification by flash chromatography on silica gel (10%  $\text{Et}_2\text{O}$ /pentane). The enantiomeric ratio was determined by GLC using a Hydrodex-B-TBDAC (50 m  $\times$  0.25 mm) column (90 °C isotherm, 1 mL/min.); (*R*) isomer  $t_r = 35.2$  min. and (*S*) isomer  $t_r = 37.9$  min. IR (film) 2927, 2854, 1732, 1708, 1449, 1412, 1381, 1286, 1164, 954, 892  $\text{cm}^{-1}$ ;  $^1\text{H}$  NMR (300 MHz,  $\text{CDCl}_3$ )  $\delta$  9.79 (t, 1H,  $J = 2.4.3$  Hz,  $\text{CHO}$ ), 2.44, (ddd, 1H,  $J = 2.1, 5.8, 16.4$  Hz,  $\text{CH}$ ), 2.28 (ddd, 1H,  $J = 2.7, 7.2, 16.2$  Hz,  $\text{CH}$ ), 1.82 – 1.61 (m, 5H), 1.47 – 0.99 (m, 12H);  $^{13}\text{C}$  NMR (75 MHz,  $\text{CDCl}_3$ )  $\delta$  203.9, 45.7, 40.3, 39.9, 30.4, 29.2, 26.74, 26.69,

(12) Tanaka, K.; Fu, G. C. *J. Org. Chem.* **2001**, *66*, 8177. (Reported a rotation of  $+7.4^\circ$  for a product that was 74% ee.)

26.67, 24.3, 11.8; HRMS ( $\text{EI}^+$ ) exact mass calculated for  $[\text{M}]^+$  ( $\text{C}_{11}\text{H}_{20}\text{O}$ ) requires  $m/z$  168.1514, found  $m/z$  168.1522;  $[\alpha]_D^{22} = +6.2^\circ$  ( $c = 1.03$ ,  $\text{CHCl}_3$ ).

**(S)-methyl 2-methyl-4-oxobutanoate:** Prepared according to the general procedure from (*E*)-methyl 3-formyl-2-methylacrylate (100 mg, 0.781 mmol) for 26 hours to provide the title compound (83% conversion, 91% ee). Conversion was determined via  $^1\text{H}$  NMR by comparison with an internal standard (BnOMe). The physical data were identical in all respects to those previously reported.<sup>13</sup> The enantiomeric ratio was determined by GLC using a Bodman Chiraldex  $\Gamma$ -TA (30 m  $\times$  0.25 mm) column (100  $^\circ\text{C}$  isotherm, 1 mL/min.); (*S*) isomer  $t_r = 6.7$  min. and (*R*) isomer  $t_r = 7.7$  min.  $[\alpha]_D^{22} = +1.4^\circ$  ( $c = 1.15$ ,  $\text{CHCl}_3$ ).

**(S)-3-[tris-(1-methylethyl)silyloxymethyl]butanal:** Prepared according to the general procedure from (*E*)-3-[tris-(1-methylethyl)silyloxymethyl]but-2-enal (245 mg, 1 mmol) for 72 hours, using workup procedure A to provide the title compound as a colorless oil (190 mg, 74% yield, 87% ee) after purification by flash chromatography on Iatrobeads<sup>®</sup> (10%  $\text{Et}_2\text{O}$ /pentane). The enantiomeric ratio was determined by HPLC (the aldehyde was reduced and protected using  $\text{BzCl}$ ) on Chiralcel<sup>®</sup> OD-H (0.46 mm  $\times$  25 cm) Isocratic 5%  $\text{EtOH}$ /Hexanes, 1 mL/min., 25  $^\circ\text{C}$ ); (*S*) isomer  $t_r = 19.2$  min. and (*R*) isomer  $t_r = 22.2$  min. IR (film) 2944, 2867, 2716, 1728, 1464, 1385, 1101  $\text{cm}^{-1}$ ;  $^1\text{H}$  NMR (300 MHz,  $\text{CDCl}_3$ )  $\delta$  9.80 (t, 1H  $J = 2.4$  Hz, **CHO**), 3.66 (dd, 1H,  $J = 5.1, 9.9$  Hz, **TIPSOCH**), 3.47 (dd, 1H,  $J = 6.9, 9.6$  Hz, **TIPSOCH**), 2.58 (m, 1H, **CHCHO**), 2.28 (m, 2H, **MeCHCH**),

(13) Kollar, L.; Consiglio, K.; Pino, P. *J. Organomet. Chem.* **1987**, 330, 305. (Reported a rotation of  $+0.58^\circ$  for a product that was 10% ee.)

1.06 (m, 21H, TIPS0), 0.97 (d,  $J = 6.9$  Hz,  $\text{CH}_3$ );  $^{13}\text{C}$  NMR (75 MHz,  $\text{CDCl}_3$ )  $\delta$  202.7, 68.0, 48.2, 31.6, 17.9, 16.7, 11.9; HRMS ( $\text{EI}^+$ ) exact mass calculated for  $[\text{M}-\text{H}]^+$  ( $\text{C}_{14}\text{H}_{29}\text{O}_2\text{Si}$ ) requires  $m/z$  257.1930 found  $m/z$  257.1937;  $[\alpha]_D^{22} = -2.7^\circ$  ( $c = 1.07$ ,  $\text{CHCl}_3$ ).

**(*S*)-3,4,4-trimethylpentanal:** Prepared according to the general procedure, at room temperature, from (*E*)-3,4,4-trimethylpent-2-enal (70 mg, 0.56 mmol) for 30 minutes to provide the title compound (95% conversion, 97% ee). Conversion was determined using  $^1\text{H}$  NMR by comparison with an internal standard (BnOMe). The physical data were identical in all respects to those previously reported.<sup>14</sup> The enantiomeric ratio was determined by GLC using a Bodman Chiraldex  $\beta$ -DM (30 m  $\times$  0.25 mm) column (60  $^\circ\text{C}$  isotherm, 1 mL/min.); (*R*) isomer  $t_r = 19.29$  min. and (*S*) isomer  $t_r = 20.32$  min.  $[\alpha]_D^{22} = +29.3^\circ$  ( $c = 1.00$ ,  $\text{CHCl}_3$ ).

---

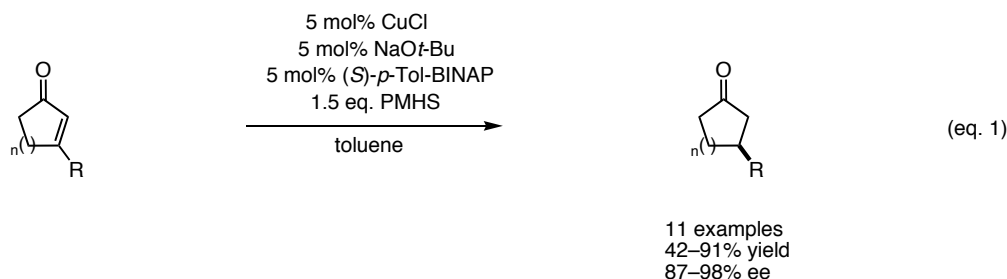
(14) Berlan, J.; Besace, Y.; Pourcelot, G.; Cresson, P. *Tetrahedron* **1986**, 42, 4757. (Reported a rotation of  $+3.4^\circ$  for a product that was 16% ee.)

## Chapter 3

### Design and Development of an Organocatalytic Reduction of Enones

#### Introduction

We sought to extend our hydrogenation technologies<sup>1</sup> towards  $\alpha,\beta$ -unsaturated cyclic enones, an important class of structurally related molecules. Access to carbocycles containing stereogenicity is an ongoing focus of asymmetric catalysis due to their broad utility in the preparation of natural isolates and medicinal agents. Considerable effort has focused on the conjugate reduction of  $\beta$ -substituted enones using transition metal complexes as catalysts.<sup>2</sup> Recently, chiral ligands have been developed and applied towards catalytic enantioselective conjugate enone reduction. The first account was reported in 2000 by the Buchwald group<sup>3</sup> (eq. 1) and has been complimented by similar work.<sup>4</sup>



(1) Ouellet, S. G.; Tuttle, J. B.; MacMillan, D. W. C. *J. Am. Chem. Soc.* **2005**, *127*, 32-33.

(2) (a) Kienan, E. G., N. *Comprehensive Organic Synthesis*; Perfamin Press: Oxford, 1991. (b) Mori, A.; Fujita, A.; Kajiro, H.; Nishihara, Y.; Hiyama, T. *Tetrahedron* **1999**, *55*, 4573-4582. (c) Mahoney, W. S.; Stryker, J. M. *J. Am. Chem. Soc.* **1989**, *111*, 8818-8823. (d) Jurkauskas, V.; Sadighi, J. P.; Buchwald, S. L. *Org. Lett.* **2003**, *5*, 2417-2420. (e) Lipshutz, B. H.; Keith, J.; Papa, P.; Vivian, R. *Tetrahedron Lett.* **1998**, *39*, 4627-4630.

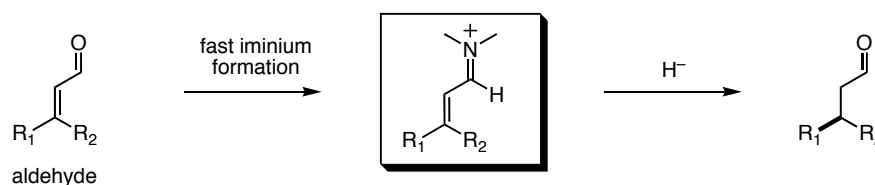
(3) Moritani, Y.; Appella, D. H.; Jurkauskas, V.; Buchwald, S. L. *J. Am. Chem. Soc.* **2000**, *122*, 6797-6798.

(4) Lipshutz, B. H.; Servesko, J. M.; Petersen, T. B.; Papa, P. P.; Lover, A. A. *Org. Lett.* **2004**, *6*, 1273-1275.

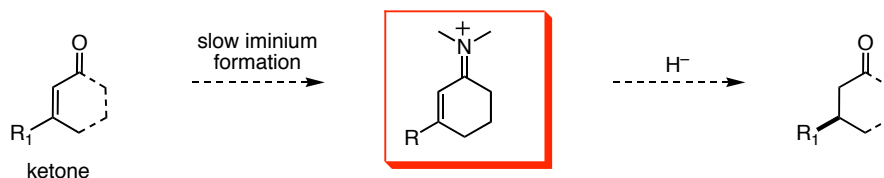
In the realm of organocatalytic iminium activation, cyclic ketones remain a challenging class of substrates. First, these compounds are less reactive compared to their aldehyde counterparts (Fig. 1). This characteristic is attributed to the subtle replacement of an aldehyde hydrogen with a methylene unit. The resulting increase in the steric component at that position leads to slower iminium formation.

**Figure 1. Reactivity Differences Between Unsaturated Aldehydes and Ketones**

■ Proven broadly useful for organocatalysis

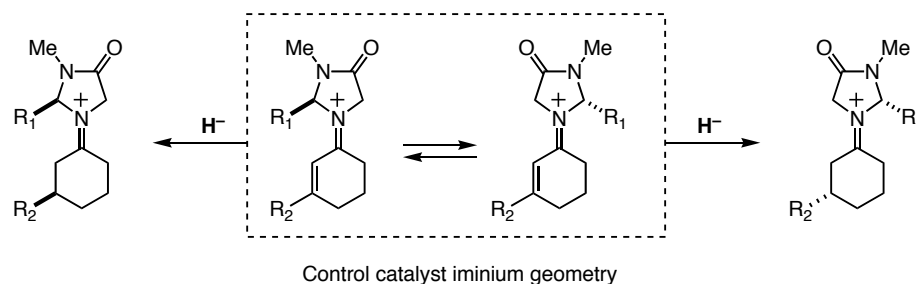


■ A difficult substrate class for organocatalysis



Second, a catalyst has to effectively distinguish the subtle, but significant, steric differences between methane and methylene groups in order to achieve enantioselectivity (Fig. 2). If conformational interchange is a facile process, then enantioselectivity will erode due to poor facial selectivity in the hydride addition step.

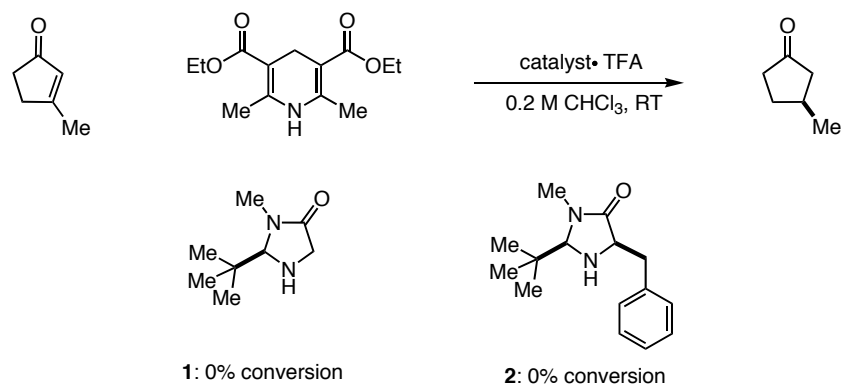
**Figure 2. Challenges for Stereocontrol**



### Development of an Organocatalytic Enone Hydrogenation Reaction

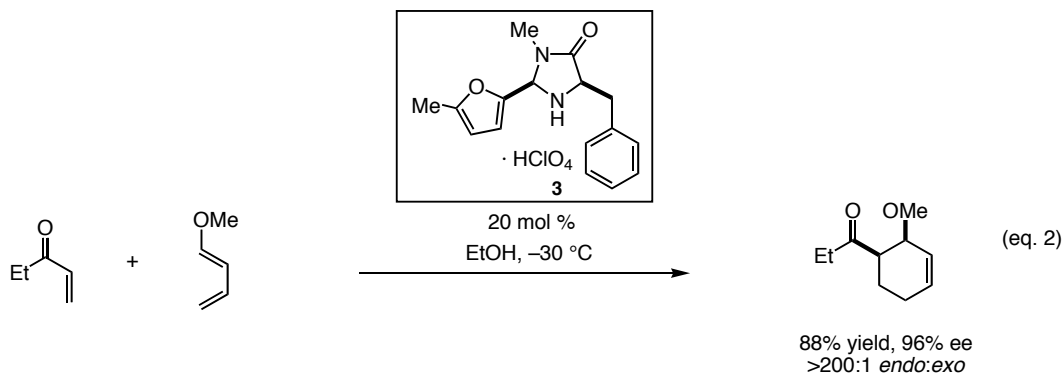
Initial forays into developing this methodology were hindered by these challenges (Fig. 3). Indeed, imidazolidinone catalyst **1** and 2<sup>nd</sup>-generation catalyst **2** failed to catalyze the reduction of 3-methylcyclopentenone, obviating the need for a different catalyst structure that is more appropriate for this type of substrate.

**Figure 3. Typical Organocatalysts Failed to Catalyze a Reaction**



Inspiration for a more effective catalyst came from within our group.<sup>5</sup> In 2002, Alan Northrup developed imidazolidinone catalyst **3** to activate  $\alpha,\beta$ -unsaturated ketones towards Diels-Alder cycloadditions (eq. 2). The basis for this enhanced reactivity is attributed to the ability of the furan to accommodate the methylene protons by, one, rotating out of the chemical space occupied by the hydrogens and, two, engaging in a

■ A privileged enone catalyst

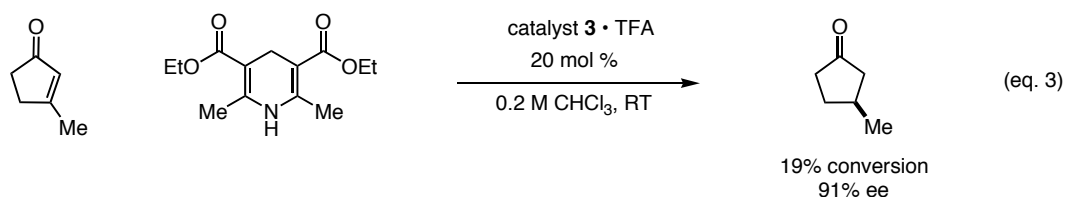


(5) Northrup, A. B.; MacMillan, D. W. C. *J. Am. Chem. Soc.* **2002**, *124*, 2458-2460.



CH- $\pi$  stabilizing interaction.<sup>6</sup> In the first reaction with catalyst **3**, we were gratified to discover the model system was activated towards hydride reduction and provided the desired product in good ee albeit low yield (eq. 3). This is the first demonstration of a conjugate nucleophilic addition reaction to an  $\alpha,\beta$ -unsaturated ketone utilizing imidazolidinone **3** as a catalyst.

■ Preliminary results for the enone hydrogenation reaction development



Having found an effective catalyst, the next step was to improve product conversion while maintaining good levels of enantioselectivity. Exploring a range of solvents indicated Et<sub>2</sub>O improved conversion and maintained good levels of ee (Table 1,

**Table 1. Optimizing the Enone Hydrogenation**

entry	solvent	co-catalyst	[C]	% conversion <sup>a</sup>	% ee <sup>b</sup>
1	CHCl <sub>3</sub>	TFA	0.2 M	19	91
2	MeOH	TFA	0.2 M	63	33
3	Toluene	TFA	0.2 M	56	91
4	Et <sub>2</sub> O	TFA	0.2 M	63	90
5	Et <sub>2</sub> O	HCl	0.2 M	16	78
6	Et <sub>2</sub> O	TCA	0.2 M	77	93
7	Et <sub>2</sub> O	TCA	0.5 M	77	96
8	Et <sub>2</sub> O	TCA	1.0 M	77	96

<sup>a</sup>Conversion determined by GC analysis comparison to an internal standard.

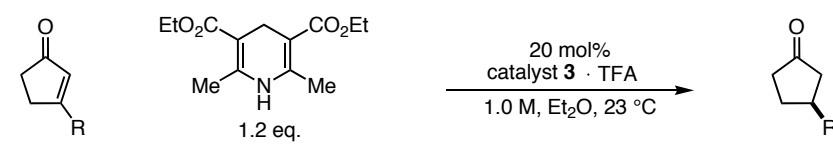
<sup>b</sup>Enantiomeric excess determined by chiral GC analysis

(6) Northrup, A. B., Ph. D. Thesis, California Institute of Technology, 2005.

entries 1-4). A co-catalyst survey indicated weaker acids improved product conversion as opposed to stronger variants presumably due to more efficient proton shuttling (Table 1, entries 5-7). Concentration had little effect on the transformation as the high conversion and ee was maintained across a range of molarities (Table 1, entries 7-9).

### ***Substrate Scope***

With these optimal conditions in hand, a range of enones that are amenable to this new process was examined (Table 2). Analysis of alkyl groups representing a spectrum of steric demand indicate enones containing methyl (Table 2, entry 1) and benzyl substituents (Table 4, entry 2) were reduced in high yield and with good enantiocontrol. Sterically congested centers, that are typically difficult to reduce using organometallic catalysts, readily react under enantioselective organocatalytic hydride conditions (EOHR) (Table 2, entries 3-4). We were pleased to discover that protected alcohol equivalents (Table 2, entry 5) are tolerated under these conditions. Variation of the electronic nature of the enone substituent has an effect on the observed enantioinduction. Iminium-stabilizing substituents decrease the enantiomeric excess (Table 2, entry 6). Conversely, a high level of selectivity is maintained in the reduction of enones that do not readily participate in iminium formation (Table 2, entry 7). Gratifyingly, the catalyst differentiates between enones of comparable electronics but different steric demand (Table 2, entry 8).

**Table 2. Substrate Scope: Cyclopentenones**


entry	R	time (h)	% yield	% ee <sup>a</sup>
1	Me	26	77 <sup>b</sup>	95
2	Bn	24	91	90 <sup>c</sup>
3	<i>c</i> -hex	8	85	96
4	<i>t</i> -bu	9	93	96
5	CH <sub>2</sub> OBn	24	76	91 <sup>c</sup>
6	Ph	8.5	89	74
7	CO <sub>2</sub> Me	24	76	90 <sup>c</sup>
8	COMe	24	82	93 <sup>c</sup>

<sup>a</sup>Enantiomeric excess determined by GLC analysis. <sup>b</sup>Yield determined by GLC. <sup>c</sup>Reaction run at 0 °C.

Importantly, functional groups sensitive to metal-mediated hydrogenation, such as ketones and benzyl protecting groups, withstand these mild conditions.

Assessing the effect of larger rings on EOHR was explored (Table 3). In the six-membered-ring series both alkyl (Table 3, entry 1) and cycloalkyl substituents (Table 3, entry 2) were reduced in good yield and selectivity. Moreover, EOHR successfully reduced substrates that contain sterically demanding functionality proximal to the reaction center (Table 5, entry 3). Further increasing the ring size to cycloheptenone (Table 3, entry 4) provided the product in moderate yield and enantioselectivity.

**Table 3. Substrate Scope: Larger Rings**

entry	R	time (h)	% yield	% ee <sup>a</sup>
1	<i>n</i> -Bu	43	75	88
2	<i>c</i> -Hex	43	80	90
3		48	65	97
4		48	63	82

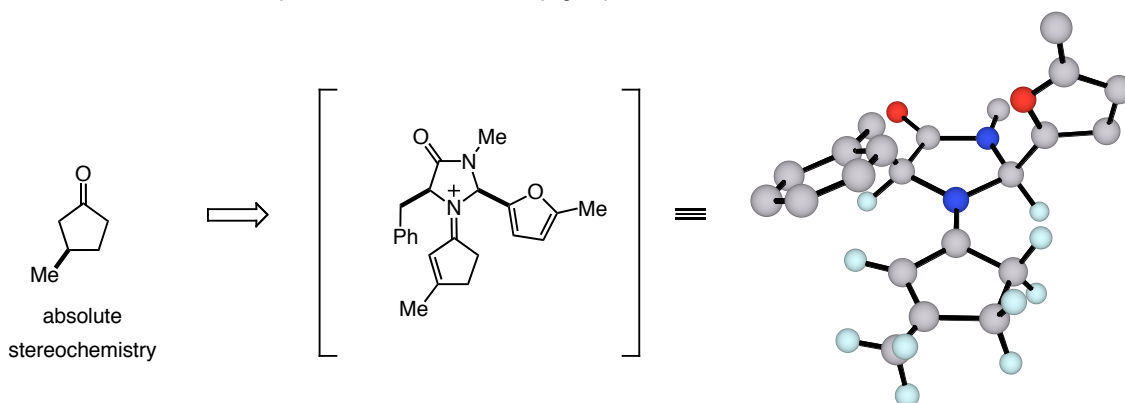
<sup>a</sup>Enantiomeric excess determined by GLC analysis.***Absolute Sense of Enantioinduction***

Comparing the GC retention time of reduced product 3-methylcyclopentanone to a commercially available, enantiopure sample proves the (*R*)-enantiomer is produced (Fig. 3). This indicates the catalyst forms an iminium intermediate that has the benzyl group shielding the *Re*-face of the substrate and favoring the *Si*-face for hydride delivery. This orientation is entirely consistent with that found for the ketone Diels-Alder chemistry where MM3 calculations indicate this type of iminium is favored by 11.3 KJ/mol.<sup>7</sup>

(7) Northrup, A. B. Ph. D. Thesis California Institute of Technology, 2005.

**Figure 4. Absolute Sense of Enantioinduction**

- Product stereochemistry matches that of an (*R*)-configured commercially available sample
- The absolute stereochemistry is consistent with the benzyl group oriented over the alkene

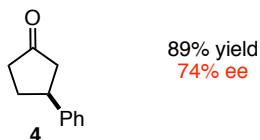


### *Challenges Associated with this Chemistry*

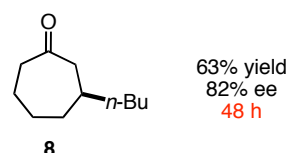
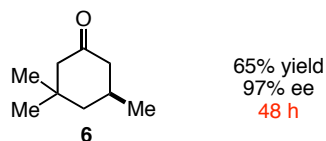
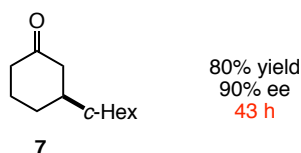
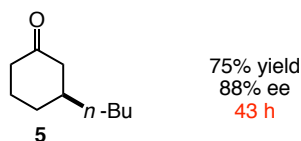
While developing the substrate scope, we discovered certain limitations to this methodology (Fig. 5). In the cyclopentane series, the phenyl ring bearing substrate **4** was reduced with low enantioselectivity (Fig. 5, 74% ee). Additionally, larger rings (Fig. 5, **5-7**) are reduced very slowly (typically 48 h) and the cycloheptenone substrate **8** exhibits a low yield and poor enantioselectivity (Fig. 5, 63% yield, 82% ee).

**Figure 5. Challenges Associated with the Reduction Chemistry**

- The phenyl derivative is reduced with low enantioselectivity



- Larger rings suffer from long reaction times



Attempts to overcome the low enantioselectivity exhibited by 3-phenylcyclopentenone **4** by varying solvent, temperature, catalyst, and co-catalyst did not improve the initial results. Our next efforts focused on varying the hydride component (Table 4). Decreasing the steric component on the 2,6-positions slightly increased the enantioselectivity but led to an undesired decrease in conversion (Table 4, Entries 1-3). Alternatively, substituting the ethoxy group with an isopropoxy group gave a good yield and a slightly improved ee (Table 4, entry 5). Unexpectedly, increasing the bulk of the ester dramatically improved the enantioselectivity while maintaining good levels of conversion (Table 4, entry 6).

**Table 4. Analyzing Hantzsch Derivatives for Efficacy**

entry	CO <sub>2</sub> R	X	time (h)	% conversion <sup>a</sup>	% ee <sup>b</sup>
1	CO <sub>2</sub> Et	H	3	93	73
2	CO <sub>2</sub> Et	Et	4	76	82
3	CO <sub>2</sub> Me	<i>i</i> -Pr	24	57	86
4	CO <sub>2</sub> Et	Me	3	96	74
5	CO <sub>2</sub> <i>i</i> -Pr	Me	3	78	78
6 <sup>c</sup>	CO <sub>2</sub> <i>t</i> -Bu	Me	6	86	91

<sup>a</sup>Conversion determined by GC analysis comparison to an internal standard.

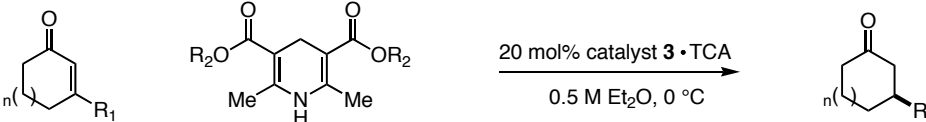
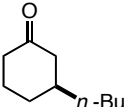
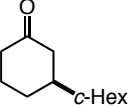
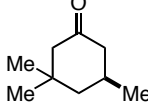
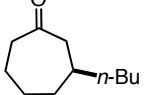
<sup>b</sup>Enantiomeric excess determined by chiral GC analysis.

<sup>c</sup>Reaction run at 0 °C.

Having solved the problem of enantioselectivity for the phenyl substrate, we sought to improve the reaction rates of the larger rings. To achieve this goal, Hantzsch ester **9** was utilized for reducing these less-reactive species (Table 5). Remarkably, in almost every instance, the reaction rate was nearly doubled, while high levels of enantioselectivities and yields were maintained (Table 5 entries 1-2, 4). Gratifyingly, the

cycloheptenone substrate now exhibited improvements in yield and ee from the initial result (Table 5, entry 4). Isophorone exhibited only slightly improved levels of reactivity, presumably owing to the influence the bulky *gem*-dimethyl group has on the reacting center (Table 5, entry 4).

**Table 5. Comparison of Ethyl and *t*-Butyl Hantzsch Reduction Reactions with Larger Rings**

			
entry	product	R <sub>2</sub> = ethyl	R <sub>2</sub> = <i>t</i> -butyl, <b>9</b>
1		75% yield 88% ee 43 h	82% yield 90% ee 25 h
2		80% yield 90% ee 43h	71% yield 88% ee 24 h
3		65% yield 97% ee 48 h	66% yield 98% ee 40 h
4		63% yield 82% ee 48 h	70% yield 92% ee 9 h

The increased reduction rate exhibited by Hantzsch **9** is not limited to larger rings. Indeed, subjecting 5-membered rings to these conditions provided the reduced products with shorter reaction times (Table 6). As shown in table 6, in many cases reduction rates were nearly doubled (Table 6 entries 1-2) or better (Table 6, entries 3-4). This remarkable difference in reactivity prompted us to assess the effect this reductant would have on  $\alpha,\beta$ -unsaturated aldehydes.

**Table 6. Comparison of Ethyl and *t*-Butyl Hantzsch Reductions of Cyclopentenones**

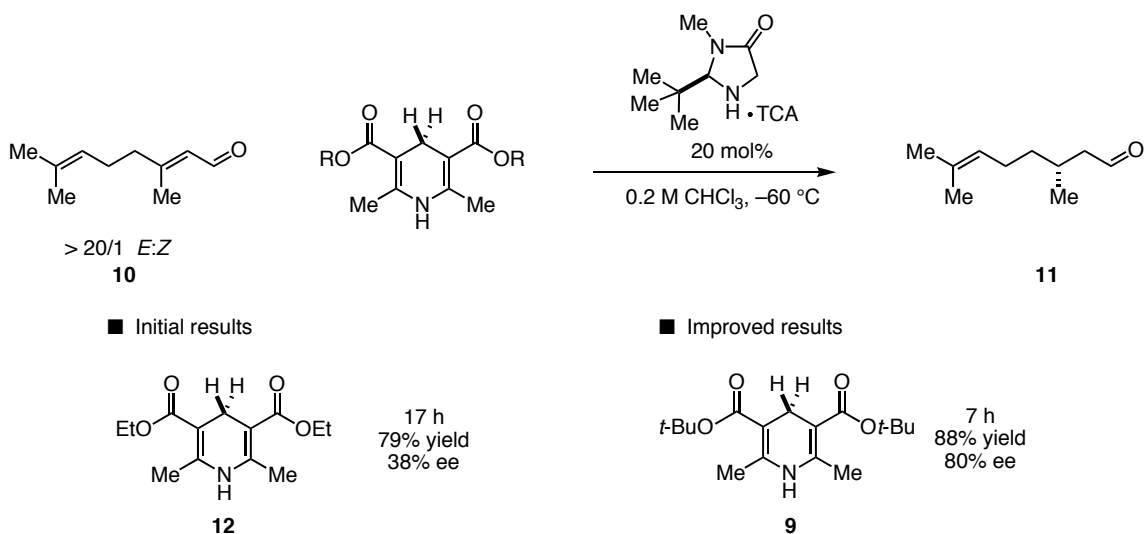
<div style="display: flex; align-items: center; justify-content: space-around;"> <div> </div> </div>			
entry	product	R <sub>2</sub> = ethyl	R <sub>2</sub> = <i>t</i> -butyl, <b>9</b>
1		76% yield 91% ee 24 h	77% yield 91% ee 13 h
2		91% yield 90% ee 24h	78% yield 90% ee 11 h
3		76% yield 90% ee 24 h	78% yield 93% ee 1 h
4		63% yield 93% ee 24 h	83% yield 93% ee 1 h

### *Utilizing *t*-Butyl Hantzsch Dihydropyridine in the Reduction of Geranial*

During the course of our enal studies, one important substrate class posed a significant problem. In particular,  $\beta,\beta$ -methyl, ethyl substituted olefins, such as geranial **10**, were reduced in very low ee using dihydropyridine **12** (Fig. 6). Remarkably, Hantzsch ester **9** continued its trend of reaction improvement, providing citronellal **11** at a faster rate, with an improved yield, and a dramatically increased ee under the same conditions (compare ethyl derivative **12**: 17h, 79% yield, 38% ee to *t*-butyl derivative **9**: 7h, 88% yield, 80% ee).

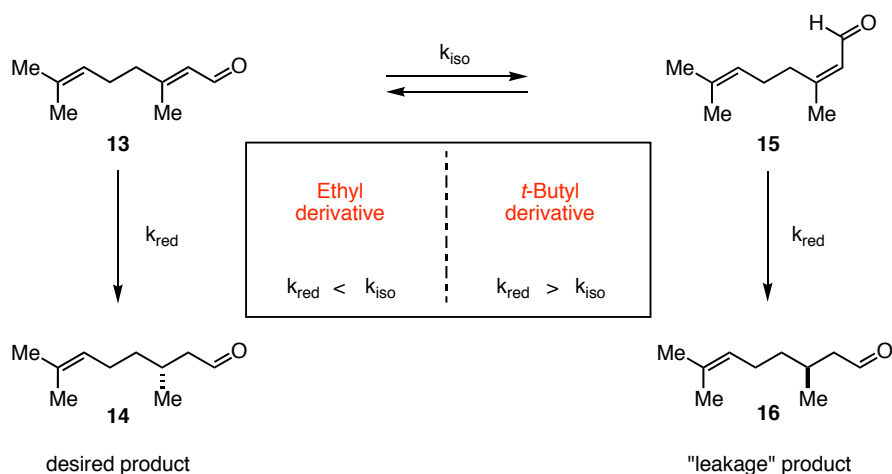


Figure 6. Methyl Versus Ethyl Stereodifferentiation: Comparing the Hantzsch Ester Derivatives



Insight into this effect is gleaned by analyzing a simple rate diagram (Fig. 7). In the case of dihydropyridine **12**, the rate of reduction is slower than the rate of isomerization. As a result, more *E*-isomer **13** is isomerized to *Z*-isomer **15** that is subsequently reduced to undesired enantiomer **16**, causing a decrease in enantioselectivity. Conversely, the rate of reduction is faster than isomerization in the case of dihydropyridine **9**. Less of the *Z*-isomer **15** is produced during the reaction and more of the *E*-isomer **13** is reduced to give desired product **14** with an increase in enantioselectivity.

Figure 7. Explaining the Increase in Enantioselectivity Demonstrated by the *t*-Butyl Hantzsch



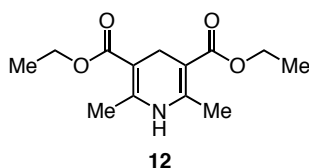
While this explanation accounts for the contrast in enantioselectivities between the two Hantzsch derivatives, it does not provide insight into why the *t*-butyl analog is more reactive.

### ***Explanation of the Reactivity Differences***

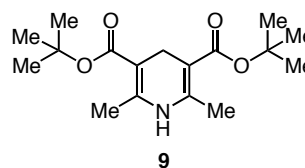
The first observation to probe these rate differences was a qualitative analysis of the reaction conditions (Fig. 8). In CHCl<sub>3</sub>, reductions that utilize ethyl Hantzsch **12** are heterogeneous. Conversely, in the same solvent, *t*-butyl Hantzsch **9** reductions are homogeneous. These solubility differences may contribute to the rate discrepancies. In the homogeneous case, a larger effective concentration of reductant would explain why the *t*-butyl derivative is more reactive. In the heterogeneous case, a lower concentration of reductant decreases the reaction rate, allows more isomerization to occur (*vide supra*), leading to the erosion of enantioselectivity.

**Figure 8. Explaining the Hantzsch Ester Rate Differences**

■ The Hantzsch derivatives exhibit different degrees of solubility



Heterogeneous reactions



Homogeneous reactions

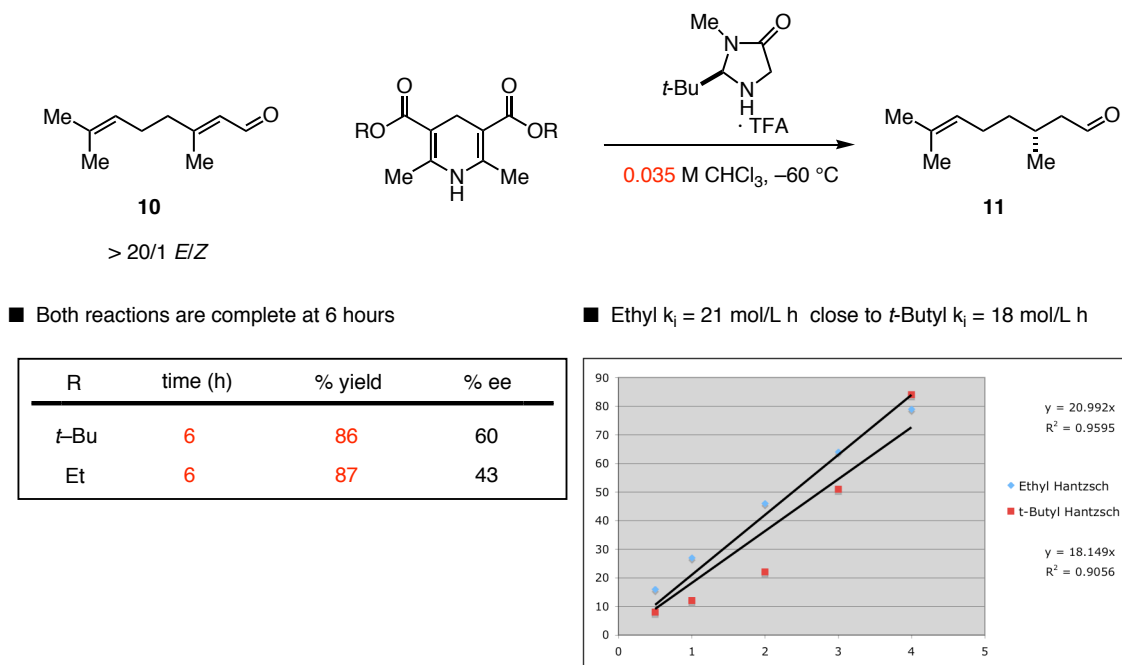
■ Hypothesis: The *t*-butyl reactions have a larger effective concentration of reductant

$$\left[ \text{H}^- \right]_{\text{ethyl derivative}} < \left[ \text{H}^- \right]_{t\text{-butyl derivative}}$$

A GC time course experiment was used to test this hypothesis. In the event, two reactions were set up using geometrically pure geranial **10**, under standard reduction conditions. Both were set up at 0.035 M, the concentration where *both* reactions are homogeneous (Fig. 9). The time course indicated both transformations reached their

endpoints after six hours and produced citronellal in comparable yields. Furthermore, a plot of various time points against product conversion indicated both reactions exhibited similar initial rates of reaction. Interestingly, the higher dilution eroded the ee in the case of dihydropyridine **9** and exhibited a slight improvement for dihydropyridine **12**, as compared to the optimized conditions shown in Figure 6 (85% ee versus 60% ee). These results support our hypothesis that the increased solubility of Hantzsch **9** is a principal contributor to the different reaction rates.

**Figure 9. Comparing Homogeneous Reactions of Both Hantzsch Ester Derivatives**

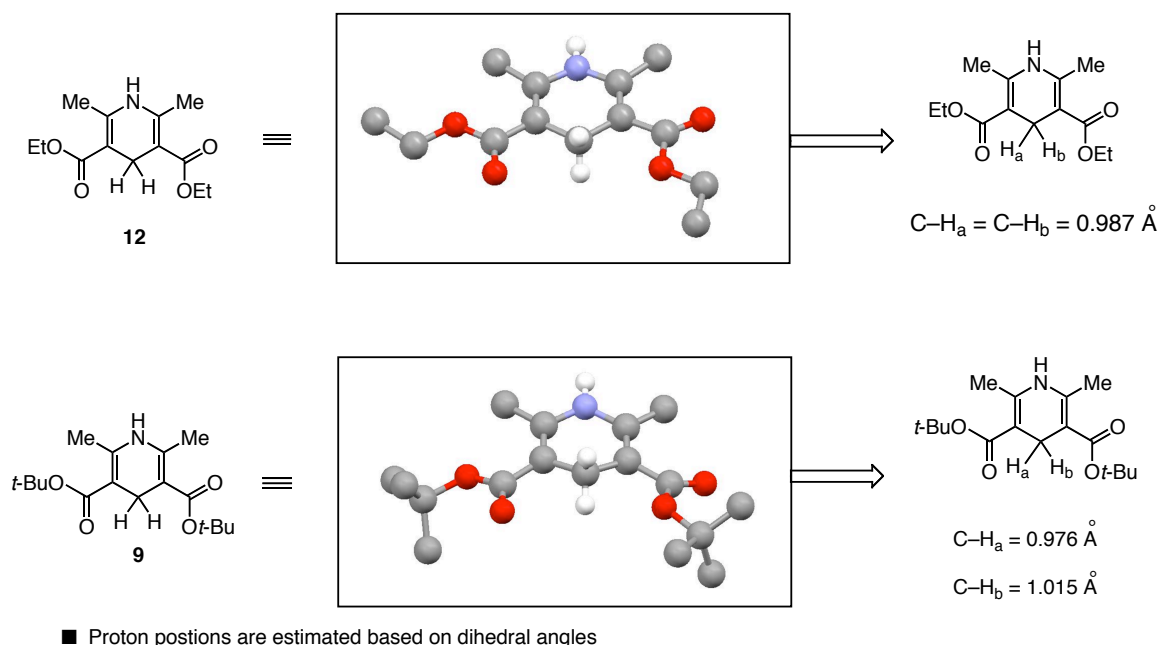


### *Structural Differences that May Further Contribute to Reactivity Differences*

While solubility plays a clear role in reactivity differences between the two dihydropyridines, it may not be the only explanation for rate enhancement. Indeed, structural differences may also have an effect. To examine this possibility, x-ray analysis was performed on each derivative (Fig. 10). Intriguingly, these analogs exhibit

differences in their ground state conformations: A non-intuitive observation, considering the seemingly benign effect ester substitution could have on their ring structures. Initial observations indicated the estimated proton-carbon bond lengths ( $H_a/H_b$ , Fig. 10) on ethyl derivative **12** are equivalent, while those on *t*-butyl derivative **9** are non-equivalent.

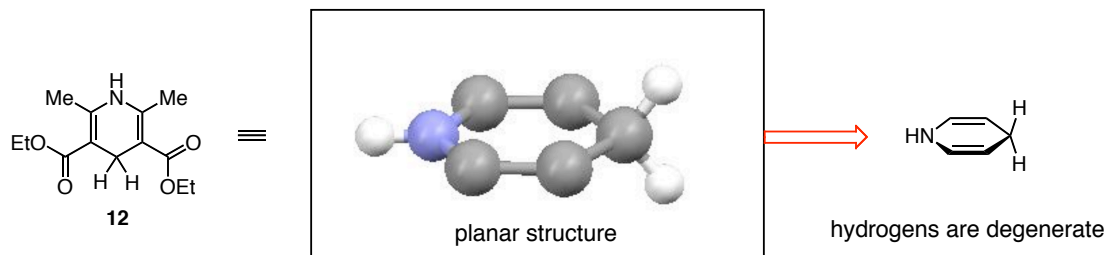
**Figure 10. X-Ray Crystallography Analysis of Both Hantzsch Derivatives**



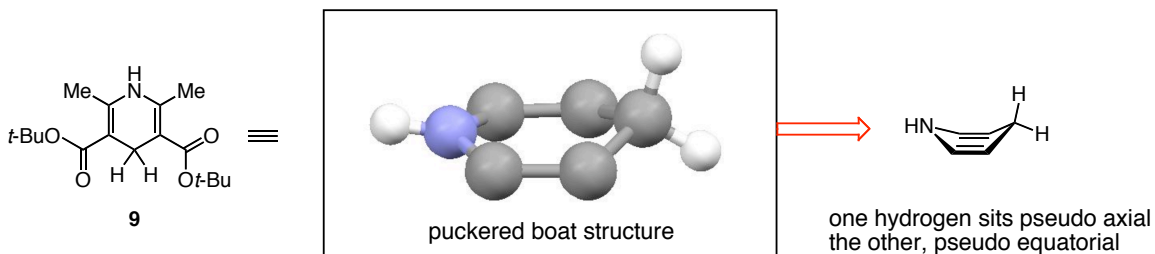
A closer examination indicates differences in the dihydropyridine ring geometries (Fig. 11). It was found ethyl Hantzsch **12** exists as a planar structure, explaining why carbon-proton bond distances are equivalent. Interestingly, *t*-butyl Hantzsch **9** adopts a *pseudo*-boat conformation, causing one proton to orient in an axial position and the other in an equatorial position, thereby accounting for the observed difference in carbon proton bond distances.

**Figure 11. Analyzing the Dihydropyridine Rings**

- The ethyl Hantzsch prefers a planar structure in the ground state



- The *t*-butyl Hantzsch analog prefers a pseudo-boat structure in the ground state

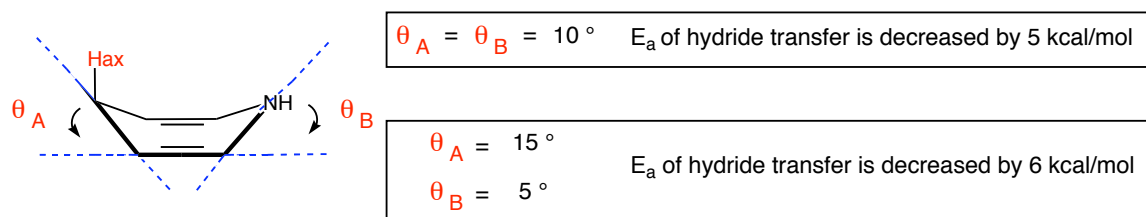


These fascinating structural differences may also contribute to reactivity differences between the two analogues. One important feature of dihydropyridine reactivity is its ability to pucker during the reduction event. For instance, in NADPH mediated enzymatic reductions, the nicotinamide hydride source adopts a puckered boat conformation and delivers a pro-*S* hydride to the electrophile. Indeed, it is the degree of puckering that has a large impact on dihydropyridine reactivity (Fig. 12). Specifically, angles  $\theta_A$  and  $\theta_B$  are metrics for the hydride-donating ability of the dihydropyridine.<sup>8</sup> Larger angles, especially for  $\theta_A$ , decrease the activation energy required for the hydride transfer.

(8) (a) Wu, Y. D.; Lai, D. K. W.; Houk, K. N. *J. Am. Chem. Soc.* **1995**, *117*, 4100-4108. (b) Almarsson, O.; Bruice, T. C. *J. Am. Chem. Soc.* **1993**, *115*, 2125-2138. (c) Almarsson, O.; Karaman, R.; Bruice, T. C. *J. Am. Chem. Soc.* **1992**, *114*, 8702-8704.

**Figure 12. Effect of Puckering on Hydride Transfer**

- Theoretical calculations show the activation energy of hydride transfer of the puckered conformation is lower than the planar conformation



The effect of these angle differences on reactivity may be explained by orbital analysis. Increased puckering improves p-orbital overlap, creating an intermediate having more aromatic character, resulting in a transition state structure resembling the more stable pyridinium product (Fig. 13). Moreover, this puckering allows the nitrogen lone pair to delocalize into the  $\pi$ -system, creating a more electron rich axial hydrogen that, as a result, is a more reactive hydride.

**Figure 13. Assessing the Puckering Effect on Dihydropyridine Reactivity**

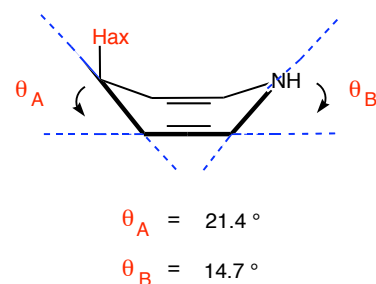
- Molecular orbital analysis of the puckered conformation



- The actual angles of the *t*-butyl Hantzsch may be significant

For NADH calculated at the AM-1 level

$\theta_A$	$\theta_B$	$\Delta H_f$ (kcal/mol)
$0^\circ$	$0^\circ$	0
$10^\circ$	$10^\circ$	1.72
$20^\circ$	$20^\circ$	9.32



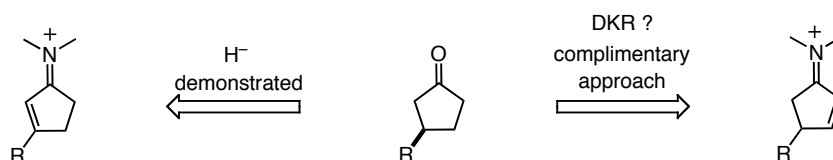
For this chemistry, while we postulate both Hantzsch derivatives will adopt a puckered boat conformation in their transition states, the *larger* puckering angles (Fig. 13,  $\theta_A$  and  $\theta_b$ ,) exhibited by the *t*-butyl Hantzsch **9** may contribute to the observed increase in reactivity. It is this degree of puckering that may not be energetically accessible by the ethyl Hantzsch **12**, making it less reactive (Fig. 13, see table).

### Dynamic Kinetic Resolution

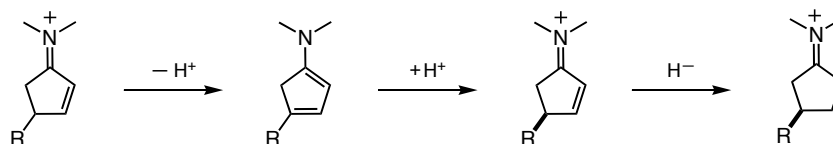
Due to the intriguing electronic effects as noted with 3-phenylcyclopenten-2-one, it was reasoned that a complementary approach to the  $\beta$ -aryl stereogenicity could be achieved by a dynamic kinetic resolution (Fig. 14). In order to test this hypothesis a

**Figure 14. An Alternative Approach to Cyclic Enone Stereogenicity**

■ Utilizing dynamic kinetic resolution (DKR) may provide the desired product

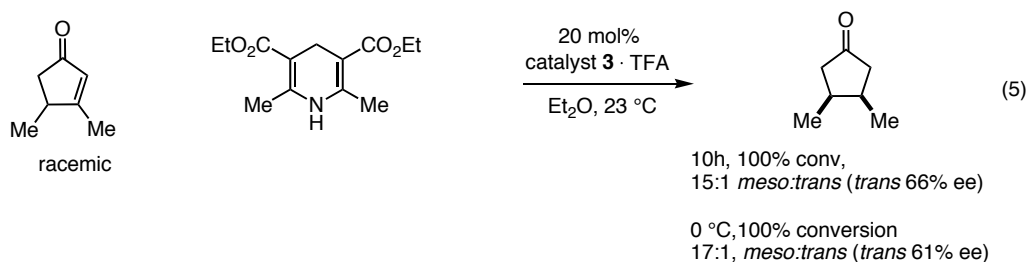
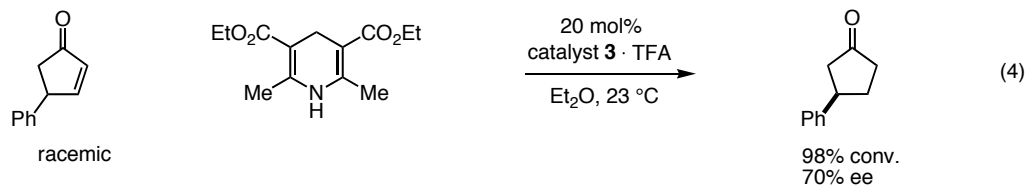


■ Possible mechanism

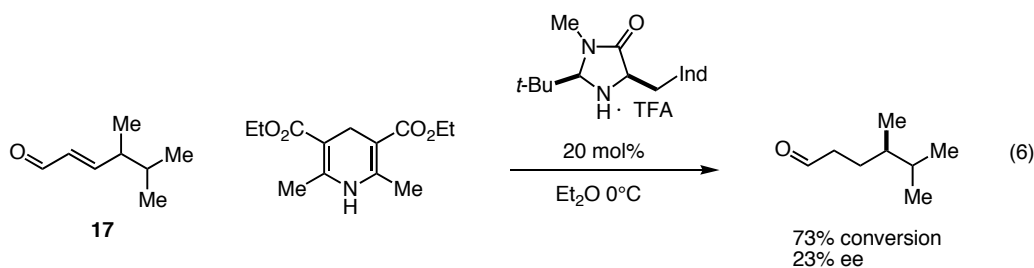


racemic sample of 4-phenylcyclopenten-2-one was subjected to EOHR conditions. We were delighted to isolate enantioenriched (*R*)-3-phenylcyclopentanone in near quantitative conversion with moderate enantioselectivity (eq. 4). Furthermore, 3,4-dimethylcyclopenten-2-one was tested for DKR and a clear preference for *meso*-

selectivity was found. Interestingly, the minor *trans* isomers were also enantioenriched (eq. 5).



Subjecting racemic acyclic substrate **17** to these reduction conditions produced saturated product with some enantioenrichment and good yield (eq. 6). Though unoptimized, these results are encouraging due to the possibility of developing a broadly applicable method for the generation of cyclic benzylic and alkyl stereogenicity in the realm of DKR.

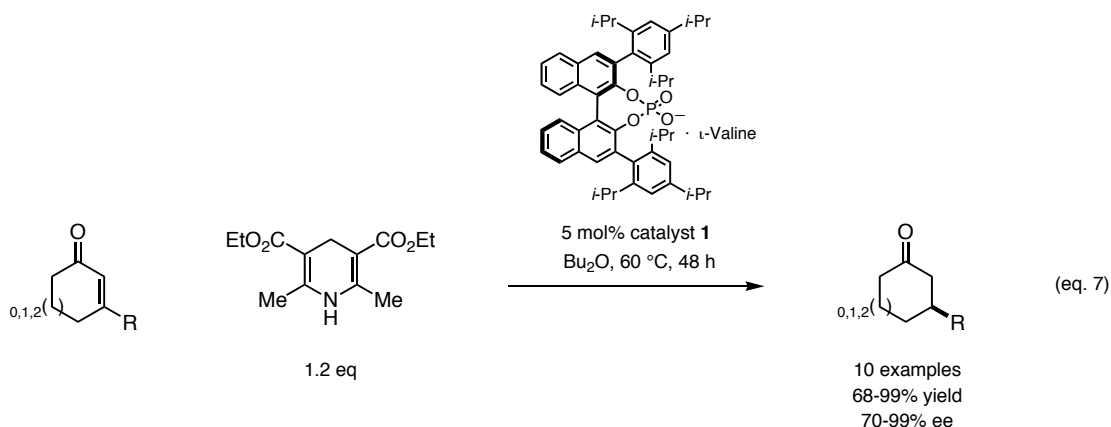


### Recent Developments

Soon after this methodology was published, the List Group reported an asymmetric reduction of  $\alpha,\beta$ -unsaturated ketones using asymmetric counterion directed



catalysis (ACDC) technology in conjunction with a Hantzsch hydride source (eq. 7).<sup>9</sup> Significantly, this paper reports the reduction of two acyclic  $\alpha,\beta$ -unsaturated ketones that have, so far, not been reactive to our hydrogenation conditions.



## Conclusion

A new organocatalytic enantioselective catalytic hydrogenation method of  $\alpha,\beta$ -unsaturated enones has been developed using iminium activation technology. Optimization efforts led to the discovery of a more reactive hydride source and preliminary investigations provide insight to the reasons why the *t*-butyl Hantzsch dihydropyridine derivative is a more reactive hydride donor compared to the ethyl derivative. Furthermore, early efforts outlining the entry into a general dynamic kinetic resolution of both ketone and aldehyde substrates have been reported. Future directions include extending this chemistry into tandem catalysis and further developing the DKR into a broadly useful methodology.

(9) Martin, N. J. A.; List, B. *J. Am. Chem. Soc.* **2006**, *128*, 13368-13369.

## Supporting Information

**General Information.** Commercial reagents were purified prior to use following the guidelines of Perrin and Armarego.<sup>1</sup> Non-aqueous reagents were transferred under nitrogen via syringe or cannula and purified according to the method of Grubbs.<sup>2</sup> Organic solutions were concentrated under reduced pressure on a Büchi rotary evaporator. Chromatographic purification of products was accomplished using forced-flow chromatography on ICN 60 32-64 mesh silica gel and Iatrobeads<sup>®</sup> according to the method of Still.<sup>3</sup> Thin-layer chromatography (TLC) was performed on EM Reagents 0.25 mm silica gel 60-F plates. Chromatograms were visualized by fluorescence quenching or by staining using either potassium permanganate or anisaldehyde stain.

<sup>1</sup>H and <sup>13</sup>C NMR spectra were recorded on a Varian Mercury 300 Spectrometer, and are internally referenced to residual solvent signals. Data for <sup>1</sup>H NMR are reported as follows: chemical shift (δ ppm), multiplicity (s = singlet, d = doublet, t = triplet, q = quartet, m = multiplet), integration, coupling constant (Hz), and assignment. Data for <sup>13</sup>C NMR are reported in terms of chemical shift. IR spectra were recorded on a Perkin Elmer Paragon 1000 spectrometer and are reported in terms of frequency of absorption (cm<sup>-1</sup>). Mass spectra were obtained from the Caltech Mass Spectrometry Facility by electron ionization, chemical ionization, or fast atom/ion bombardment techniques. Gas liquid chromatography (GLC) was performed on Hewlett-Packard 6850 and 6890 Series gas chromatographs equipped with a split-mode capillary injection system and flame

---

(1) Perrin, D. D.; Armarego, W. L. F. *Purification of Laboratory Chemicals*; 3rd ed., Pergamon Press, Oxford, 1988.

(2) Pangborn, A. B.; Giardello, M. A.; Grubbs, R. H.; Rosen, R. K.; Timmers, F. J. *Organometallics* **1996**, *15*, 1518.

(3) Still, W. C.; Kahn, M.; Mitra, A. J. *J. Org. Chem.* **1978**, *43*, 2923.

ionization detectors using a Bodman Chiraldex b-DM (30 m × 0.25 mm), a Bodman Chiraldex  $\Gamma$ -TA (30 m × 0.25 mm), or a Hydrodex-B-TBDAC (50 m × 0.25 mm) column as noted. Optical rotations were measured on a Jasco P-1010 polarimeter, and  $[\alpha]_D$  values are reported in  $10^{-1} \text{ dg cm}^2 \text{ g}^{-1}$ ; concentration (c) is in g/100 mL.

### Preparation of the starting materials

These  $\alpha,\beta$ -unsaturated cyclic enones are commercially available from Aldrich: 3-methyl-2-cyclopenten-1-one and isophorone (3,5,5-trimethylcyclohex-2-enone). The following  $\alpha,\beta$ -unsaturated cyclic enones have already been described in the literature: 3-hexylcyclopent-2-enone, 3-cyclohexylcyclopent-2-enone,<sup>4</sup> 3-*tert*-butylcyclopent-2-enone,<sup>5</sup> 3-phenylcyclopent-2-enone,<sup>6</sup> 3-benzylcyclopent-2-enone,<sup>7</sup> 3-(benzyloxymethyl)cyclopent-2-enone,<sup>8</sup> methyl 3-oxocyclopent-1-enecarboxylate, 3-acetylcyclopent-2-enone,<sup>9</sup> 3-butylcyclohex-2-enone,<sup>10</sup> 3-cyclohexylcyclohex-2-one.<sup>11</sup>

**Column-free preparation of di-*tert*-butyl 2,6-dimethyl-1,4-dihydropyridine-3,5-dicarboxylate:** A suspension of hexamethylenetetramine (67 g, 474 mmol) and ammonium acetate (73 g, 948 mmol) in neat *tert*-butyl acetoacetate (150 g, 948 mmol) was reacted in a 1 L beaker using a conventional microwave on “high” power, with thorough stirring for 30 seconds after each heating period, as follows: 2 x 45 seconds, 3 x 30 seconds. The light green solution was next heated for another 30 seconds and was followed by VIGOROUS bubbling. The solution was stirred with the spatula vigorously for ~5 minutes. The resulting amorphous orange solid was heated for another 15 seconds

(4) Collins, S.; Hong, Y.; Mataoka, M.; Nguyen, T. *J. Org. Chem.* **1990**, *55*, 3395.

(5) Ponaras, A. A.; Zaim, O.; Pazo, Y.; Ohannesian, L. *J. Org. Chem.* **1988**, *53*, 1110. and Garbisch, E. W., Jr.; Sprecher, R. F. *J. Am. Chem. Soc.* **1969**, *91*, 6785.

(6) Jurkauskas, V.; Sadigni, J. P.; Buchwald, S. L. *Org. Lett.* **2003**, *5*, 2417.

(7) Moritani, Y.; Appella, D. H.; Jurkauskas, V.; Buchwald, S. L. *J. Am. Chem. Soc.* **2000**, *122*, 6797.

(8) Dauben, W. G.; Warshawsky, A. M. *J. Org. Chem.* **1990**, *55*, 3075.

(9) Yu, J.-Q.; Corey, E. J. *J. Am. Chem. Soc.* **2003**, *125*, 3232. And Catino, A. J.; Forslund, R. E.; Doyle, M. P. *J. Am. Chem. Soc.* **2004**, *126*, 13622.

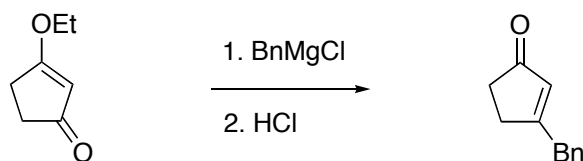
(10) Mudryk, B.; Cohen, T. *J. Am. Chem. Soc.* **1993**, *115*, 3854.

(11) Snider, B. B.; Rodini, D. J.; van Straten, J. *J. Am. Chem. Soc.* **1980**, *102*, 5872.

and stirred for 5 minutes. The orange solid was allowed to harden and cool to room temperature, after which it was dissolved in dichloromethane (500 mL) with the aid of a spatula. To this red solution was added sodium sulfate (20 g) and the mixture was stirred for 20 minutes. The dissolving/drying process should take less than 1 hour to minimize pyridine formation. The solution was vacuum filtered using a glass fritted Buchner filter funnel and then concentrated to an orange solid. After ensuring complete removal of dichloromethane via high vacuum, the solid was transferred to a glass fritted Buchner filter funnel in pentane and thoroughly triturated, in order, with 10% NaOH (3 x 200 mL), water (2 x 200 mL), 5% HCl (4 x 200 mL), water (2 x 200 mL), and pentane (4 x 200 mL). The resulting light yellow crude solid is dissolved in EtOH (ratio 140 g: 500 mL EtOH) by gently heating with a heat gun. Here the EtOH should not boil. The resulting solution was allowed to cool to room temperature and then placed at 4 °C for 2 hours. The resulting solid was filtered off and triturated 3 x 150 mL ice cold EtOH. SAVE THE FILTRATE. The solid was next triturated 4 x 200 mL pentane. The resulting solid was dried on high vacuum for 16 hours to provide 42 g of a light yellow solid (30% yield)

It is possible to recrystallize the EtOH filtrate by re-cooling to 4 °C overnight and repeating the steps above. Due to the presence of pyridine in the second crop of crystals a second recrystallization sequence was repeated as above.

**General procedure for the preparation of the starting materials:**



**3-benzylcyclopent-2-enone:** To a  $-78\text{ }^{\circ}\text{C}$  solution of benzyl magnesium chloride (14.3 mL, 28.5 mmol, 1.2 eq., 2 M solution in THF) in ether (50 mL) was slowly added 3-ethoxycyclopent-2-enone (2.84 mL, 23.8 mmol, 1 eq.). The reaction mixture was warmed up to  $-30\text{ }^{\circ}\text{C}$  over 1 hour followed by addition of a 1 M solution of HCl until the pH was adjusted to 1 as indicated by litmus paper. The solution was warmed up to room temperature and the layers were separated. The aqueous phase was extracted with 40 mL of Et<sub>2</sub>O (3×) and the combined organic layers were washed with 100 mL of brine (1×), dried over anhydrous MgSO<sub>4</sub>, and concentrated *in vacuo*. The residual oil was purified by flash chromatography (25% EtOAc/hexanes) to afford the title compound as a colorless oil (3.1 g, 76% yield).

**(Z)-1-butylcyclohept-2-enol:** To a clear solution of 2-cyclohepten-1-one (5 g, 45.5 mmol) in ether (50 mL), cooled to  $0\text{ }^{\circ}\text{C}$ , was added *n*-BuLi (2.0 M in hexanes, 25 mL, 50.0 mmol) dropwise to produce an opaque yellow solution. The reaction was stirred for 2 hours at  $0\text{ }^{\circ}\text{C}$  and then warmed to room temperature. After 1 hour, the reaction was complete as determined by TLC, and quenched in 50 mL NH<sub>4</sub>Cl. The organic layer was separated and the aqueous layer was extracted with 50 mL of Et<sub>2</sub>O (3×). The combined

organic layers were dried over  $\text{Na}_2\text{SO}_4$ , filtered and concentrated *in vacuo*. The resulting residue was purified by flash chromatography (10%  $\text{Et}_2\text{O}$ /pentane) to afford the title compound as a light yellow oil (2 g, 26% yield). IR (film) 3377, 3015, 2930, 2860, 1456, 1378, 1335, 1223, 1121, 1103, 1043, 997  $\text{cm}^{-1}$ ;  $^1\text{H}$  NMR (300 MHz,  $\text{CDCl}_3$ )  $\delta$  5.69 (dt, 1H,  $J = 11.9, 5.6$  Hz,  $\text{CCH}=\text{CH}$ ), 5.59 (d, 1H,  $J = 11.9$  Hz,  $\text{CCH}=\text{CH}$ ), 2.17 – 2.09 (m, 2H), 1.84 – 1.45 (m, 9H), 1.38 – 1.27 (m, 4H), 0.93 – 0.88 (m, 3H);  $^{13}\text{C}$  NMR (75 MHz,  $\text{CDCl}_3$ )  $\delta$  139.1, 130.0, 76.1, 41.1, 38.5, 27.6, 27.5, 25.6, 24.1, 23.2, 14.1; HRMS ( $\text{EI}^+$ ) exact mass calculated for  $[\text{M}]^+$  ( $\text{C}_{11}\text{H}_{20}\text{O}$ ) requires  $m/z$  168.1514, found  $m/z$  168.1516.

**(Z)-3-butylcyclohept-2-enone:** To a solution of (Z)-1-butylcyclohept-2-enol (2 g, 11.9 mmol) dissolved in dichloromethane (60 mL) was added pyridine chlorochromate on basic alumina (20 wt.%, 25.7 g, 23.8 mmol). The resulting reddish solution was stirred at room temperature for 2 hours until determined to be complete by TLC. The mixture was diluted in 100 mL  $\text{Et}_2\text{O}$  and stirred for 1 hour after which it was poured over filter paper that was subsequently washed with the  $\text{Et}_2\text{O}$ . The filtrate was partially concentrated (30 mL) and passed through a Florisil column with  $\text{Et}_2\text{O}$  (100 mL). The resulting colorless solution was concentrated and purified by flash chromatography (5%  $\text{Et}_2\text{O}$ /Pentane) to provide a colorless oil (920 mg, 47 % yield). IR (film) 2933, 2864, 1662, 1458, 1421, 1375, 1344, 1322, 1267, 1201, 1124, 1103, 1048, 937, 875, 855  $\text{cm}^{-1}$ ;  $^1\text{H}$  NMR (300 MHz,  $\text{CDCl}_3$ )  $\delta$  5.89 (s, 1H,  $\text{COCH}$ ), 2.58 – 2.53 (m, 2H,  $\text{C}=\text{OH}_2$ ), 2.41– 2.38 (m, 2H,  $\text{HC}=\text{CCH}_2$ ), 2.18 (t, 2H,  $J = 6.91$  Hz,  $\text{HC}=\text{CCH}_2(\text{CH}_2)_2\text{CH}_3$ ), 1.80 – 1.74 (m, 2H,  $\text{COCH}_2\text{CH}_2$ ), 1.50 – 1.40 (m, 2H,  $\text{HC}=\text{CCH}_2\text{CH}_2$ ), 1.38 – 1.25 (m, 2H,  $\text{HC}=\text{C}(\text{CH}_2)_2\text{CH}_2\text{CH}_3$ ), 0.90 (t, 3H,  $J = 7.18$  Hz,  $\text{CH}_2\text{CH}_3$ );  $^{13}\text{C}$  NMR (75 MHz,  $\text{CDCl}_3$ )  $\delta$

204.4, 162.4, 128.2, 42.1, 40.8, 32.5, 29.7, 25.1, 22.4, 21.2, 13.9; HRMS (EI<sup>+</sup>) exact mass calculated for [M]<sup>+</sup> (C<sub>11</sub>H<sub>18</sub>O) requires *m/z* 166.1358, found *m/z* 166.1359.

**General Procedures for the enantioselective hydrogenation of cyclic enones:**

Procedure A: To a room temperature solution of 3-substituted-cyclopent-2-enone (1 mmol) dissolved in 1 mL of Et<sub>2</sub>O (1 M) was added trichloroacetic acid (33 mg, 0.2 mmol, 0.2 eq.), (2*S*,5*S*)-5-benzyl-3-methyl-2-(5-methylfuran-2-yl)imidazolidin-4-one (54 mg, 0.2 mmol, 0.2 eq.), and ethyl Hantzsch ester (304 mg, 1.2 mmol, 1.2 eq.). The resulting yellow suspension was stirred at room temperature until the reaction was judged to be complete by TLC. The reaction mixture was passed through a short pad of silica gel and eluted with Et<sub>2</sub>O. The resulting solution was concentrated *in vacuo* and purified by flash chromatography (solvent noted) to provide the title compound.

Procedure B: To a solution of 3-substituted-cyclopent-2-enone (1 mmol) dissolved in 0.5 mL of Et<sub>2</sub>O (0.5 M), cooled to 4 °C using an ice bath, was added trichloroacetic acid (33 mg, 0.2 mmol, 0.2 eq.), (2*S*,5*S*)-5-benzyl-3-methyl-2-(5-methylfuran-2-yl)imidazolidin-4-one (54 mg, 0.2 mmol, 0.2 eq.), and *t*-Butyl Hantzsch ester (340 mg, 1.1 mmol, 1.1 eq.). The resulting yellow suspension was stirred at 4 °C until the reaction was judged to be complete by TLC. The reaction mixture was passed through a short pad of silica gel and eluted with Et<sub>2</sub>O. The resulting solution was concentrated *in vacuo* and purified by flash chromatography (solvent noted) to provide a crude mixture of the title compound

and pyridine by-product. The pyridine was removed by washing with 5 mL 6 M HCl (3×), 5 mL H<sub>2</sub>O (1×) and 5 mL sat. NaHCO<sub>3</sub> (1×) to provide the title compound.

**(*R*)-3-methylcyclopentanone:** Prepared according to the general procedure A from 3-methylcyclopent-2-enone (20 mg, 0.204 mmol) for 26 hours to provide the title compound (77% conversion, 95% ee). Conversion was determined via GLC analysis by comparison with an internal standard (BnOMe). The physical data were identical in all respects to those of the commercially available (*R*)-3-methylcyclopentanone. The enantiomeric ratio was determined by GLC using a Bodman Chiraldex Γ-TA (30 m × 0.25 mm) column (100 °C isotherm, 1 mL/min.); (*S*) isomer  $t_r$  = 25.1 min. and (*R*) isomer  $t_r$  = 25.8 min.

General procedure B provided the title compound (72% conversion, 95% ee) after 8.5 hours.

**(*R*)-3-cyclohexylcyclopentanone:** Prepared according to the general procedure A from 3-cyclohexylcyclopent-2-enone (164 mg, 1 mmol) for 23 hours to provide the title compound as a yellow oil (152 mg, 93% yield, 96% ee) after purification by flash chromatography on Iatrobeds® (15 – 20% Et<sub>2</sub>O/pentane). The physical data were identical in all respects to those previously reported.<sup>12</sup> The enantiomeric ratio was determined by GLC using a Hydrodex-B-TBDAC (50 m × 0.25 mm) column (105 °C isotherm, 1 mL/min.); (*S*) isomer  $t_r$  = 127.7 min. and (*R*) isomer  $t_r$  = 127.9 min.  $[\alpha]_D^{22}$  = +8.6 ° (c = 1.00, CHCl<sub>3</sub>).

---

(12) Jones, P.; Reddy, C. K.; Knochel, P. *Tetrahedron* **1998**, *54*, 1471. (Racemic product, no optical rotation.)



General procedure B provided the title compound (82% yield, 93% ee) after 11 hours.

**(*R*)-3-*tert*-butylcyclopentanone:** Prepared according to the general procedure A from 3-*tert*-butylcyclopent-2-enone (138 mg, 1 mmol) for 8 hours to provide the title compound as a colorless oil (126 mg, 85% yield, 96% ee) after purification by flash chromatography on Iatrobeads® (20% Et<sub>2</sub>O/pentane). The physical data were identical in all respects to those previously reported.<sup>13</sup> The enantiomeric ratio was determined by GLC using a Bodman Chiraldex Γ-TA (30 m × 0.25 mm) column (90 °C isotherm, 1 mL/min.); (*S*) isomer *t*<sub>r</sub> = 14.4 min. and (*R*) isomer *t*<sub>r</sub> = 15.0 min.  $[\alpha]_D^{22} = +150.3^\circ$  (c = 1.00, CHCl<sub>3</sub>).

General procedure B provided the title compound (81% conversion, 96% ee) after 5.5 hours.

**(*R*)-3-benzylcyclopentanone:** Prepared according to the general procedure A from 3-benzylcyclopent-2-enone (172 mg, 1 mmol) for 24 hours at 0 °C. After the reaction mixture was passed through a short pad of silica gel, the resulting mixture was poured into 5 mL of a 10% HCl solution and diluted with 5 mL of Et<sub>2</sub>O. The layers were separated, then the organic layer was washed with 5 mL of a 10% HCl solution (4×) and with 5 mL of water (1×). The resulting solution was dried over MgSO<sub>4</sub> and concentrated *in vacuo* to provide the title compound as a colorless oil (158 mg, 91% yield, 90% ee) after purification by flash chromatography on Iatrobeads® (2% Et<sub>2</sub>O/benzene). The physical data were identical in all respects to those previously reported.<sup>14</sup> The enantiomeric ratio

(13) Ahlbrecht, H.; Weber, P. *Synthesis* **1992**, 1019. (Racemic product, no optical rotation.)

(14) Yanagisawa, A.; Habaue, S.; Yasue, K.; Yamamoto, H. *J. Am. Chem. Soc.* **1994**, *116*, 6130. and Moritani, Y.; Appella, D. H.; Jurkauskas, V.; Buchwald, S. L. *J. Am. Chem. Soc.* **2000**, *122*, 6797. (Reported an optical rotation of  $-96^\circ$  for the (*S*)-isomer that is 96% e.)

was determined by GLC using a Hydrodex-B-TBDAC (50 m  $\times$  0.25 mm) column (145 °C isotherm, 1 mL/min.); (*S*) isomer  $t_r$  = 91.5 min. and (*R*) isomer  $t_r$  = 90.1 min.  $[\alpha]_D^{22}$  = +83.9 ° (c = 1.00, CHCl<sub>3</sub>).

General procedure B provided the title compound (78% yield, 90% ee) after 11 hours.

**(*R*)-3-(benzyloxymethyl)cyclopentanone:** Prepared according to the general procedure A from 3-(benzyloxymethyl)cyclopent-2-enone (202 mg, 1 mmol) for 24 h at 0 °C. After the reaction mixture was passed through a short pad of silica gel, the resulting solution was poured into 5 mL of a 10% HCl solution and diluted with 5 mL of Et<sub>2</sub>O. The layers were separated, then the organic layer was washed with 5 mL of a 10% HCl solution (4 $\times$ ) and with 5 mL of water (1 $\times$ ). The resulting solution was dried over MgSO<sub>4</sub> and concentrated *in vacuo* to provide the title compound as a colorless oil (155 mg, 76% yield, 91% ee) after purification by flash chromatography on silica gel (15% Et<sub>2</sub>O/pentane). The enantiomeric ratio was determined by GLC using a Hydrodex-B-TBDAC (50 m  $\times$  0.25 mm) column (150 °C isotherm, 1 mL/min.); (*S*) isomer  $t_r$  = 151.2 min. and (*R*) isomer  $t_r$  = 153.2 min. IR (film) 3030, 2860, 1740, 1404, 1100 cm<sup>-1</sup>; <sup>1</sup>H NMR (300 MHz, CDCl<sub>3</sub>)  $\delta$  7.42 – 7.28 (m, 5H, ArH<sub>5</sub>), 4.55 (s, 2H, CH<sub>2</sub>Ph), 3.51 (d, 2H, *J* = 6.3 Hz, CHCH<sub>2</sub>O), 2.61 – 2.49 (m, 1H), 2.44 – 2.25 (m, 2H), 2.23 – 2.01 (m, 3H), 1.84 – 1.71 (m, 1H); <sup>13</sup>C NMR (75 MHz, CDCl<sub>3</sub>)  $\delta$  219.2, 138.1, 128.3, 127.4, 126.8, 73.2, 73.0, 41.9, 37.8, 36.7, 26.0; HRMS (EI<sup>+</sup>) exact mass calculated for [M]<sup>+</sup> (C<sub>13</sub>H<sub>16</sub>O<sub>2</sub>) requires *m/z* 204.1150, found *m/z* 204.1144;  $[\alpha]_D^{22}$  = +31.2 ° (c = 1.0, CHCl<sub>3</sub>).

General procedure B provided the title compound (77% yield, 91% ee) after 13 hours.

**(R)-3-phenylcyclopentanone:** Prepared according to the general procedure A from 3-phenylcyclopent-2-enone (158 mg, 1 mmol) for 8.5 hours to provide the title compound as a light yellow oil (140 mg, 89% yield, 74% ee) after purification by flash chromatography on Iatrobeds® (0 - 2% Et<sub>2</sub>O/benzene). The physical data were identical in all respects to those previously reported.<sup>15</sup> The enantiomeric ratio was determined by GLC using a Hydrodex-B-TBDAC (50 m × 0.25 mm) column (145 °C isotherm, 1 mL/min.); (*S*) isomer  $t_r$  = 56.3 min. and (*R*) isomer  $t_r$  = 61.3 min.  $[\alpha]_D^{22} = +60.2^\circ$  ( $c = 1.00$ , CHCl<sub>3</sub>).

General procedure B provided the title compound (73% yield, 91% ee) after 9 hours.

**(R)-methyl 3-oxocyclopentanecarboxylate:** Prepared according to the general procedure A from methyl 3-oxocyclopent-1-enecarboxylate (140 mg, 1 mmol) for 24 hours at 0 °C to provide the title compound as a colorless oil (108 mg, 76% yield, 90% ee) after purification by flash chromatography on silica gel (40% Et<sub>2</sub>O/pentane). The physical data were identical in all respects to those previously reported.<sup>16</sup> The enantiomeric ratio was determined by GLC using a Hydrodex-B-TBDAC (50 m × 0.25 mm) column (130 °C isotherm, 1 mL/min.); (*S*) isomer  $t_r$  = 41.9 min. and (*R*) isomer  $t_r$  = 43.5 min.  $[\alpha]_D^{22} = +28.0^\circ$  ( $c = 1.00$ , CHCl<sub>3</sub>).

General procedure B provided the title compound (78% yield, 93% ee) after 1 hour.

---

(15) Gadwood, R. C.; Mallick, I. M.; DeWinter, A. J. *J. Org. Chem.* **1987**, *52*, 774. Gomez-Bengoa, E.; Heron, N. M.; Didiuk, M. T.; Luchaco, C. A.; Hoveyda, A. H. *J. Am. Chem. Soc.* **1998**, *120*, 7649. and Hashimoto, S.-I.; Watanabe, N.; Ikegami, S. *Synlett.* **1994**, 353.

(16) Ranu, B. C.; Dutta, J. Guchhait, S. K. *Org. Lett.* **2001**, *3*, 2603. The absolute stereochemistry was assigned by analogy.

**(R)-3-acetylcyclopentanone:** Prepared according to the general procedure A from 3-acetylcyclopent-2-enone (124 mg, 1 mmol) for 24 hours at 0 °C to provide the title compound as a colorless oil (103 mg, 82% yield, 93% ee) after purification by flash chromatography on silica gel (50% Et<sub>2</sub>O/benzene). The physical data were identical in all respects to those previously reported.<sup>17</sup> The enantiomeric ratio was determined by GLC using a Hydrodex-B-TBDAC (50 m × 0.25 mm) column (145 °C isotherm, 1 mL/min.); (*S*) isomer  $t_r$  = 52.0 min. and (*R*) isomer  $t_r$  = 53.3 min.  $[\alpha]_D^{22} = +56.3^\circ$  (c = 1.0, CHCl<sub>3</sub>).

General procedure B provided the title compound (83% yield, 93% ee) after 1 hour.

**(R)-3-butylcyclohexanone:** Prepared according to the general procedure A from 3-butylcyclohexen-2-one (168 mg, 1.09 mmol) in 0.2 M Et<sub>2</sub>O for 43 hours at room temperature to provide the title compound as a colorless oil (128.3 mg, 75% yield, 88% ee) after purification by flash chromatography on silica gel (5% Et<sub>2</sub>O/pentane). The physical data were identical in all respects to those previously reported.<sup>18</sup> The enantiomeric ratio was determined by GLC using a Hydrodex-B-TBDAC (50 m × 0.25 mm) column (150 °C isotherm, 1 mL/min.); (*S*) isomer  $t_r$  = 37.0 min. and (*R*) isomer  $t_r$  = 36.0 min.  $[\alpha]_D^{22} = +15.5^\circ$  (c = 1.00, CHCl<sub>3</sub>).

General procedure B provided the title compound (82% yield, 90% ee) after 25 hours.

---

(17) Monte, W. T.; Baizer, M. M.; Little, R. D. *J. Org. Chem.* **1983**, *48*, 803. (Racemic product, no optical rotation.)

(18) Jones, P.; Reddy, C. K.; Knowche, P. *Tetrahedron* **1998**, *54*, 1471. and Moritani, Y.; Appella, D. H.; Jurkauskas, V.; Buchwald, S. L. *J. Am. Chem. Soc.* **2000**, *122*, 6797. (Reported a rotation of  $-17^\circ$  for the (*S*)-enantiomer that is 87% ee.)

**(R)-3-cyclohexylcyclohexanone:** Prepared according to the general procedure A from 3-cyclohexylcyclohexen-2-one (178 mg, 1.09 mmol) in 0.2 M Et<sub>2</sub>O for 43 hours at room temperature to provide the title compound as a colorless oil (157 mg, 80% yield, 90% ee) after purification by flash chromatography on silica gel (5% Et<sub>2</sub>O/pentane). The enantiomeric ratio was determined by GLC using a Hydrodex-B-TBDAC (50 m × 0.25 mm) column (110 °C isotherm, 1 mL/min.); (*S*) isomer  $t_r$  = 73.5 min. and (*R*) isomer  $t_r$  = 65.2 min. IR (film) 2924, 2853, 1715, 1449, 14223, 1346, 1317, 1263, 1225, 1101, 1056, 982, 892, 866 cm<sup>-1</sup>; <sup>1</sup>H NMR (300 MHz, CDCl<sub>3</sub>)  $\delta$  2.44 – 2.21 (m, 3H), 2.16 – 2.04 (m, 2H), 1.93 – 1.85 (m, 1H), 1.80 – 1.54 (m, 8H), 1.47 – 1.33 (m, 1H), 1.32 – 1.11 (m, 3H), 1.08 – 0.92 (m, 2H); <sup>13</sup>C NMR (75 MHz, CDCl<sub>3</sub>)  $\delta$  212.9, 45.6, 44.7, 42.7, 41.6, 30.0, 29.9, 28.4, 26.6, 26.59, 25.54, 25.6; HRMS (EI<sup>+</sup>) exact mass calculated for [M]<sup>+</sup> (C<sub>12</sub>H<sub>20</sub>O) requires  $m/z$  180.1514, found  $m/z$  180.1508;  $[\alpha]_D^{22}$  = +11.9 ° (c = 1.05, CHCl<sub>3</sub>). General procedure B provided the title compound (71% yield, 88% ee) after 24 hours.

**(R)-3,3,5-trimethylcyclohexanone:** Prepared according to the general procedure A from isophorone (138 mg, 1.09 mmol) in 0.2 M Et<sub>2</sub>O for 48 hours at room temperature to provide the title compound as a colorless oil (100 mg, 65% yield, 97% ee) after purification by flash chromatography on silica gel (5% Et<sub>2</sub>O/pentane). The physical data were identical in all respects to those previously reported.<sup>19</sup> The enantiomeric ratio was determined by GLC using a Hydrodex-B-TBDAC (50 m × 0.25 mm) column (110 °C isotherm, 1 mL/min.); (*S*) isomer  $t_r$  = 11.8 min. and (*R*) isomer  $t_r$  = 12.4 min.  $[\alpha]_D^{22}$  = – 18.7 ° (c = 1.03, CHCl<sub>3</sub>).

(19) Allinger, N. L.; Riew, C. K. *J. Org. Chem.* **1975**, *40*, 1316. (Reported a rotation of +20.3 ° for the (*S*)-enantiomer that is 75% ee.)

General procedure B provided the title compound (66% yield, 98% ee) after 40 hours.

**(*R*)-3-butylcycloheptanone:** Prepared according to the general procedure A from 3-butylcyclohept-2-enone (166.3 mg, 1 mmol) for 48 hours at room temperature to provide the title compound as a light yellow oil (106 mg, 63% yield, 82% ee) after purification by flash chromatography on silica gel (5% Et<sub>2</sub>O/pentane). The physical data were identical in all respects to those previously reported.<sup>20</sup> The enantiomeric ratio was determined by GLC using a Hydrodex-B-TBDAC (50 m × 0.25 mm) column (105 °C isotherm, 1 mL/min.); (*S*) isomer  $t_r$  = 100.6 min. and (*R*) isomer  $t_r$  = 102.7 min.  $[\alpha]_D^{22} = +40.3^\circ$  (c = 1.05, CHCl<sub>3</sub>).

General procedure B provided the title compound (70% yield, 92% ee) after 9 hours.

---

(20) Strangeland, E. L.; Sammakia, T. *Tetrahedron* **1997**, *53*, 16503. (Reported a rotation of +31.4 ° for a product that is 92% ee.)

CALIFORNIA INSTITUTE OF TECHNOLOGY  
BECKMAN INSTITUTE  
X-RAY CRYSTALLOGRAPHY LABORATORY

Date 17 January 2006

**Crystal Structure Analysis of:**

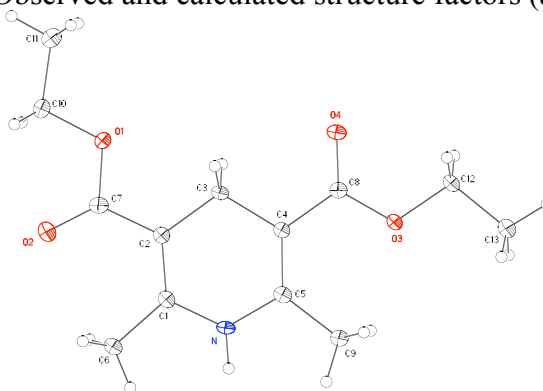
**JBT02**

(shown below)

**For** Investigator: Jamie Tuttle ext. 6061  
Advisor: D. W. C. MacMillan ext. 6044  
Account Number: DWCM.45100-1-ENDOW.451000  
**By** Michael W. Day 116 Beckman ext. 2734  
e-mail: mikeday@caltech.edu

Contents

Table 1. Crystal data
Figures Figures
Table 2. Atomic Coordinates
Table 3. Full bond distances and angles
Table 4. Anisotropic displacement parameters
Table 5. Hydrogen atomic coordinates
Table 6. Hydrogen bond distances and angles
Table 7. Observed and calculated structure factors (available upon request)



JBT02

**Note:** The crystallographic data have been deposited in the Cambridge Database (CCDC) and has been placed on hold pending further instructions from me. The deposition number is 295385. Ideally the CCDC would like the publication to contain a footnote of the type: "Crystallographic data have been deposited at the CCDC, 12 Union Road, Cambridge CB2 1EZ, UK and copies can be obtained on request, free of charge, by quoting the publication citation and the deposition number 295385."



**Table 1. Crystal data and structure refinement for JBT02 (CCDC 295385).**

Empirical formula	$C_{13}H_{19}NO_4$	
Formula weight	253.29	
Crystallization Solvent	Not given	
Crystal Habit	Block	
Crystal size	0.34 x 0.22 x 0.15 mm <sup>3</sup>	
Crystal color	Pale yellow	
<b>Data Collection</b>		
Type of diffractometer	Bruker SMART 1000	
Wavelength	0.71073 Å MoK $\alpha$	
Data Collection Temperature	100(2) K	
$\theta$ range for 5978 reflections used in lattice determination	2.73 to 33.41°	
Unit cell dimensions	a = 24.3323(16) Å b = 6.8424(5) Å c = 7.4651(5) Å	$\beta = 92.078(2)^\circ$
Volume	1242.06(15) Å <sup>3</sup>	
Z	4	
Crystal system	Monoclinic	
Space group	C2/m	
Density (calculated)	1.355 Mg/m <sup>3</sup>	
F(000)	544	
Data collection program	Bruker SMART v5.630	
$\theta$ range for data collection	1.67 to 33.82°	
Completeness to $\theta = 33.82^\circ$	91.8 %	
Index ranges	$-35 \leq h \leq 34, -10 \leq k \leq 10, -11 \leq l \leq 11$	
Data collection scan type	$\omega$ scans at 5 $\phi$ settings	
Data reduction program	Bruker SAINT v6.45A	
Reflections collected	12600	
Independent reflections	2457 [ $R_{int} = 0.0584$ ]	
Absorption coefficient	0.100 mm <sup>-1</sup>	
Absorption correction	None	
Max. and min. transmission	0.9851 and 0.9667	

**Table 1 (cont.)****Structure solution and Refinement**

Structure solution program	Bruker XS v6.12
Primary solution method	Direct methods
Secondary solution method	Difference Fourier map
Hydrogen placement	Difference Fourier map
Structure refinement program	Bruker XL v6.12
Refinement method	Full matrix least-squares on $F^2$
Data / restraints / parameters	2457 / 0 / 152
Treatment of hydrogen atoms	Unrestrained
Goodness-of-fit on $F^2$	2.363
Final R indices [ $I > 2\sigma(I)$ , 1961 reflections]	$R1 = 0.0465$ , $wR2 = 0.0870$
R indices (all data)	$R1 = 0.0595$ , $wR2 = 0.0892$
Type of weighting scheme used	Sigma
Weighting scheme used	$w = 1/\sigma^2(F_o^2)$
Max shift/error	0.000
Average shift/error	0.000
Largest diff. peak and hole	0.505 and -0.402 e.Å <sup>-3</sup>

**Special Refinement Details**

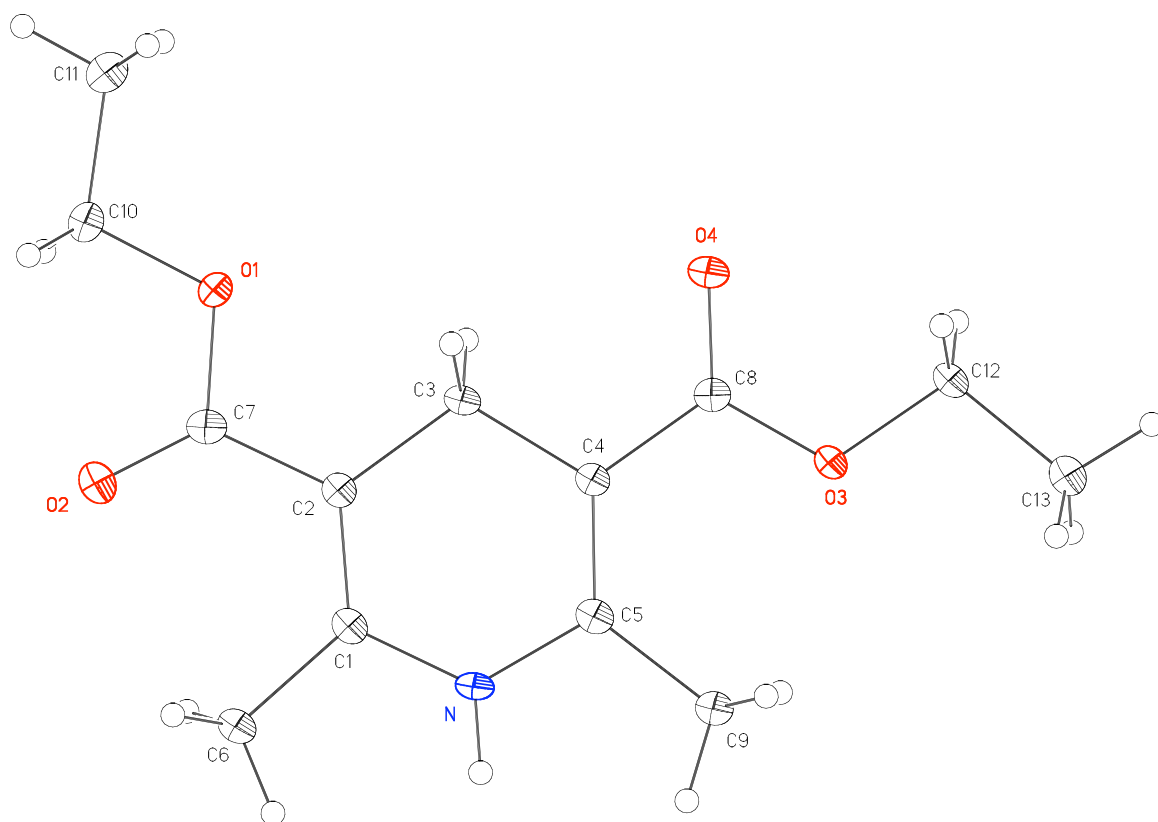
This structure has been previously reported 21 and appears in the CSD as deposition EXCMHP. The structure presented here is not substantially different than the previously reported structure. However, I believe the structure is more correctly described in the monoclinic system with space group  $C2/m$ . The data collected here is substantially more complete than the previously reported structure and warrants inclusion as such in any future publication.

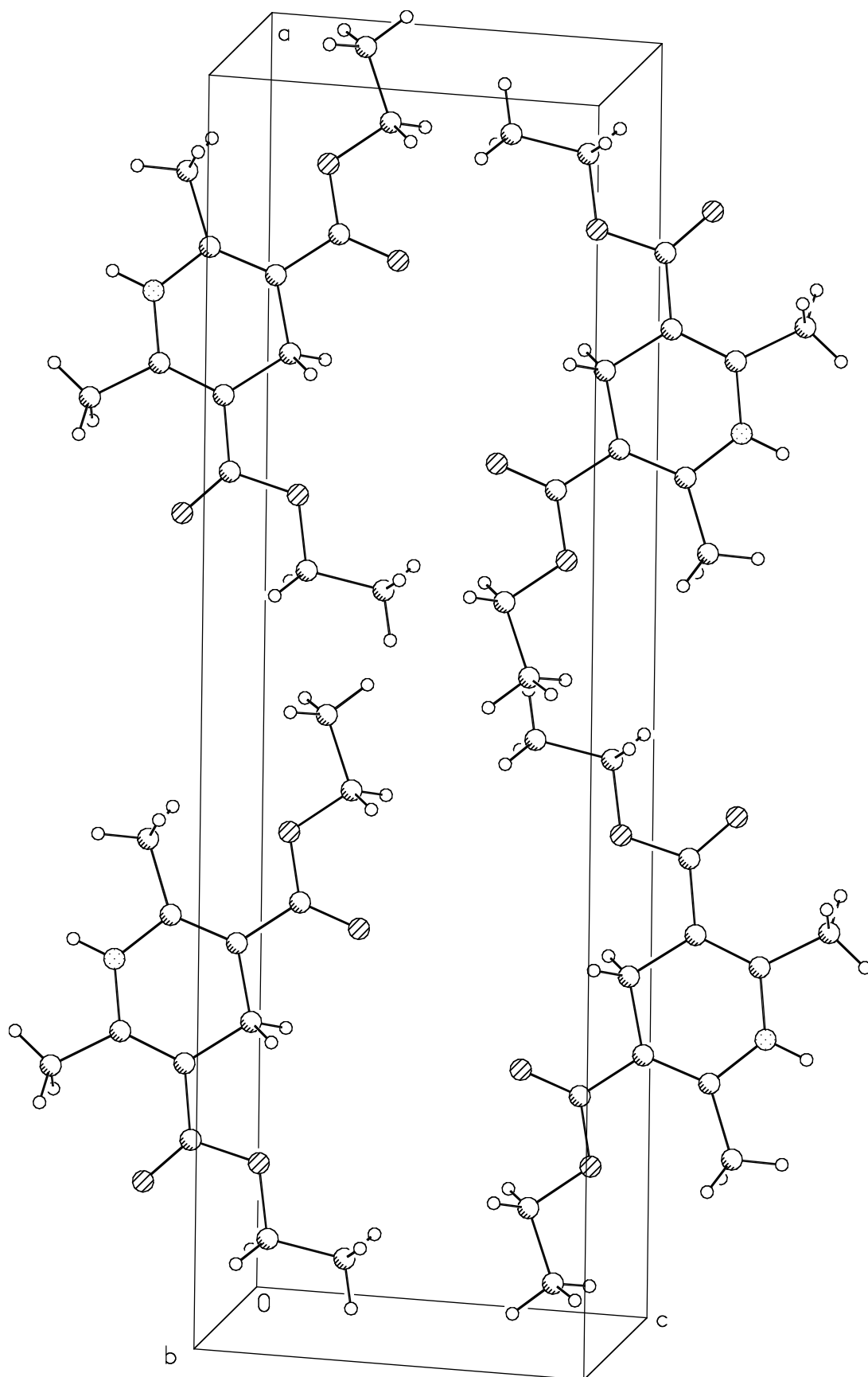
Refinement of  $F^2$  against ALL reflections. The weighted R-factor ( $wR$ ) and goodness of fit ( $S$ ) are based on  $F^2$ , conventional R-factors ( $R$ ) are based on  $F$ , with  $F$  set to zero for negative  $F^2$ . The threshold expression of  $F^2 > 2\sigma(F^2)$  is used only for calculating R-factors(gt) etc. and is not relevant to the choice of reflections for refinement. R-factors based on  $F^2$  are statistically about twice as large as those based on  $F$ , and R-factors based on ALL data will be even larger.

All esds (except the esd in the dihedral angle between two l.s. planes) are estimated using the full covariance matrix. The cell esds are taken into account individually in the estimation of esds in distances, angles and torsion angles; correlations between esds in cell parameters are only used when they are defined by crystal symmetry. An approximate (isotropic) treatment of cell esds is used for estimating esds involving l.s. planes.

---

21 Lenstra, A.T.H., *Molecular-Structure of 3,5-Diethoxycarbonyl-2,6-Dimethyl-1,4-Dihydropyridine - X-ray Study*. Bulletin des Societes Chimiques Belges, 1979. **88**(3): p. 133-141.





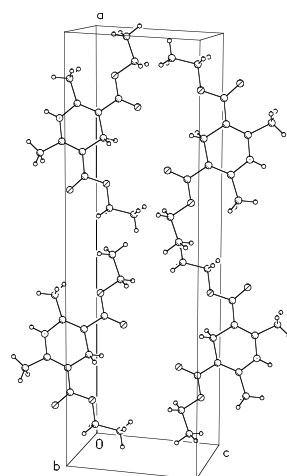
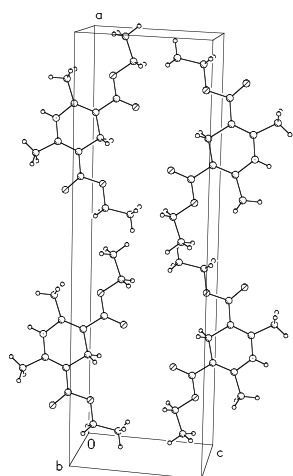


**Table 2. Atomic coordinates ( $\times 10^4$ ) and equivalent isotropic displacement parameters ( $\text{\AA}^2 \times 10^3$ ) for JBT02 (CCDC 295385).  $U(\text{eq})$  is defined as the trace of the orthogonalized  $U^{ij}$  tensor.**

	x	y	z	$U_{\text{eq}}$
O(1)	3765(1)	0	-810(1)	17(1)
O(2)	3980(1)	0	2152(1)	24(1)
O(3)	1150(1)	0	-1489(1)	18(1)
O(4)	1866(1)	0	-3306(1)	18(1)
N	2253(1)	0	2957(1)	15(1)
C(1)	2816(1)	0	2782(2)	13(1)
C(2)	3029(1)	0	1129(2)	13(1)
C(3)	2663(1)	0	-566(2)	13(1)
C(4)	2054(1)	0	-175(2)	12(1)
C(5)	1874(1)	0	1529(2)	13(1)
C(6)	3129(1)	0	4556(2)	19(1)
C(7)	3625(1)	0	947(2)	15(1)
C(8)	1695(1)	0	-1787(2)	13(1)
C(9)	1292(1)	0	2129(2)	18(1)
C(10)	4354(1)	0	-1059(2)	19(1)
C(11)	4461(1)	0	-3032(2)	22(1)
C(12)	786(1)	0	-3072(2)	19(1)
C(13)	209(1)	0	-2416(2)	25(1)

**Table 3. Bond lengths [Å] and angles [°] for JBT02 (CCDC 295385).**

O(1)-C(7)	1.3673(15)	C(7)-O(1)-C(10)	113.89(10)
O(1)-C(10)	1.4498(17)	C(8)-O(3)-C(12)	116.07(10)
O(2)-C(7)	1.2241(15)	C(1)-N-C(5)	124.32(11)
O(3)-C(8)	1.3546(16)	C(1)-N-H(1)	119.5(10)
O(3)-C(12)	1.4506(15)	C(5)-N-H(1)	116.2(10)
O(4)-C(8)	1.2218(15)	C(2)-C(1)-N	119.94(10)
N-C(1)	1.3811(18)	C(2)-C(1)-C(6)	127.18(12)
N-C(5)	1.3849(16)	N-C(1)-C(6)	112.88(11)
N-H(1)	0.862(16)	C(1)-C(2)-C(7)	119.87(11)
C(1)-C(2)	1.3557(17)	C(1)-C(2)-C(3)	121.66(12)
C(1)-C(6)	1.5021(17)	C(7)-C(2)-C(3)	118.47(11)
C(2)-C(7)	1.4606(19)	C(4)-C(3)-C(2)	112.73(10)
C(2)-C(3)	1.5221(16)	C(4)-C(3)-H(3A)	109.6(6)
C(3)-C(4)	1.5183(18)	C(2)-C(3)-H(3A)	108.5(6)
C(3)-H(3A)	0.987(10)	C(5)-C(4)-C(8)	124.46(12)
C(4)-C(5)	1.3612(17)	C(5)-C(4)-C(3)	121.99(10)
C(4)-C(8)	1.4611(16)	C(8)-C(4)-C(3)	113.55(10)
C(5)-C(9)	1.501(2)	C(4)-C(5)-N	119.36(12)
C(6)-H(6A)	0.952(13)	C(4)-C(5)-C(9)	128.26(11)
C(6)-H(6B)	0.94(2)	N-C(5)-C(9)	112.38(11)
C(9)-H(9A)	0.965(12)	C(1)-C(6)-H(6A)	110.9(7)
C(9)-H(9B)	0.959(18)	C(1)-C(6)-H(6B)	109.1(11)
C(10)-C(11)	1.505(2)	H(6A)-C(6)-H(6B)	110.7(9)
C(10)-H(10A)	0.994(11)	O(2)-C(7)-O(1)	120.72(12)
C(11)-H(11A)	0.965(12)	O(2)-C(7)-C(2)	127.40(12)
C(11)-H(11B)	0.958(17)	O(1)-C(7)-C(2)	111.87(10)
C(12)-C(13)	1.502(2)	O(4)-C(8)-O(3)	121.38(11)
C(12)-H(12A)	0.975(11)	O(4)-C(8)-C(4)	123.44(12)
C(13)-H(13A)	0.982(12)	O(3)-C(8)-C(4)	115.18(10)
C(13)-H(13B)	0.981(18)	C(5)-C(9)-H(9A)	113.2(8)
		C(5)-C(9)-H(9B)	110.9(11)
		H(9A)-C(9)-H(9B)	108.3(9)
		O(1)-C(10)-C(11)	109.46(11)
		O(1)-C(10)-H(10A)	107.4(6)
		C(11)-C(10)-H(10A)	112.3(6)
		C(10)-C(11)-H(11A)	111.4(7)
		C(10)-C(11)-H(11B)	110.6(9)
		H(11A)-C(11)-H(11B)	106.9(9)
		O(3)-C(12)-C(13)	106.49(11)
		O(3)-C(12)-H(12A)	108.2(6)
		C(13)-C(12)-H(12A)	112.1(7)
		C(12)-C(13)-H(13A)	110.1(8)
		C(12)-C(13)-H(13B)	109.4(11)
		H(13A)-C(13)-H(13B)	110.1(9)

**Table 4. Anisotropic displacement parameters ( $\text{\AA}^2 \times 10^4$ ) for JBT02 (CCDC 295385). The anisotropic displacement factor exponent takes the form:  $-2\pi^2 [h^2 a^{*2} U^{11} + \dots + 2 h k a^* b^* U^{12}]$**

	$U^{11}$	$U^{22}$	$U^{33}$	$U^{23}$	$U^{13}$	$U^{12}$
O(1)	107(5)	257(5)	130(4)	0	16(3)	0
O(2)	161(6)	400(6)	154(4)	0	-27(4)	0
O(3)	120(5)	322(6)	96(4)	0	-14(3)	0
O(4)	173(5)	252(5)	101(4)	0	17(3)	0
N	156(6)	207(6)	76(4)	0	20(4)	0
C(1)	144(7)	132(6)	119(5)	0	-12(5)	0
C(2)	127(7)	145(6)	119(5)	0	-2(5)	0
C(3)	146(7)	162(7)	88(5)	0	9(4)	0
C(4)	126(7)	117(6)	105(5)	0	1(4)	0
C(5)	156(7)	121(6)	119(5)	0	0(4)	0
C(6)	166(8)	279(8)	110(5)	0	-8(5)	0
C(7)	166(7)	165(6)	126(5)	0	19(5)	0
C(8)	138(7)	138(6)	120(5)	0	12(4)	0
C(9)	150(7)	270(8)	117(5)	0	8(5)	0
C(10)	124(7)	274(8)	173(6)	0	8(5)	0
C(11)	163(8)	317(9)	188(6)	0	33(6)	0
C(12)	147(7)	312(8)	103(5)	0	-20(5)	0
C(13)	158(8)	455(10)	146(6)	0	-20(5)	0



**Table 5. Hydrogen coordinates ( $\times 10^4$ ) and isotropic displacement parameters ( $\text{\AA}^2 \times 10^3$ ) for JBT02 (CCDC 295385).**

	x	y	z	$U_{\text{iso}}$
H(1)	2121(6)	0	4010(20)	18(4)
H(3A)	2750(4)	1166(15)	-1280(13)	16(3)
H(6A)	3367(6)	1101(18)	4655(15)	39(4)
H(6B)	2879(8)	0	5480(20)	42(5)
H(9A)	1080(5)	1100(18)	1681(16)	38(3)
H(9B)	1282(7)	0	3410(20)	39(5)
H(10A)	4509(4)	1173(17)	-438(13)	22(3)
H(11A)	4312(5)	1152(18)	-3614(15)	33(3)
H(11B)	4849(7)	0	-3220(20)	24(4)
H(12A)	863(4)	1164(17)	-3772(14)	25(3)
H(13A)	151(5)	1154(18)	-1665(17)	40(4)
H(13B)	-53(7)	0	-3450(20)	37(5)

**Table 6. Hydrogen bonds for JBT02 (CCDC 295385) [ $\text{\AA}$  and  $^\circ$ ].**

D-H...A	d(D-H)	d(H...A)	d(D...A)	<(DHA)
N-H(1)...O(4)#1	0.862(16)	2.117(16)	2.9767(14)	175.0(14)

Symmetry transformations used to generate equivalent atoms:  
 #1 x,y,z+1

CALIFORNIA INSTITUTE OF TECHNOLOGY  
BECKMAN INSTITUTE  
X-RAY CRYSTALLOGRAPHY LABORATORY

Date 11 January 2006

**Crystal Structure Analysis of:**

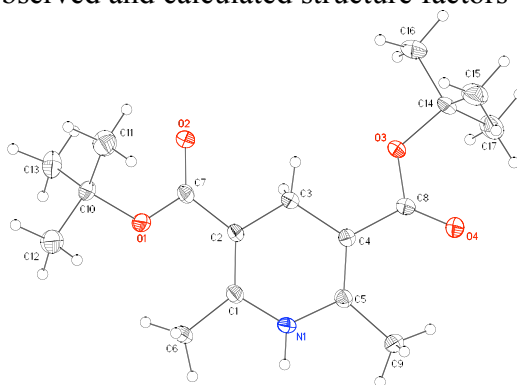
**JBT01**

(shown below)

<b>For</b>	Investigator: Jamie Tuttle	ext. 6061
	Advisor: D. W. C. MacMillan	ext. 6044
	Account Number: DWCM.45100-1-ENDOW.451000	
<b>By</b>	Michael W. Day	116 Beckman ext. 2734 e-mail: mikeday@caltech.edu

Contents

Table 1.	Crystal data
Figures	Figures
Table 2.	Atomic Coordinates
Table 3.	Full bond distances and angles
Table 4.	Anisotropic displacement parameters
Table 5.	Hydrogen atomic coordinates
Table 6.	Hydrogen bond distances and angles
Table 7.	Observed and calculated structure factors (available upon request)



**JBT01**

**Note:** The crystallographic data have been deposited in the Cambridge Database (CCDC) and has been placed on hold pending further instructions from me. The deposition number is 294051. Ideally the CCDC would like the publication to contain a footnote of the type: "Crystallographic data have been deposited at the CCDC, 12 Union Road, Cambridge CB2 1EZ, UK and copies can be obtained on request, free of charge, by quoting the publication citation and the deposition number 294051."

**Table 1. Crystal data and structure refinement for JBT01 (CCDC 294051).**

Empirical formula	$C_{17}H_{27}NO_4$	
Formula weight	309.40	
Crystallization Solvent	Not given	
Crystal Habit	Block	
Crystal size	0.37 x 0.28 x 0.18 mm <sup>3</sup>	
Crystal color	Pale yellow	
<b>Data Collection</b>		
Type of diffractometer	Bruker SMART 1000	
Wavelength	0.71073 Å MoK $\alpha$	
Data Collection Temperature	100(2) K	
$\theta$ range for 9125 reflections used in lattice determination	2.71 to 34.25°	
Unit cell dimensions	a = 7.9678(4) Å b = 20.8362(11) Å c = 11.2805(6) Å	$\beta = 106.0340(10)^\circ$
Volume	1799.92(16) Å <sup>3</sup>	
Z	4	
Crystal system	Monoclinic	
Space group	P2 <sub>1</sub> /n	
Density (calculated)	1.142 Mg/m <sup>3</sup>	
F(000)	672	
Data collection program	Bruker SMART v5.630	
$\theta$ range for data collection	1.95 to 35.06°	
Completeness to $\theta = 35.06^\circ$	89.7 %	
Index ranges	$-12 \leq h \leq 12, -31 \leq k \leq 33, -14 \leq l \leq 17$	
Data collection scan type	$\omega$ scans at 7 $\phi$ settings	
Data reduction program	Bruker SAINT v6.45A	
Reflections collected	30215	
Independent reflections	7143 [ $R_{int} = 0.0670$ ]	
Absorption coefficient	0.080 mm <sup>-1</sup>	
Absorption correction	None	
Max. and min. transmission	0.9857 and 0.9708	

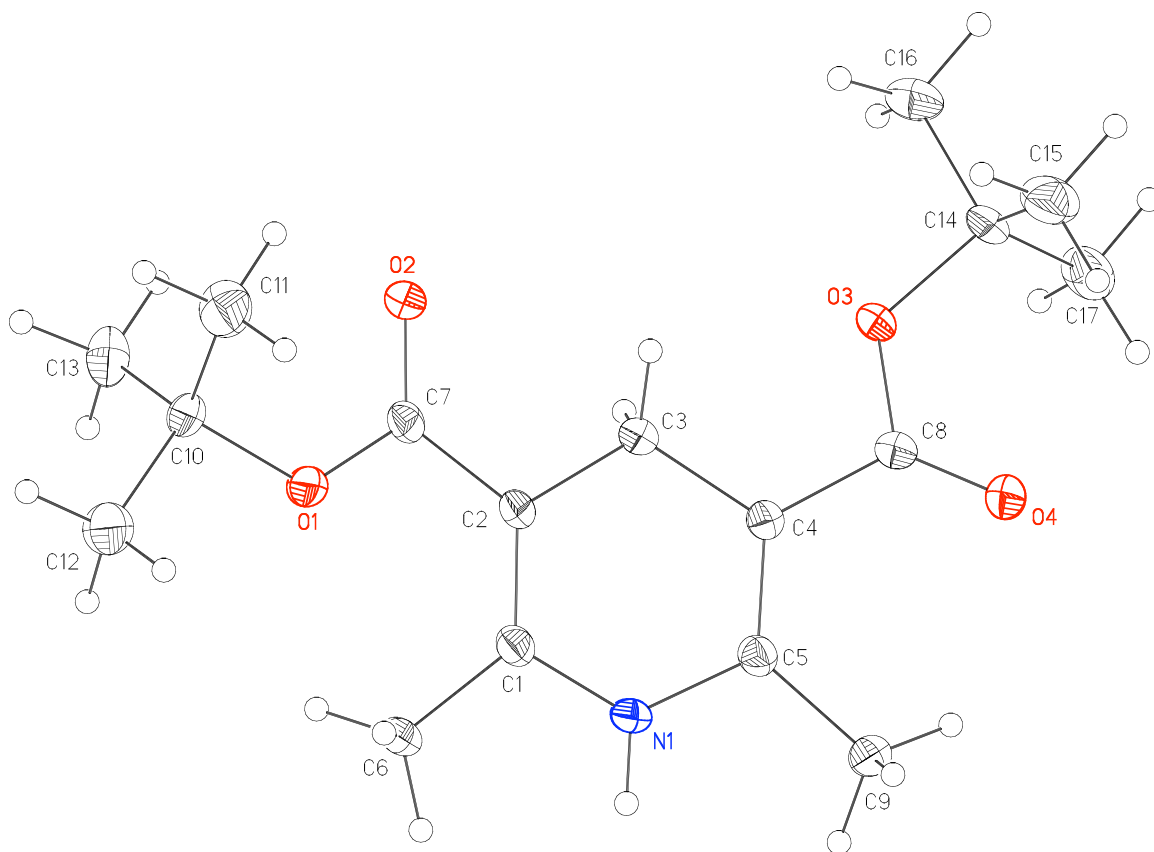
**Table 1 (cont.)****Structure solution and Refinement**

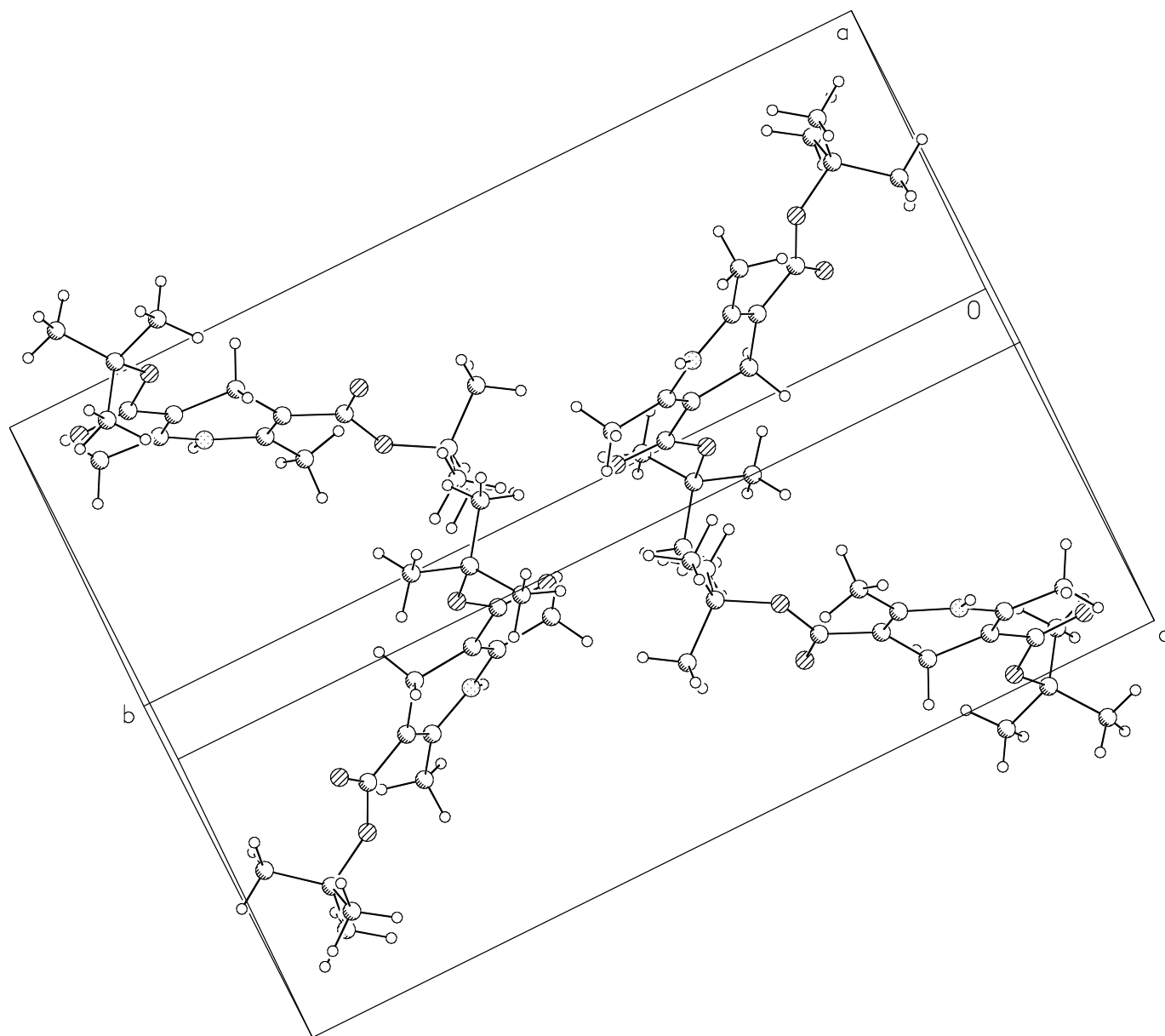
Structure solution program	Bruker XS v6.12
Primary solution method	Direct methods
Secondary solution method	Difference Fourier map
Hydrogen placement	Difference Fourier map
Structure refinement program	Bruker XL v6.12
Refinement method	Full matrix least-squares on $F^2$
Data / restraints / parameters	7143 / 0 / 307
Treatment of hydrogen atoms	Unrestrained
Goodness-of-fit on $F^2$	1.445
Final R indices [ $I > 2\sigma(I)$ , 4432 reflections]	$R1 = 0.0483$ , $wR2 = 0.0751$
R indices (all data)	$R1 = 0.0851$ , $wR2 = 0.0784$
Type of weighting scheme used	Sigma
Weighting scheme used	$w = 1/\sigma^2(F_o^2)$
Max shift/error	0.000
Average shift/error	0.000
Largest diff. peak and hole	0.386 and -0.310 e.Å <sup>-3</sup>

**Special Refinement Details**

Refinement of  $F^2$  against ALL reflections. The weighted R-factor ( $wR$ ) and goodness of fit ( $S$ ) are based on  $F^2$ , conventional R-factors ( $R$ ) are based on  $F$ , with  $F$  set to zero for negative  $F^2$ . The threshold expression of  $F^2 > 2\sigma(F^2)$  is used only for calculating R-factors(gt) etc. and is not relevant to the choice of reflections for refinement. R-factors based on  $F^2$  are statistically about twice as large as those based on  $F$ , and R-factors based on ALL data will be even larger.

All esds (except the esd in the dihedral angle between two l.s. planes) are estimated using the full covariance matrix. The cell esds are taken into account individually in the estimation of esds in distances, angles and torsion angles; correlations between esds in cell parameters are only used when they are defined by crystal symmetry. An approximate (isotropic) treatment of cell esds is used for estimating esds involving l.s. planes.





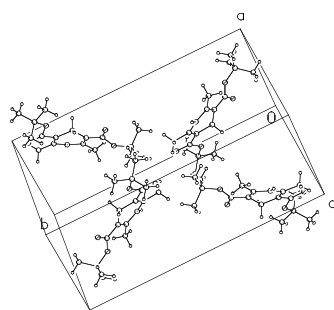
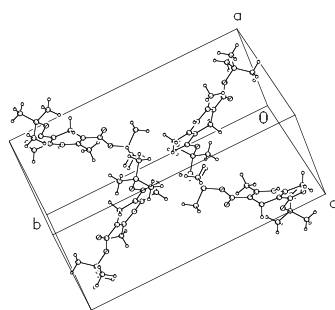




**Table 2. Atomic coordinates ( $\times 10^4$ ) and equivalent isotropic displacement parameters ( $\text{\AA}^2 \times 10^3$ ) for JBT01 (CCDC 294051).  $U(\text{eq})$  is defined as the trace of the orthogonalized  $U^{ij}$  tensor.**

	x	y	z	$U_{\text{eq}}$
O(1)	3978(1)	3496(1)	8437(1)	23(1)
O(2)	1041(1)	3515(1)	7653(1)	21(1)
O(3)	-2143(1)	1573(1)	7851(1)	20(1)
O(4)	-746(1)	622(1)	8363(1)	24(1)
N(1)	3546(1)	1815(1)	10321(1)	21(1)
C(1)	3723(1)	2408(1)	9824(1)	18(1)
C(2)	2336(1)	2662(1)	8970(1)	17(1)
C(3)	568(1)	2338(1)	8696(1)	19(1)
C(4)	746(1)	1626(1)	8972(1)	16(1)
C(5)	2182(1)	1395(1)	9805(1)	18(1)
C(6)	5527(1)	2688(1)	10314(1)	25(1)
C(7)	2369(1)	3260(1)	8301(1)	18(1)
C(8)	-735(1)	1204(1)	8382(1)	17(1)
C(9)	2558(1)	719(1)	10255(1)	22(1)
C(10)	4280(1)	4096(1)	7823(1)	22(1)
C(11)	3630(2)	4026(1)	6433(1)	31(1)
C(12)	6262(1)	4148(1)	8239(1)	36(1)
C(13)	3440(2)	4658(1)	8301(1)	31(1)
C(14)	-3826(1)	1293(1)	7148(1)	21(1)
C(15)	-3594(2)	937(1)	6032(1)	33(1)
C(16)	-4936(1)	1891(1)	6751(1)	32(1)
C(17)	-4567(2)	879(1)	7987(1)	34(1)

**Table 3. Bond lengths [Å] and angles [°] for JBT01 (CCDC 294051).**

O(1)-C(7)	1.3414(10)	C(8)-O(3)-C(14)	122.11(7)
O(1)-C(10)	1.4814(11)	C(1)-N(1)-C(5)	123.32(8)
O(2)-C(7)	1.2280(10)	C(1)-N(1)-H(1)	118.7(7)
O(3)-C(8)	1.3547(10)	C(5)-N(1)-H(1)	117.7(7)
O(3)-C(14)	1.4762(10)	C(2)-C(1)-N(1)	118.87(8)
O(4)-C(8)	1.2147(10)	C(2)-C(1)-C(6)	128.08(9)
N(1)-C(1)	1.3794(12)	N(1)-C(1)-C(6)	113.04(8)
N(1)-C(5)	1.3929(11)	C(1)-C(2)-C(7)	124.85(8)
N(1)-H(1)	0.878(11)	C(1)-C(2)-C(3)	120.05(8)
C(1)-C(2)	1.3567(12)	C(7)-C(2)-C(3)	115.03(8)
C(1)-C(6)	1.5086(13)	C(2)-C(3)-C(4)	111.44(7)
C(2)-C(7)	1.4623(13)	C(2)-C(3)-H(3A)	109.3(5)
C(2)-C(3)	1.5144(12)	C(4)-C(3)-H(3A)	109.5(5)
C(3)-C(4)	1.5152(13)	C(2)-C(3)-H(3B)	111.1(6)
C(3)-H(3A)	0.976(10)	C(4)-C(3)-H(3B)	110.0(6)
C(3)-H(3B)	1.015(11)	H(3A)-C(3)-H(3B)	105.4(8)
C(4)-C(5)	1.3528(12)	C(5)-C(4)-C(8)	121.31(8)
C(4)-C(8)	1.4739(12)	C(5)-C(4)-C(3)	120.31(8)
C(5)-C(9)	1.4987(13)	C(8)-C(4)-C(3)	118.22(7)
C(6)-H(6A)	0.966(13)	C(4)-C(5)-N(1)	118.61(8)
C(6)-H(6B)	0.981(12)	C(4)-C(5)-C(9)	128.41(8)
C(6)-H(6C)	0.984(11)	N(1)-C(5)-C(9)	112.96(8)
C(9)-H(9A)	0.986(11)	C(1)-C(6)-H(6A)	111.3(7)
C(9)-H(9B)	0.979(12)	C(1)-C(6)-H(6B)	110.1(6)
C(9)-H(9C)	0.973(12)	H(6A)-C(6)-H(6B)	108.3(9)
C(10)-C(11)	1.5160(15)	C(1)-C(6)-H(6C)	111.1(6)
C(10)-C(13)	1.5197(15)	H(6A)-C(6)-H(6C)	106.9(9)
C(10)-C(12)	1.5216(14)	H(6B)-C(6)-H(6C)	109.0(9)
C(11)-H(11A)	1.010(12)	O(2)-C(7)-O(1)	123.33(8)
C(11)-H(11B)	0.994(12)	O(2)-C(7)-C(2)	122.70(8)
C(11)-H(11C)	0.992(12)	O(1)-C(7)-C(2)	113.95(8)
C(12)-H(12A)	0.995(13)	O(4)-C(8)-O(3)	123.94(8)
C(12)-H(12B)	0.961(12)	O(4)-C(8)-C(4)	127.16(8)
C(12)-H(12C)	1.014(11)	O(3)-C(8)-C(4)	108.90(7)
C(13)-H(13A)	0.986(12)	C(5)-C(9)-H(9A)	112.2(6)
C(13)-H(13B)	0.998(11)	C(5)-C(9)-H(9B)	109.2(6)
C(13)-H(13C)	0.992(13)	H(9A)-C(9)-H(9B)	110.5(9)
C(14)-C(17)	1.5154(15)	C(5)-C(9)-H(9C)	110.0(7)
C(14)-C(15)	1.5159(15)	H(9A)-C(9)-H(9C)	109.8(9)
C(14)-C(16)	1.5219(14)	H(9B)-C(9)-H(9C)	104.9(9)
C(15)-H(15A)	0.967(14)	O(1)-C(10)-C(11)	110.39(8)
C(15)-H(15B)	0.982(12)	O(1)-C(10)-C(13)	109.86(8)
C(15)-H(15C)	0.992(12)	C(11)-C(10)-C(13)	112.57(9)
C(16)-H(16A)	0.977(13)	O(1)-C(10)-C(12)	101.79(8)
C(16)-H(16B)	0.985(11)	C(11)-C(10)-C(12)	110.82(10)
C(16)-H(16C)	0.992(12)	C(13)-C(10)-C(12)	110.89(9)
C(17)-H(17A)	0.979(11)	C(10)-C(11)-H(11A)	110.1(7)
C(17)-H(17B)	0.966(12)	C(10)-C(11)-H(11B)	110.2(7)
C(17)-H(17C)	1.009(14)	H(11A)-C(11)-H(11B)	107.6(9)
		C(10)-C(11)-H(11C)	110.6(7)
C(7)-O(1)-C(10)	121.92(7)	H(11A)-C(11)-H(11C)	109.5(9)

H(11B)-C(11)-H(11C)	108.8(9)
C(10)-C(12)-H(12A)	111.2(7)
C(10)-C(12)-H(12B)	108.0(6)
H(12A)-C(12)-H(12B)	110.5(10)
C(10)-C(12)-H(12C)	109.9(6)
H(12A)-C(12)-H(12C)	107.6(9)
H(12B)-C(12)-H(12C)	109.5(9)
C(10)-C(13)-H(13A)	111.4(7)
C(10)-C(13)-H(13B)	107.2(6)
H(13A)-C(13)-H(13B)	109.4(9)
C(10)-C(13)-H(13C)	110.7(7)
H(13A)-C(13)-H(13C)	109.8(10)
H(13B)-C(13)-H(13C)	108.4(9)
O(3)-C(14)-C(17)	110.02(8)
O(3)-C(14)-C(15)	109.80(8)
C(17)-C(14)-C(15)	113.45(10)
O(3)-C(14)-C(16)	101.68(8)
C(17)-C(14)-C(16)	110.75(9)
C(15)-C(14)-C(16)	110.51(9)
C(14)-C(15)-H(15A)	110.7(8)
C(14)-C(15)-H(15B)	108.5(7)
H(15A)-C(15)-H(15B)	108.6(11)
C(14)-C(15)-H(15C)	112.3(7)
H(15A)-C(15)-H(15C)	108.5(10)
H(15B)-C(15)-H(15C)	108.3(10)
C(14)-C(16)-H(16A)	109.6(7)
C(14)-C(16)-H(16B)	108.5(7)
H(16A)-C(16)-H(16B)	110.2(9)
C(14)-C(16)-H(16C)	109.5(6)
H(16A)-C(16)-H(16C)	108.8(10)
H(16B)-C(16)-H(16C)	110.3(9)
C(14)-C(17)-H(17A)	111.5(7)
C(14)-C(17)-H(17B)	107.3(7)
H(17A)-C(17)-H(17B)	110.3(9)
C(14)-C(17)-H(17C)	110.2(7)
H(17A)-C(17)-H(17C)	106.6(10)
H(17B)-C(17)-H(17C)	111.1(10)

**Table 4. Anisotropic displacement parameters ( $\text{\AA}^2 \times 10^4$ ) for JBT01 (CCDC 294051). The anisotropic displacement factor exponent takes the form:  $-2\pi^2 [h^2 a^{*2} U^{11} + \dots + 2 h k a^* b^* U^{12}]$**

	$U^{11}$	$U^{22}$	$U^{33}$	$U^{23}$	$U^{13}$	$U^{12}$
O(1)	179(3)	211(3)	277(4)	90(3)	10(3)	-39(3)
O(2)	204(3)	189(3)	202(4)	16(3)	-22(3)	-17(3)
O(3)	125(3)	190(3)	246(4)	13(3)	-5(3)	-17(2)
O(4)	224(3)	162(3)	295(4)	-9(3)	7(3)	-8(3)
N(1)	175(4)	208(4)	204(5)	63(3)	-38(3)	-29(3)
C(1)	184(4)	192(5)	158(5)	0(4)	17(4)	-41(3)
C(2)	166(4)	161(4)	158(5)	-12(4)	9(4)	-30(3)
C(3)	158(4)	183(5)	206(5)	19(4)	-3(4)	-15(4)
C(4)	150(4)	163(4)	175(5)	7(4)	36(4)	-15(3)
C(5)	160(4)	187(5)	177(5)	8(4)	41(4)	-24(3)
C(6)	197(5)	254(6)	230(6)	62(5)	-42(4)	-65(4)
C(7)	200(5)	167(4)	146(5)	-34(4)	17(4)	-33(3)
C(8)	147(4)	193(5)	164(5)	4(4)	31(4)	8(3)
C(9)	188(5)	196(5)	267(6)	51(4)	31(4)	-2(4)
C(10)	226(5)	181(5)	247(5)	73(4)	40(4)	-43(4)
C(11)	360(6)	327(6)	261(6)	42(5)	102(5)	-60(5)
C(12)	247(6)	343(7)	465(8)	153(6)	48(6)	-77(5)
C(13)	352(7)	222(5)	369(7)	-17(5)	103(6)	-72(5)
C(14)	127(4)	244(5)	226(5)	4(4)	-16(4)	-31(3)
C(15)	320(6)	364(7)	246(6)	-44(5)	-18(5)	23(5)
C(16)	191(5)	360(6)	357(7)	24(6)	-21(5)	42(5)
C(17)	206(5)	410(7)	393(7)	75(6)	48(5)	-96(5)

**Table 5. Hydrogen coordinates ( $\times 10^4$ ) and isotropic displacement parameters ( $\text{\AA}^2 \times 10^3$ ) for JBT01 (CCDC 294051).**

	x	y	z	$U_{\text{iso}}$
H(1)	4382(14)	1679(5)	10952(11)	32(3)
H(3A)	-54(12)	2402(4)	7829(10)	19(3)
H(3B)	-192(13)	2545(5)	9177(10)	31(3)
H(6A)	6173(15)	2669(5)	9706(12)	45(4)
H(6B)	6182(14)	2450(5)	11046(11)	35(3)
H(6C)	5470(13)	3143(6)	10535(10)	32(3)
H(9A)	1486(13)	482(5)	10255(10)	29(3)
H(9B)	3369(14)	725(5)	11084(11)	38(3)
H(9C)	3178(15)	493(6)	9750(11)	44(3)
H(11A)	4132(14)	3625(6)	6161(11)	45(3)
H(11B)	4016(14)	4397(6)	6023(10)	41(3)
H(11C)	2337(16)	4003(5)	6163(12)	46(3)
H(12A)	6702(15)	4167(5)	9154(13)	46(4)
H(12B)	6591(14)	4528(6)	7876(10)	40(3)
H(12C)	6803(14)	3758(5)	7953(11)	40(3)
H(13A)	2155(15)	4630(5)	8029(11)	41(3)
H(13B)	3824(13)	5057(5)	7963(10)	35(3)
H(13C)	3845(15)	4678(6)	9215(13)	49(4)
H(15A)	-3061(17)	1211(6)	5548(13)	59(4)
H(15B)	-4750(16)	806(6)	5518(11)	48(4)
H(15C)	-2864(15)	547(6)	6264(11)	45(3)
H(16A)	-5107(15)	2107(6)	7478(12)	49(4)
H(16B)	-6070(15)	1760(5)	6195(11)	41(3)
H(16C)	-4329(14)	2189(5)	6321(11)	39(3)
H(17A)	-3882(14)	487(6)	8230(11)	39(3)
H(17B)	-5754(16)	774(5)	7538(11)	44(3)
H(17C)	-4529(16)	1118(6)	8772(14)	56(4)

**Table 6. Hydrogen bonds for JBT01 (CCDC 294051) [ $\text{\AA}$  and  $^\circ$ ].**

D-H...A	d(D-H)	d(H...A)	d(D...A)	<(DHA)
N(1)-H(1)...O(2)#1	0.878(11)	2.047(11)	2.9088(10)	166.9(10)

Symmetry transformations used to generate equivalent atoms:

#1  $x+1/2, -y+1/2, z+1/2$

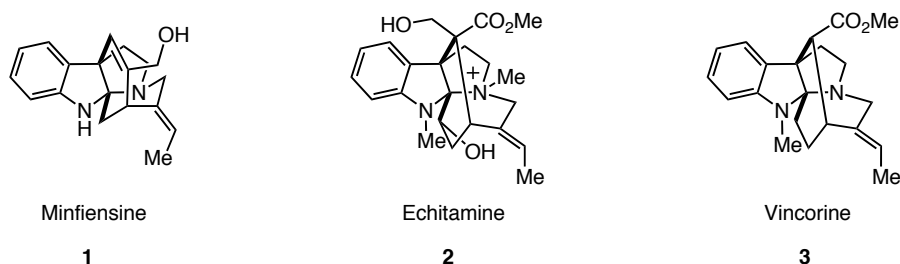
## Chapter 4

### Progress Toward the Total Synthesis of (+)-Minfiensine

#### *Isolation, Structure, and Biological Activity*

Members of the *Strychnos* family of natural products were first isolated in 1989 from the plant *Strychnos minfiensis* by Massiot *et al.*<sup>1</sup> and are comprised of indole and tryptophan units, presumably via cyclization of corynanthene intermediates (Fig. 1).<sup>2</sup> Despite recent heightened interest in related akuammiline alkaloids exhibiting interesting biological activity as isolates and as traditional medicines,<sup>3</sup> little is known about their pharmacology. The potential for new therapies and understanding their subsequent modes of action makes these molecules attractive targets for total synthesis.

**Figure 1. Structurally Related Members of the Strychnos Alkaloid Family**



Minfiensine **1** is a pentacyclic pyrroloindoline alkaloid bearing a quaternary carbon stereocenter and a fully differentiated aminal motif at the fused ring juncture. The only synthesis of this natural product was reported by the Overman group in 2005.<sup>4</sup> Their

(1) Massiot, G.; Thepenier, P.; Jacquier, M. J.; Lemenoliev, L.; Delaude, C. *Heterocycles* **1989**, 29, 1435-1438.

(2) (a) Scott, A. I. *Acc. Chem. Res.* **1970**, 3, 151-157. (b) Scott, A. I.; Cherry, P. C.; Quereschi, A. A. J. *Am. Chem. Soc.* **1969**, 91, 4932.

(3) Ramirez, A. G.-R., S. *Curr. Med. Chem.* **2003**, 10, 1891-1915.

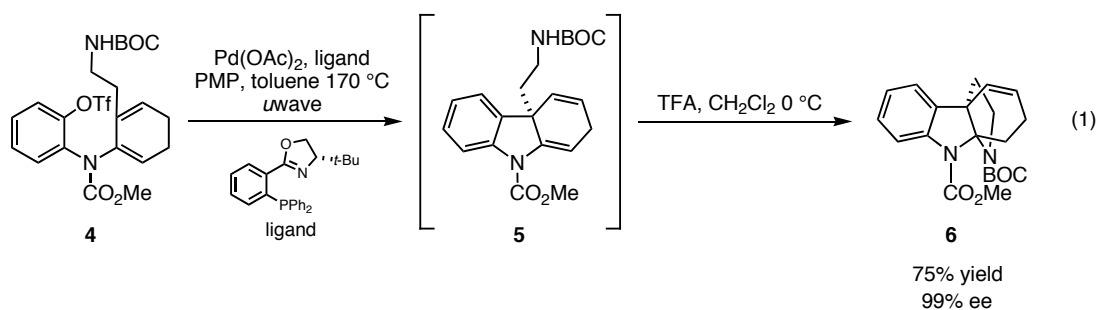
(4) (a) Dounay, A. B.; Overman, L. E.; Wroblewski, A. D. *J. Am. Chem. Soc.* **2005**, 127, 10186-10187. (b) Dounay, A. B.; Overman, L. E.; Wroblewski, A. D. *J. Am. Chem. Soc.* **2006**, 128, 2154-2154.

strategy utilized a series of intramolecular Heck reactions<sup>5</sup> to set the pentacycle, followed by oxidation state manipulations to assemble the target molecule (Fig. 2).

**Figure 2. Overman's Synthetic Strategy**



The key step in their sequence relies on an asymmetric Heck/iminium ion cyclization (eq. 1). In this reaction, triflate **4** undergoes Heck cyclization to form the quaternary carbon stereocenter in **5**. Protonation of the enamine followed by 1,2-addition to the resulting iminium by the pendant amine furnishes tetracycle **6** in good yield and high ee. In this transformation, the quaternary center is set with high levels of enantioselectivity, paving the way for substrate-controlled assembly of the remaining pyrroloindoline core.

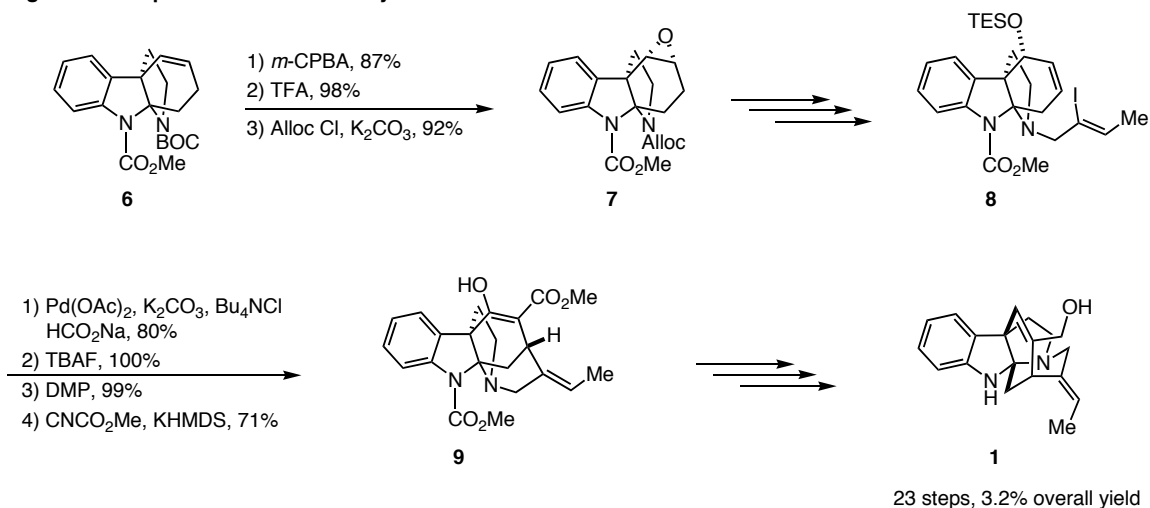


(5) (a) Douglas, C. J.; Overman, L. E. *PNAS* **2004**, *101*, 5363-5367. (b) Lebsack, A. D.; Link, J. T.; Overman, L. E.; Stearns, B. A. *J. Am. Chem. Soc.* **2002**, *124*, 9008-9009. (c) Overman, L. E.; Watson, D. A. *J. Org. Chem.* **2006**, *71*, 2600-2608. (d) Dounay, A. B.; Humphreys, P. G.; Overman, L. E.; Wroblewski, A. D. *J. Am. Chem. Soc.* **2008**, ASAP articles.



Overman *et al.* then assembled intermediate **7** that was next elaborated into vinyl iodide **8** (Fig. 3). The final ring was created by a second intramolecular Heck cyclization, followed by deprotection of the alcohol, oxidation to the ketone and subsequent alkylation to provide late-stage intermediate **9**. Five additional transformations installed the required oxidation states of (+)-minfiensine **1** in 23 steps

**Figure 3. Completion of Overman's Synthesis**



and 3.2% overall yield. Recently, the Overman group reported an improved endgame that reduced the overall number of linear steps to 15.<sup>5d</sup>

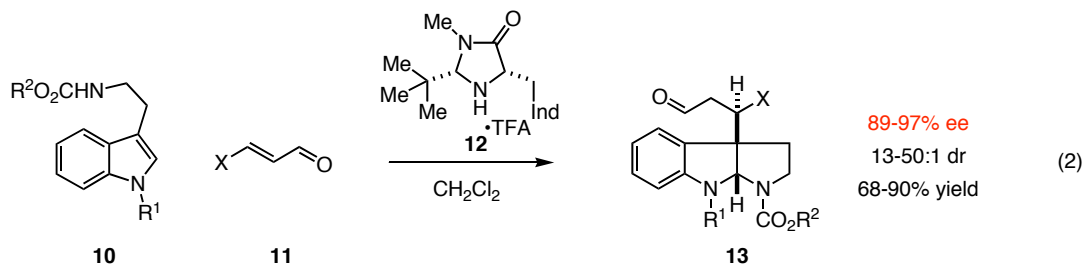
### Synthetic Strategy

Our approach to (+)-minfiensine **1** focuses on the pyrroloindoline core of the natural product. In 2004, our group reported a powerful and rapid means for entry into these tricyclic cores utilizing iminium-activation organocatalysis (eq. 2).<sup>6</sup> In this methodology, substituted tryptamine derivative **10** is reacted with  $\alpha,\beta$ -unsaturated aldehyde **11** under iminium activation conditions using imidazolidinone **12** to furnish pyrroloindoline **13**. This organocatalytic cyclization was successful in using a variety of

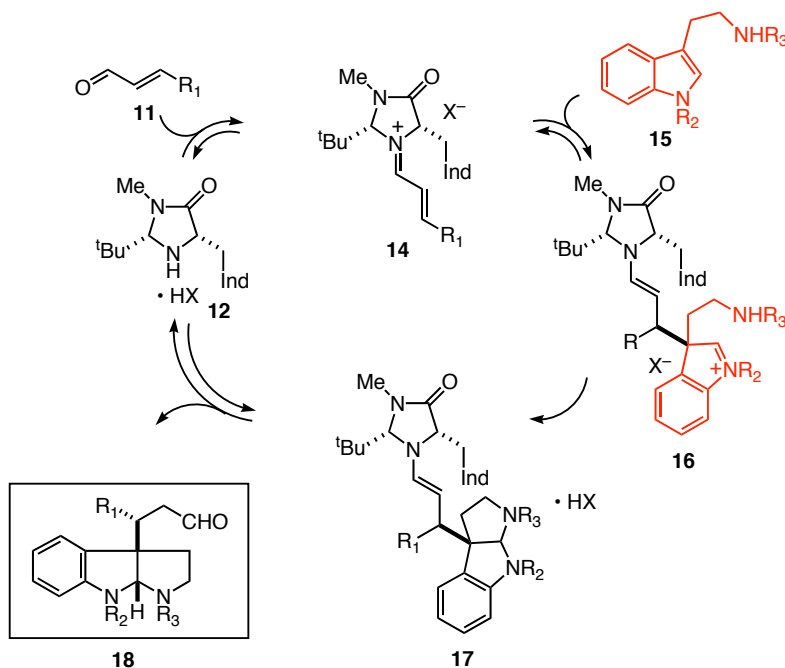
(6) (a) Austin, J. F.; Kim, S. G.; Sinz, C. J.; Xiao, W. J.; MacMillan, D. W. C. *PNAS* **2004**, *101*, 5482-5487. (b) Austin, J. F.; MacMillan, D. W. C. *J. Am. Chem. Soc.* **2002**, *124*, 1172-1173.

indole derivatives to access a broad range of elaborated pyrroloindoline cores bearing quaternary carbon stereocenters in excellent ee, good dr, and good yields. Furthermore, an assortment of  $\beta$ -substituted aldehydes was successfully utilized in this chemistry.

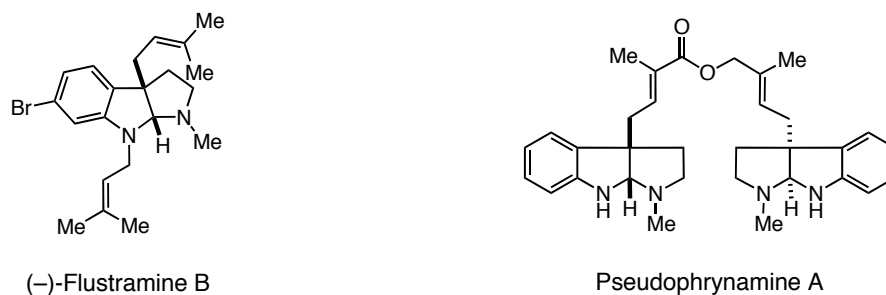
■ The pyrroloindoline forming strategy creates quaternary carbon stereocenters in excellent ee's



This methodology takes advantage of the latent indolinium created after Friedel-Crafts addition of the indole to an iminium-activated  $\alpha,\beta$ -unsaturated aldehyde **14** (Fig. 4). In the proposed catalytic cycle, imidazolidinone **12** condenses with enal **11** to provide activated intermediate **14**. Indole nucleophile **15** adds in a conjugate fashion to produce indolinium **16** that cyclizes to pyrroloindoline **17** via intramolecular attack of the pendant amine. Finally, hydrolysis releases catalyst **12** back into the cycle and unveils aldehyde **18**.

**Figure 4. Organocatalytic Pyrroloindoline Construction Relies on Interception of a Reactive Intermediate**

This strategy has been utilized in the rapid synthesis of two complex natural products, (–)-flustramine B<sup>7</sup> and pseudophrynamine A<sup>8</sup> (Fig. 5).

**Figure 5. Organocatalytic Cyclization Is a Powerful Entry into Natural Products**

Dr. Sung-Gon Kim and Dr. Wen-Jing Xiao

Dr. Shojiro Miyazaki and Dr. Sung-Gon Kim

While this methodology is broadly useful for a range of substituted indoles, one major obstacle exists. Currently, 2,3-dialkyl substituted indoles are unreactive in these reactions, presumably due to the increased non-bonding interactions that hinder approach of the electrophile to the  $\pi$ -system. Indeed, both natural products assembled using this

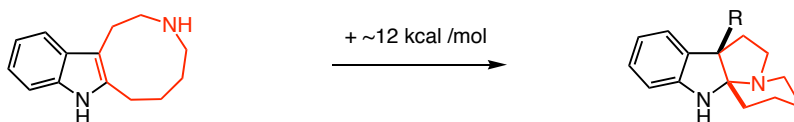
(7) Austin, J. F.; Kim, S. G.; Sinz, C. J.; Xiao, W. J.; MacMillan, D. W. C. *PNAS* **2004**, *101*, 5482-5487.

(8) Unpublished results.

technology contain hydrogens at the amination center of the pyrroloindoline core. Conversely, minfiensine bears an alkyl substituent at this position, presenting a potential problem for the key cyclization event.

In order to address this reactivity problem, an alternative driving force was proposed. We felt the release of trans-annular ring strain (up to 12.6 kcal/mol for nine-membered lactams<sup>9</sup>) characteristic of medium size rings would provide an opportunity to utilize the organocatalytic cascade cyclization (Fig. 6).

**Figure 6. Utilizing the Energy Released via the Collapse of a Nine-Membered Ring**

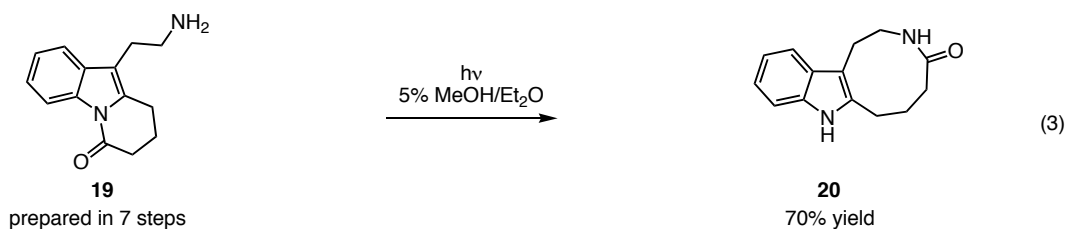


In order to test this hypothesis, a model system was synthesized via a known route reported by the Ban Group (eq. 3).<sup>10</sup> This remarkable photo-Fries rearrangement begins with free-radical cleavage of the amide bond shown in structure **21** followed by tautomerization to the more stable intermediate **22**. Radical carbon-carbon bond formation provides intermediate **23** that is in equilibrium with hemi-aminal **24**. Protonation provides indolinium **25**, which undergoes fragmentation via **26** to furnish indole caprylolactam **20** in 70% isolated yield. This method is one of the few effective ways to access nine-membered lactams in good yields.

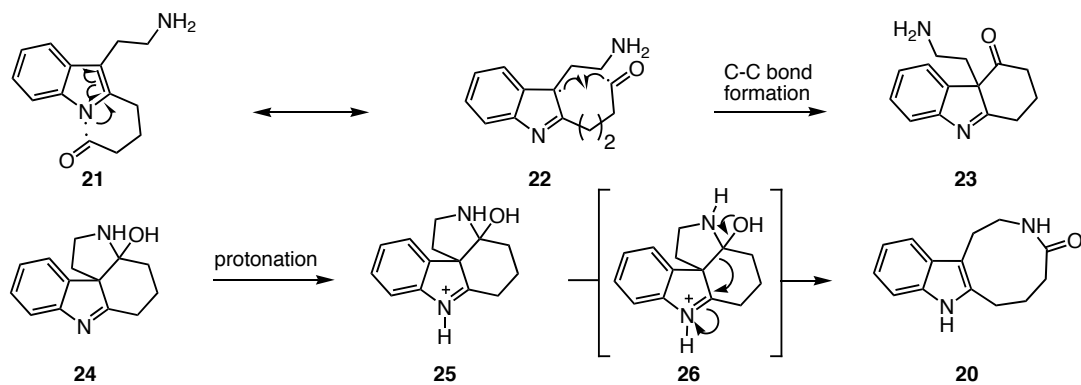
(9) Rousseau, G. *Tetrahedron* **1995**, *51*, 2777-2849.

(10) (a) Ban, Y.; Yoshida, K.; Goto, J.; Oishi, T. *J. Am. Chem. Soc.* **1981**, *103*, 6990-6992. (14) Ban, Y.; Yoshida, K.; Goto, J.; Oishi, T.; Takeda, E. *Tetrahedron* **1983**, *39*, 3657-3668.

■ Synthesis of the key rearrangement precursor was performed in multi-gram quantities



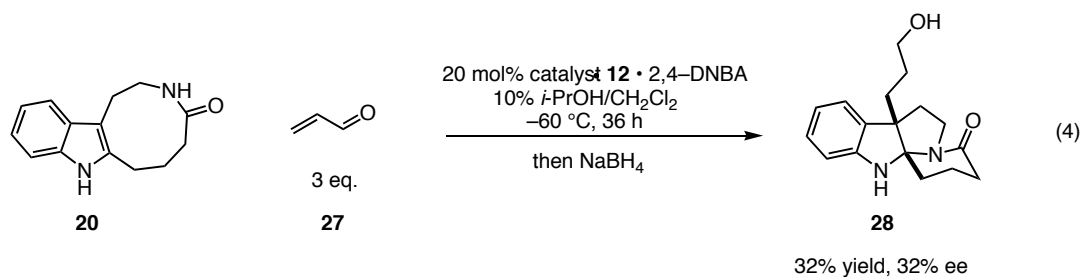
■ A photo-Fries rearrangement assembles the tricyclic structure



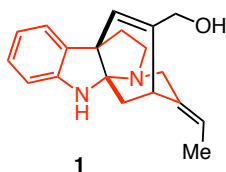
With this molecule in hand, we proceeded with the organocatalytic cyclization.

To our great delight, subjecting indole caprylactam **20** into standard pyrroloindoline forming conditions with acrolein provided the desired tetracyclic alcohol **28** after a reductive workup (eq. 4).

■ Initial result

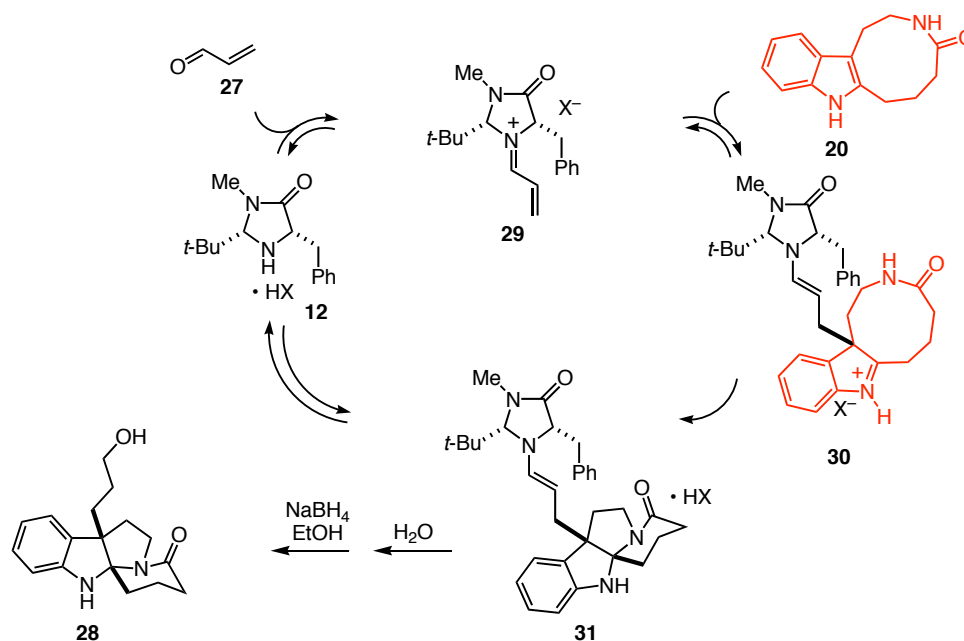


■ Four of the five rings are assembled from the tricyclic starting material



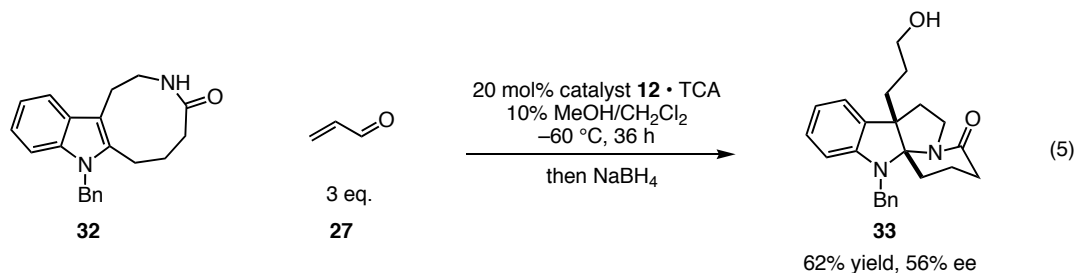
Remarkably, four of the five rings found in the natural product are assembled from the fused indole caprylactam **20** in 32% yield and 32% ee, thereby establishing this approach as a viable route for rapid entry into the [6,5,5,6]-tetracyclic framework of (+)-minfiensine. The proposed catalytic cycle provides a picture of this cyclization event (Fig. 7). Catalyst **12** condenses with acrolein to form iminium **29**. Friedel-Crafts addition of indole **20** provides indolinium intermediate **30** that is trapped by the amide nitrogen to provide pyrroloindoline **31**. Hydrolysis of the resulting enamine **31** delivers the aldehyde that is subsequently reduced to furnish the desired product **28**.

Figure 7. Assembling the Tetracyclic Ring System



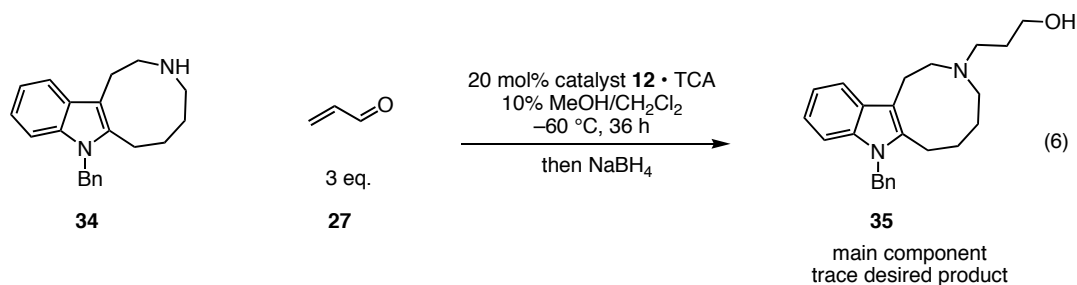
A series of experiments were performed to understand and improve this cyclization. The first problem was the formation of the bis-alkylated pyrroloindoline, isolated in 49% yield, as the major product in this first reaction. Protecting the indole nitrogen to provide **32** prevented this event and, under slightly modified conditions, tetracyclic product **33** was obtained in improved yield and ee (eq. 5).

■ Protecting the indole group prevents acrolein addition and increases yield



Next, the role of the amide group was assessed. Transformation of the amide to its corresponding secondary amine was possible under reducing conditions. Subjecting compound **34** to the cascade conditions resulted only in alkylation of the secondary amine to produce **35** in preference to the desired conjugate addition/cyclization product. Importantly, the carbonyl acts to attenuate the nucleophilicity of the amine, favoring the intramolecular cyclization over the intermolecular alkylation (eq. 6).

■ The carbonyl modulates the amine reactivity

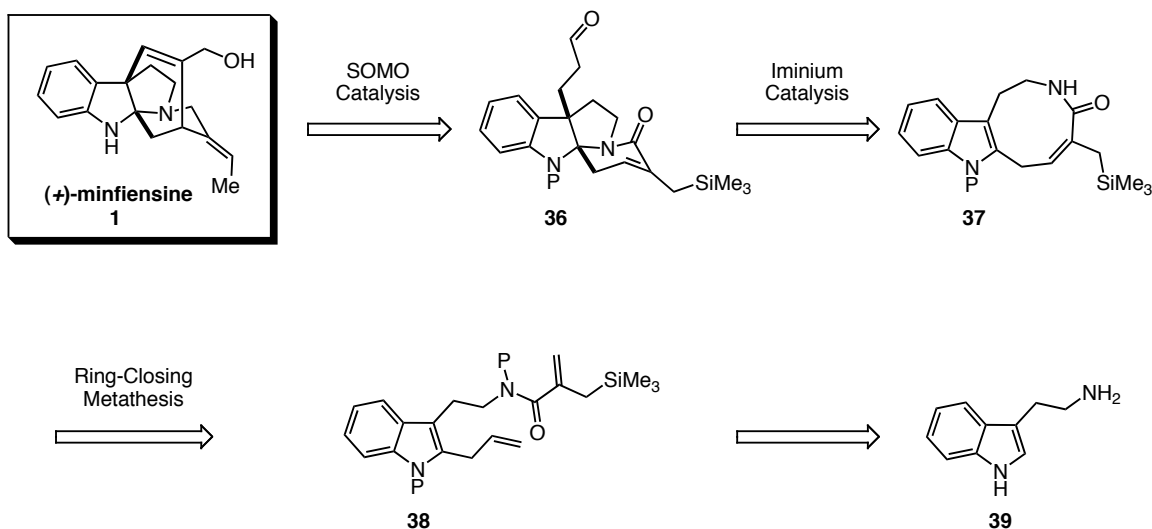


### Retrosynthetic Analysis

Having identified the structural features required in this cyclization reaction, a retrosynthesis of minfiensine was formulated (Fig. 8). The final carbon-carbon bond needed to access the final ring could be furnished by SOMO catalysis. Elaborated caprylolactam **37** should furnish SOMO substrate **36** under organocatalytic cyclization

conditions. Caprylolactam **37** could be obtained via ring-closing metathesis of intermediate **38** that can be assembled from commercially available tryptamine **39**.

Figure 8. A Retrosynthetic Analysis of Minfiensine

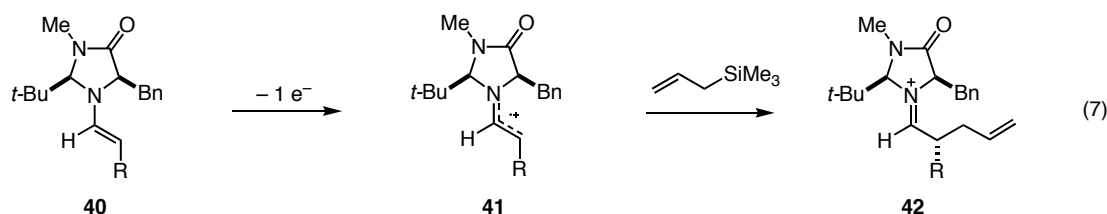


SOMO catalysis is a new mode of organocatalytic activation reported by our group in 2007.<sup>11</sup> A portion of the catalytic cycle, shown in eq. 7, outlines the mechanistic underpinnings of this powerful methodology. Enamine **40** undergoes a single electron oxidation event to generate radical cation **41**. This versatile intermediate species has been demonstrated to react enantioselectively with a variety of SOMO-nucleophiles, (i.e., allylsilane) to provide iminium **42**. The net transformation yields enantioenriched  $\alpha$ -alkyl aldehydes in good yield and ee.

(11) Beeson, T. D.; Mastracchio, A.; Hong, J. B.; Ashton, K.; MacMillan, D. W. C. *Science* **2007**, *316*, 582-585.

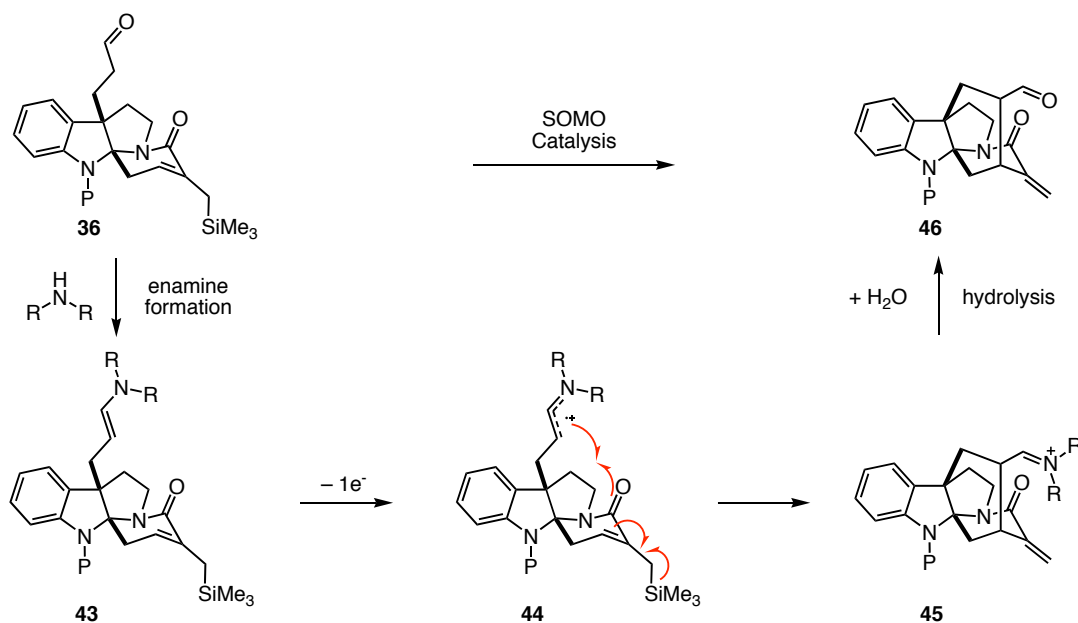


■ SOMO catalysis: Generating a radical cation via the single electron oxidation of an enamine



It was envisioned that this technology could be applied to this synthesis by installing the requisite functionality found in structure **36** (Fig. 9). After enamine formation to provide intermediate **43**, a single-electron oxidant, typically ceric ammonium nitrate (CAN) or iron(III) phenanthroline, will induce formation of radical cation **44**. Trapping by the allylsilane creates the final carbon-carbon bond in **45** and, after hydrolysis, provides late-stage pentacycle **46** that should be readily advanced to the target molecule.

Figure 9. SOMO Catalysis can Forge the Final C–C Bond of the Caged Cycle

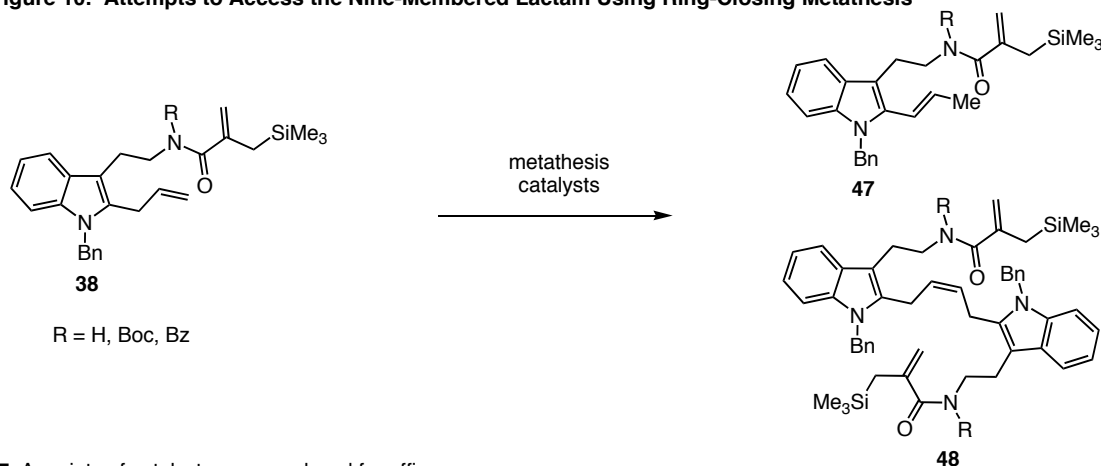


### Unsuccessful Approaches to the Elaborated Caprylactam

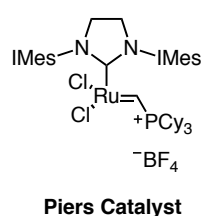
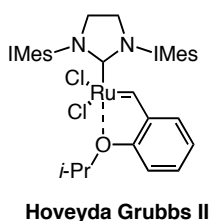
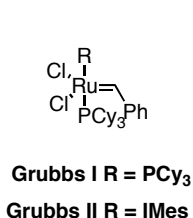
Elaboration of tryptamine into compound **38** proceeded uneventfully. The challenges arose beginning at the ring-closing metathesis step (Fig. 10). Subjecting diene **38** to

RCM failed to provide the desired caprylactam. Instead, either isomerized material **47** or dimer **48** was isolated as major components. Attempts to optimize this reaction by varying metathesis catalysts, temperatures, solvents, and concentrations never created the desired fused indole caprylactam. Efforts to re-subject dimer **48** to a variety of metathesis conditions did not produce desired lactam, as this dimer was remarkably resistant to further transformation. Finally, attempts to prevent olefin isomerization by utilizing benzoquinone and 2,6-dichlorobenzoquinone to intercept the intermediate ruthenium hydride only favored dimer production.<sup>12</sup>

**Figure 10. Attempts to Access the Nine-Membered Lactam Using Ring-Closing Metathesis**



■ A variety of catalysts were analyzed for efficacy



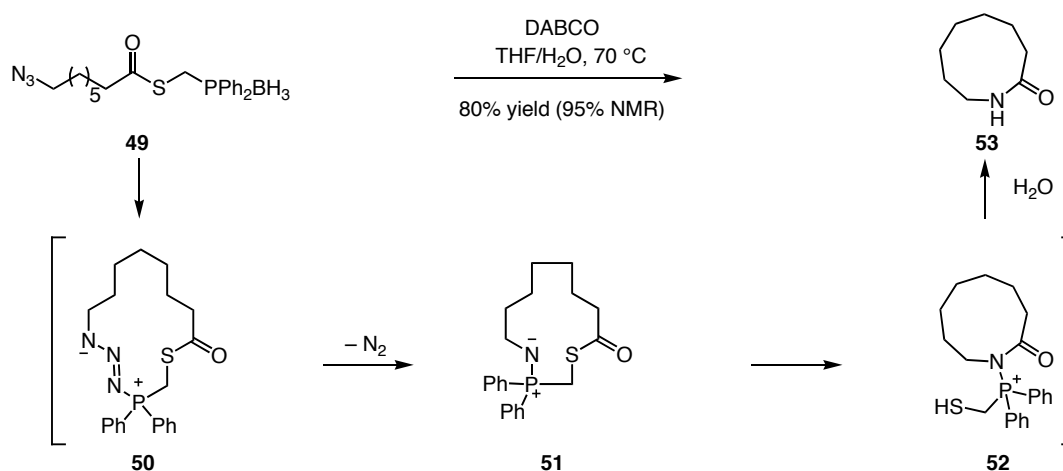
- Analysis of a broad range of temperatures, solvents, and concentrations led to the above products
- Attempts to resubject the dimer to a variety of metathesis conditions were also ineffective

Realizing the inadequacies of substrate **38** in RCM, we chose to pursue an alternative strategy. Many useful methods that access medium-size rings proceed by synthesis of a more accessible macrocycle followed by ring contraction to provide the

(12) Hong, S. H.; Sanders, D. P.; Lee, C. W.; Grubbs, R. H. *J. Am. Chem. Soc.* **2005**, *127*, 17160-17161.

desired medium ring. One very effective approach utilizes an intramolecular Staudinger cyclization to access nine-membered lactams (Fig. 11).<sup>13</sup> In the event, protected diphenylphosphine intermediate **49** is unmasked and, subsequently, attacks the azide to furnish zwitterionic macrocycle **50**. Extrusion of nitrogen gas to produce **51** brings the amine in close proximity to the thioester, facilitating a reaction to create lactam phosphonium intermediate **52** that hydrolyzes to furnish the desired lactam **53** in 80% isolated yield.

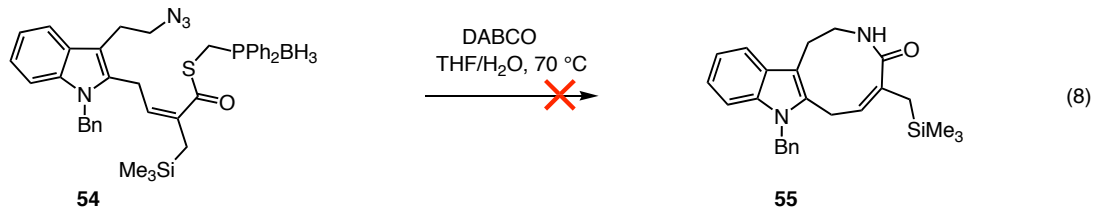
Figure 11. Van Maarseveen's Intramolecular Staudinger Ligation



Cyclization precursor **54** was synthesized as a 6:1 mixture of geometrical isomers and subjected to van Maarseveen's conditions (eq. 8). Within 15 minutes, isomerization of the (*Z*)-alkene to the more stable (*E*)-alkene was observed, instead of the desired deprotection/cyclization event. Due to the preference for this deleterious pathway over macrocyclization, this route was not explored any further.

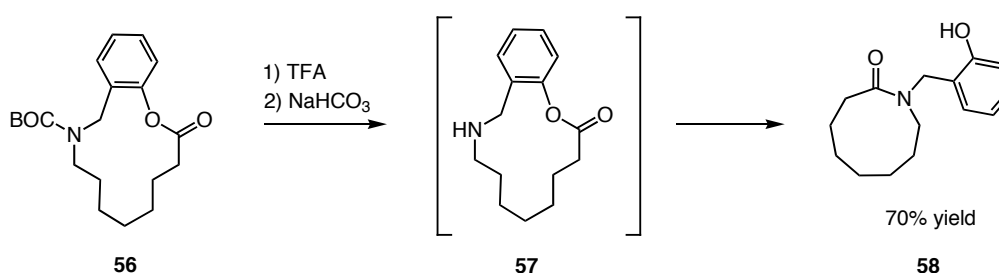
(13) Olivier, D.; Meester, W. J. N.; Bieraugel, H.; Schoemaker, H. E.; Hiemstra, H.; van Maarseveen, J. H. *Angew. Chem. Int. Ed.* **2003**, *42*, 4373-4375.

■ Alkene isomerization precluded cyclization



The van Maarseveen Group also reported a related macrocyclization/ring-contraction to access nine-membered lactams (Fig. 12).<sup>14</sup> In this strategy, a phenol-based linker is used in intermediate **56**. After BOC deprotection with TFA, basic conditions induce cyclization to the desired lactam **58** in 70% yield.

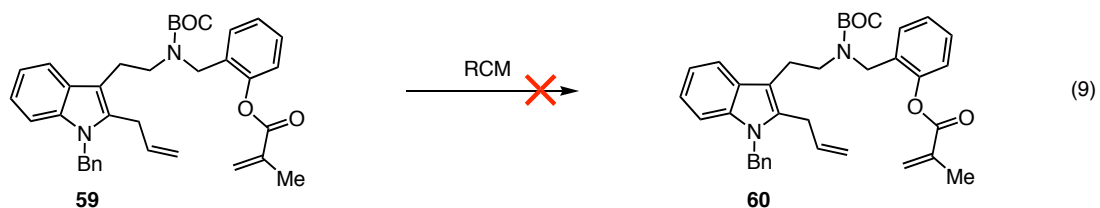
Figure 12. A Related Strategy to Access the Lactam



Application of this method required the synthesis of intermediate **59** (eq. 9). In this case, the allylsilane was omitted due to a propensity for protodesilylation under strongly acidic conditions. All attempts to access the 13-membered ring resulted in either dimerization or isomerization of the primary alkene. This substrate **59** proved to be just as poor an RCM substrate as **38**.

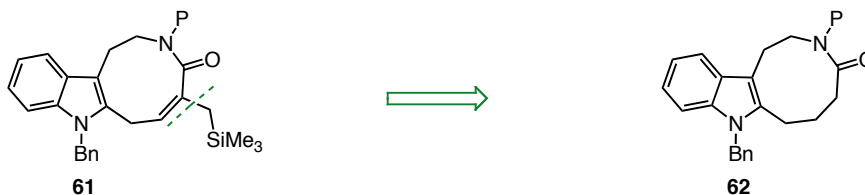
(14) Bieraugel, H.; Jansen, T. P.; Schoemaker, H. E.; Hiemstra, H.; van Maarseveen, J. H. *Org. Lett.* **2002**, *4*, 2673-2674.

■ In the event, only dimer and isomerized product was observed

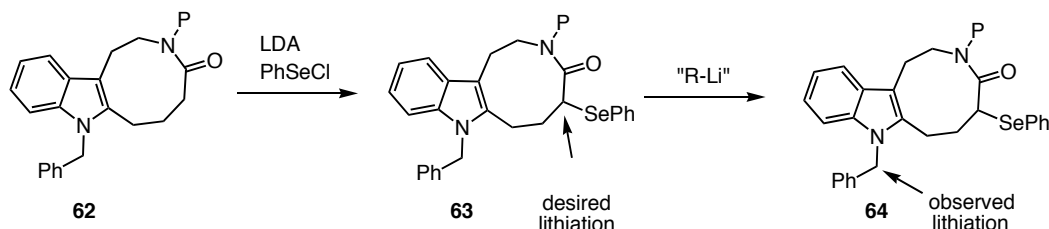


Having attempted these ring-contraction strategies without success, we re-focused our attention to functionalizing the original model system (Fig. 13). After orthogonal protection of the nitrogens,  $\alpha$ -selenenylation was accomplished using LDA and PhSeCl to provide **63**. Further attempts to introduce other functionality on **63** at the selenide-bearing carbon were met with regioselectivity issues presumably induced by torsional strain. In the event, lithiation occurred predominantly at the benzylic position shown in **64**. This undesired reaction could not be circumvented.

Figure 13. Issues with Lithiating Substituted Caprylactams



■ Regioselectivity issues prevented further desired functionalization

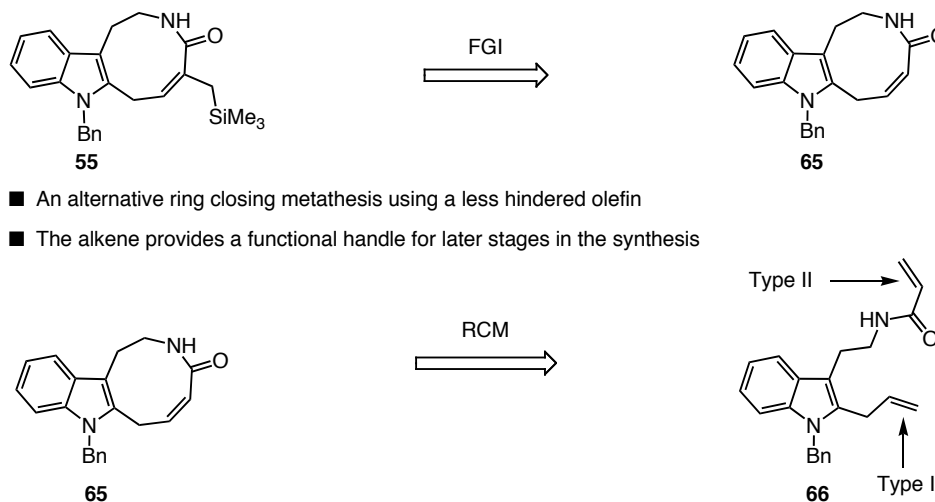


### Modifying the Strategy

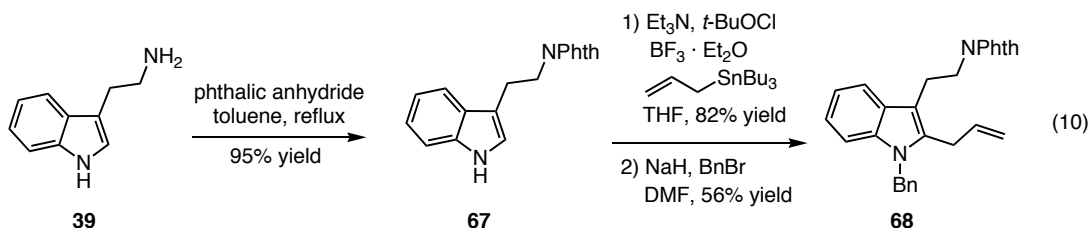
An alternate strategy was to simplify cyclization precursor **55** to  $\alpha,\beta$ -unsaturated caprylactam **65** (Fig. 14). Removing the silane appendage replaces the sterically

demanding type III alkene with a sterically less-demanding type II alkene **66**.<sup>15</sup> We hoped this combination of more reactive olefins would facilitate closure of the strained ring.

**Figure 14. Simplifying the Nine-Membered Lactam Intermediate**



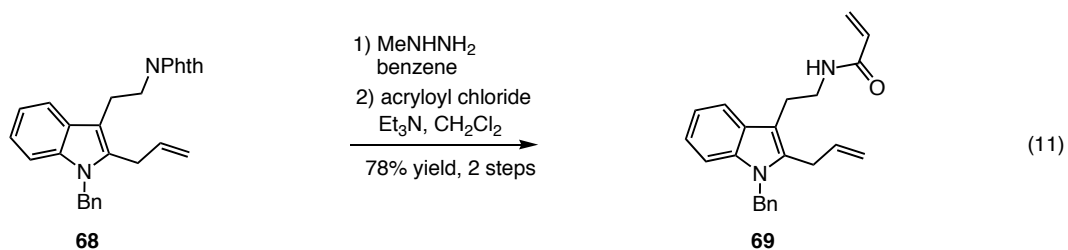
Treating tryptamine **39** with phthalic anhydride, followed by re-crystallization provided pure phthalimide-protected compound **67** (eq. 10). Following a Danishefsky procedure,<sup>16</sup> the allyl group was installed and subsequent benzyl protection provided compound **68** in 44% yield over two chemical steps. During the protection step, it was crucial to closely monitor the reaction for the exact end point, due to deleterious alkene bond isomerization. Furthermore, neutral pH 7 buffer solution was required for all subsequent aqueous workups in order to prevent this undesired event.



(15) Chatterjee, A. K.; Choi, T. L.; Sanders, D. P.; Grubbs, R. H. *J. Am. Chem. Soc.* **2003**, *125*, 11360-11370.

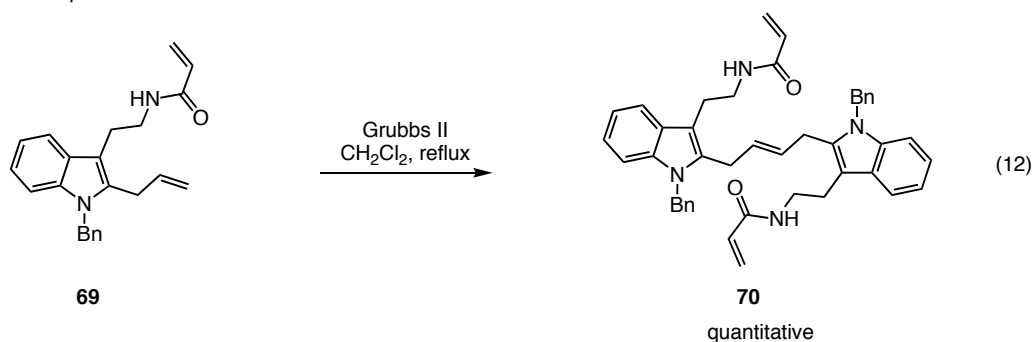
(16) Chatterjee, A. K.; Choi, T. L.; Sanders, D. P.; Grubbs, R. H. *J. Am. Chem. Soc.* **1999**, *121*, 11964-11975.

Due to the sensitivity of the alkene **68** towards isomerization, mild phthalimide deprotection conditions were sought. Methyl hydrazine was utilized to unmask the amine, as it was successful in Nicolaou's calicheamicin synthesis.<sup>17</sup> Subjecting the crude amine to acylation conditions provided amide **69** in 78% yield over two steps (eq. 11). This expedient route provided this RCM substrate in multi-gram quantities.



As an initial foray into constructing the caprylactam, amide **69** was subjected to standard RCM conditions (eq. 12). Disappointingly, only dimer **70** was formed in quantitative yield. This result is best explained in terms of amide bond *cis/trans* isomerization. The barrier to this rotation event is typically high (15–20 kcal/mol) favoring the more stable *trans* configuration.<sup>18</sup> In this case, the *trans* geometry orients the acrylamide olefin distal to the intermediate ruthenium carbene, preventing a successful cross metathesis.

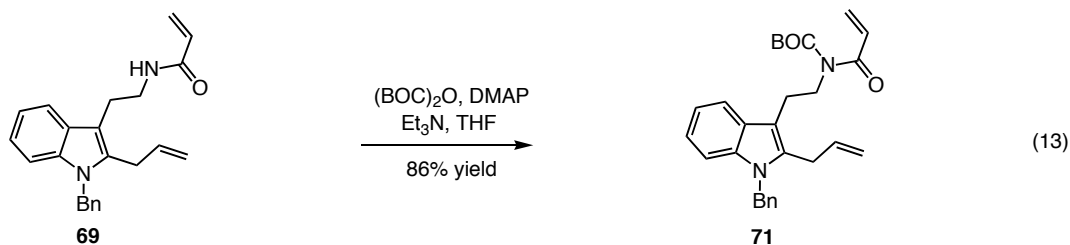
■ The unprotected amide dimerizes



(17) Smith, A. L.; Hwang, C. K.; Pitsinos, E.; Scarlato, G. R.; Nicolaou, K. C. *J. Am. Chem. Soc.* **1992**, *114*, 3134-3136.

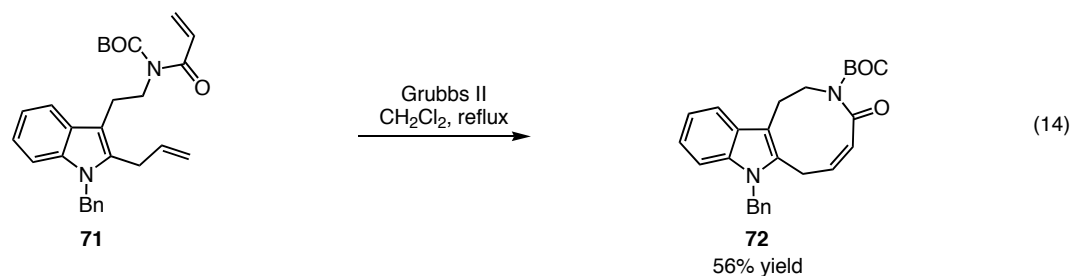
(18) Kemnitz, C. R.; Loewen, M. J. *J. Am. Chem. Soc.* **2007**, *129*, 2521-2528.

In order to overcome this barrier, a BOC group was introduced under standard conditions to provide bisalkene **71** (eq. 13).



Gratifyingly, subjecting this compound to the previous conditions provided indole caprylolactam **72** in 56% yield, and confirms the ability of imide **71** to overcome the energy barrier of C-N bond rotation to position the acrylamide alkene in close proximity to the ruthenium carbene (eq. 14).

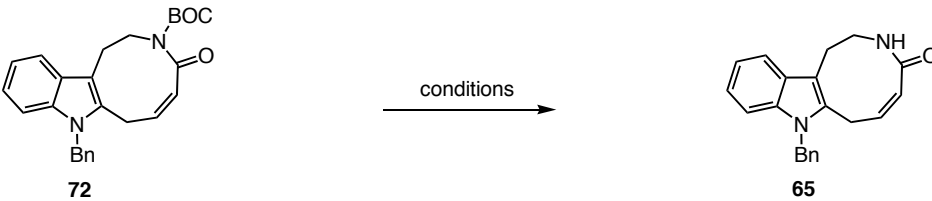
■ Tertiary amides undergo peptide bond rotation



Having solved the cyclization step, we sought to unveil cascade cyclization precursor **65** via BOC deprotection of lactam **72**. Utilizing standard TFA conditions resulted in extensive decomposition of the starting material (Table 1, entry 1). Employing alternative acids led to quantitative hydrolysis of the lactam moiety (Table 1, entry 2). The substrate was then subjected to basic conditions. Unfortunately, neither  $\text{K}_2\text{CO}_3$  nor  $\text{Cs}_2\text{CO}_3$  successfully removed the BOC group (Table 1, entries 3,4).



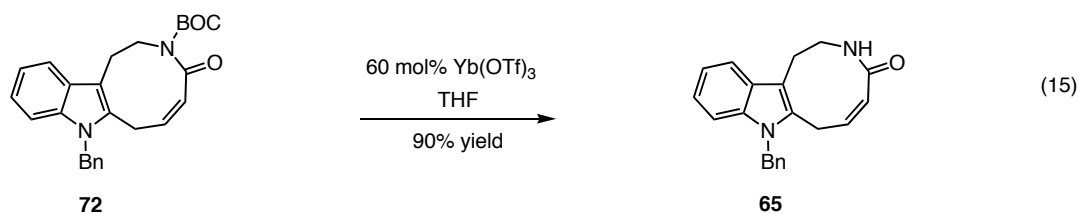
**Table 1. Subjecting the Caprylolactam to a Variety of Deprotection Conditions**



entry	conditions	result
1	2 eq. TFA/CH <sub>2</sub> Cl <sub>2</sub>	complex mixture
2	2 eq. TsOH•H <sub>2</sub> O	amide bond hydrolysis product
3	K <sub>2</sub> CO <sub>3</sub> /DME 70 °C	starting material persisted
4	Cs <sub>2</sub> CO <sub>3</sub> /imidazole/THF 70 °C	complex mixture

Due to the sensitivity of this substrate to Brønsted acid and basic conditions, substrate **72** was subjected to Lewis acid conditions.<sup>19</sup> Fortuitously, a catalytic amount of Yb(OTf)<sub>3</sub> cleanly provided deprotected material **65** in 90% yield (eq. 15).

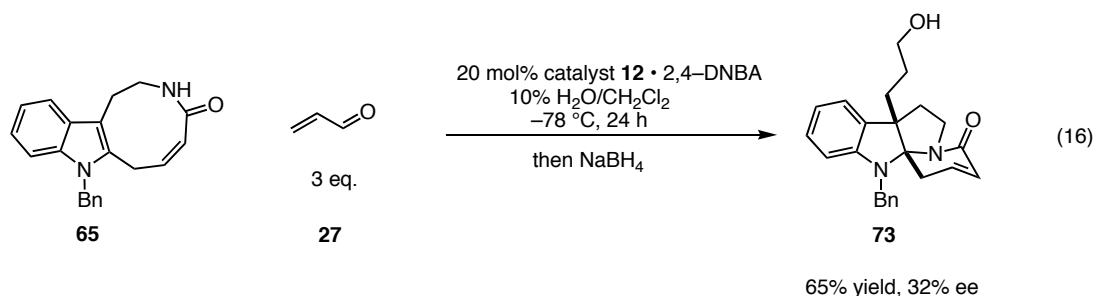
■ Successful BOC deprotection conditions



In proceeding with the synthesis, caprylolactam **65** was subjected to organocatalytic cyclization conditions. Gratifyingly, this unsaturated analogue of the model system provided desired tetracycle **73** in 65% yield and 32% ee, a promising first result (eq. 16).

(19) Calimsiz, S.; Lipton, M. A. *J. Org. Chem.* **2005**, *70*, 6218-6221.

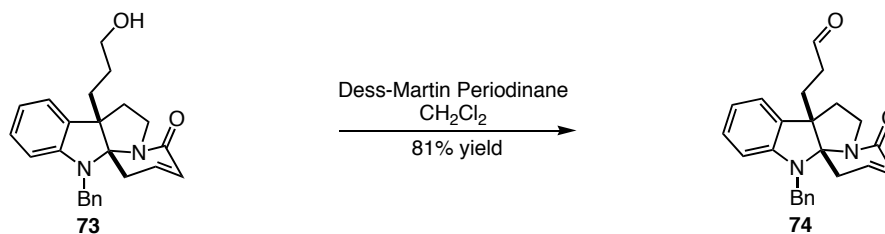
■ Organocatalytic cascade cyclization was successful on the unsaturated system



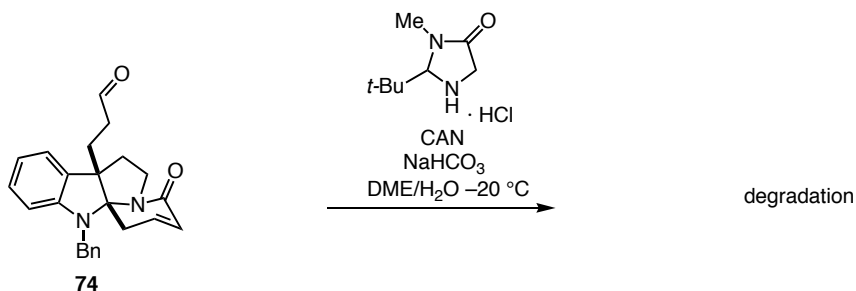
More importantly, the presence of the alkene was tolerated and, subsequently, provided a functional handle to introduce the allylsilane. Before optimizing the cascade sequence, a study was performed on tetracycle **73** to gain insight to the stability of electron-rich heterocycles under SOMO conditions (Fig. 15). Alcohol **73** was oxidized to aldehyde **74** using Dess-Martin periodinane in 81% yield. Subjecting aldehyde **74** to SOMO conditions resulted in rapid degradation to, presumably, polymeric species. Ceric ammonium nitrate (CAN) preferentially oxidizes electron-rich heterocycles over enamines.

**Figure 15. Testing the Stability of Electron-Rich Heterocycles Under SOMO Conditions**

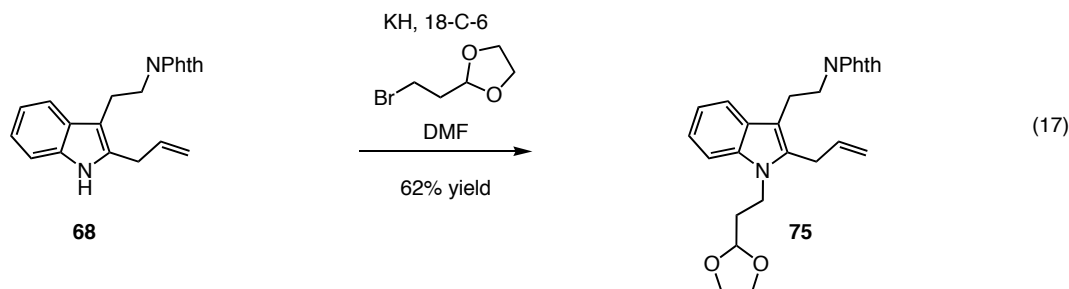
■ Oxidation of the alcohol provided the aldehyde



■ The results of the stability test provided important information

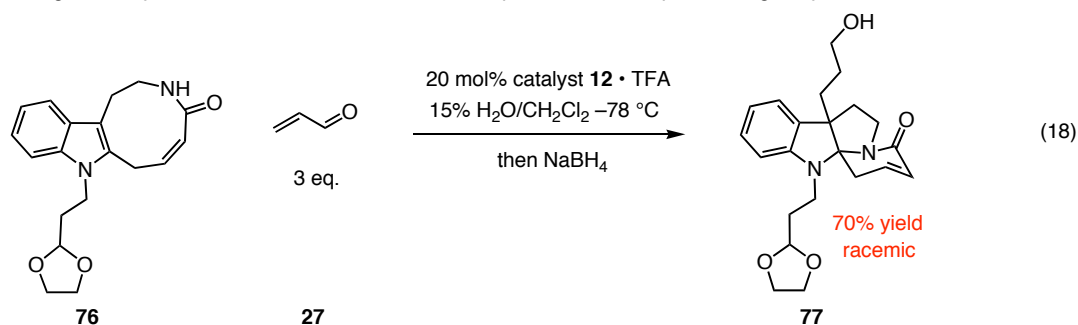


In order to overcome this issue, we postulated that decreasing the electron density of the aniline heterocycle would render CAN-mediated degradation less favorable. Indeed, in some cases, free indoles have been stable to CAN oxidation under SOMO conditions. To pursue this goal, an alternative protecting group that could be easily removed, was introduced via intermediate **68** (eq. 17).



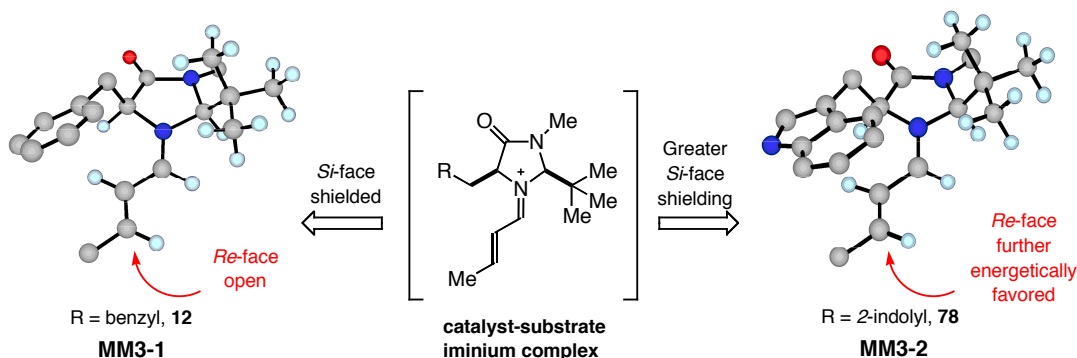
Dioxolane species **75** provides a functional group that can be cleaved under mild conditions that will leave the olefin moiety unchanged. This material was advanced to the indole caprylactam by the original sequence. Intriguingly, subjecting dioxolane **76** to cascade conditions produced desired tetracycle **77** in 70% yield as a racemic mixture (eq. 18). This result demonstrates that seemingly innocuous changes on the indole starting material have a large impact on the outcome of this organocatalytic pyrroloindoline-forming reaction. Fortunately, the sensitive nature of this methodology allows slight changes in reaction conditions to aid optimization.

■ Organocatalytic cascade reaction on the dioxolane produce racemic product in good yield



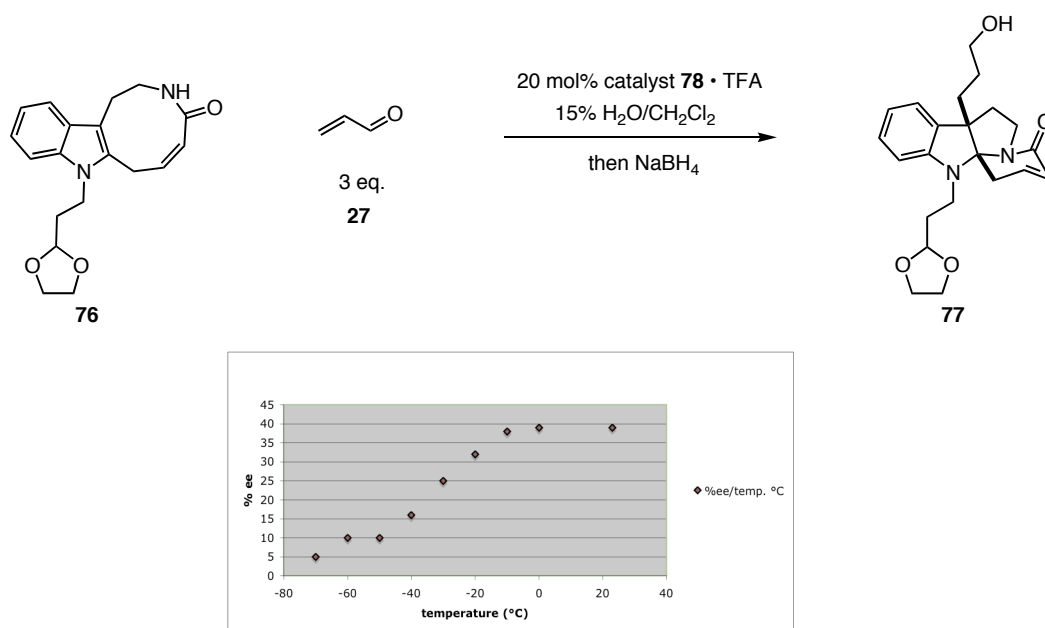
The first step to improving this reaction was to utilize an alternative imidazolidinone catalyst (Fig. 16). The increased enantiofacial coverage by substituting the phenyl group, **MM3-1**, with an indole moiety, **MM3-2**, should improve the enantioselectivity of the Friedel-Crafts addition. Furthermore, the indole moiety of **MM3-2** has a greater electrostatic surface potential than the phenyl group in **MM3-1** (compare 32.6 kcal/mol versus 27.1 kcal/mol). We believe this attribute will re-enforce the iminium geometry of the reactive intermediate by enabling a cation- $\pi$  interaction to further increase the ee of this cyclization.

Figure 16. MM3 Structures of Two Imidazolidinone Catalysts



Initial experiments utilizing the indole catalyst at  $-78\text{ }^{\circ}\text{C}$  led to nearly racemic product formation (3% ee), as was observed in the case of the related benzyl catalyst **12**. Interestingly, as the reaction temperature was warmed to room temperature, the ee was improved from 3% to 40% (Fig. 17). The improved enantioselectivity by indole catalyst **78** was not observed using benzyl catalyst **12**, as racemic material was obtained after repeating this reaction under the same conditions. These results are atypical for iminium catalyzed pyrroloindoline chemistry, where an inverse correlation between reaction temperature and enantioselectivity is generally observed.

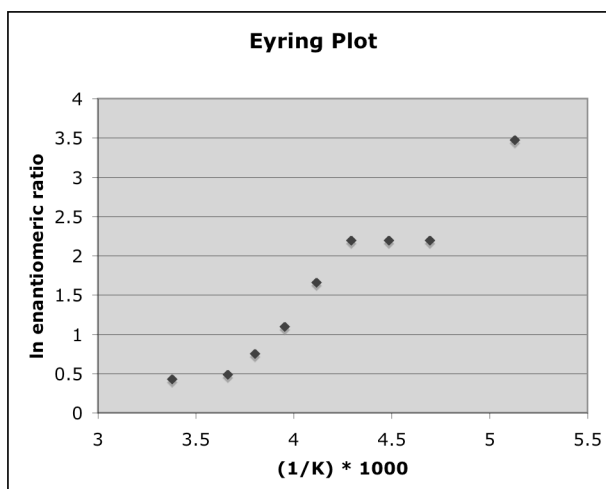
Figure 17. Increasing the Temperature Increases the Enantioselectivity



An Eyring plot analysis of these data indicates two inflection points over the range of temperatures examined in Figure 17 (Fig. 18). This indicates that two different reaction mechanisms are taking place, one below and one above  $-50\text{ }^{\circ}\text{C}$ . While the exact mechanisms remain unknown, it may be that an increased concentration of water at warmer temperatures may benefit a higher ee by introducing more acid co-catalyst (*vide infra*) into the reaction or by preventing reversibility of the acrolein addition, as is known for similar substrates, by forming a hemi-acetal. Another explanation may be the caprylolactam *cis/trans* orientation may be effected by additional acid in solution and influence the approach of the activated iminium intermediate.<sup>20</sup>

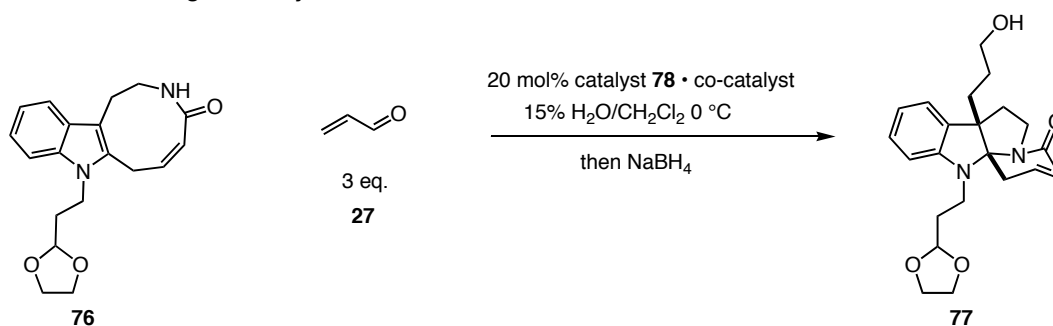
(20) Borgen, G. *Mag. Res. Chem.* **1991**, 29, 805.

Figure 18. Eyring Plot Analysis of the OC Reaction



After having determined that 0 °C was the optimal temperature, co-catalysts were surveyed for efficacy (Table 2). While no obvious trends were discovered (Table 1, entries 1-4), AcOH (entry 4) gave the highest levels of conversion and ee.

Table 2. Evaluating Co-Catalysts

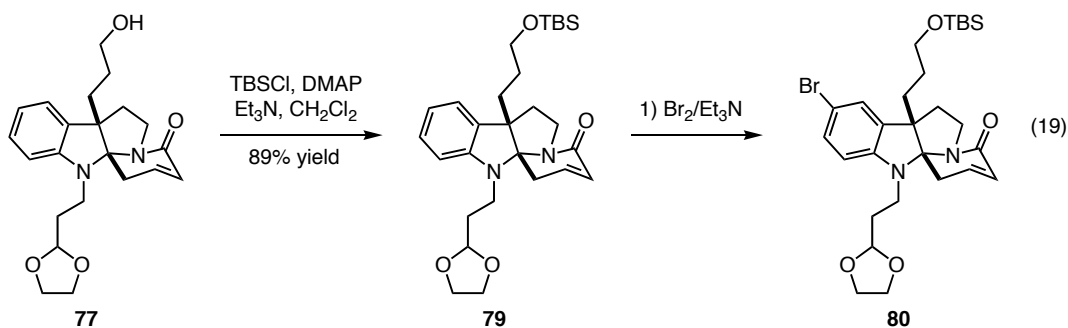


entry	cocatalyst	pKa	% yield	% ee	time (h)
1	TFA	-0.23	77	43	24
2	HCl	-8.0	82	57	24
3	DNBA	1.43	89	54	24
4	AcOH	3.77	83	60	24

While this key step was being optimized, tetracycle **77** was utilized in subsequent reactions. It was envisioned that Kumada cross-coupling conditions could install the

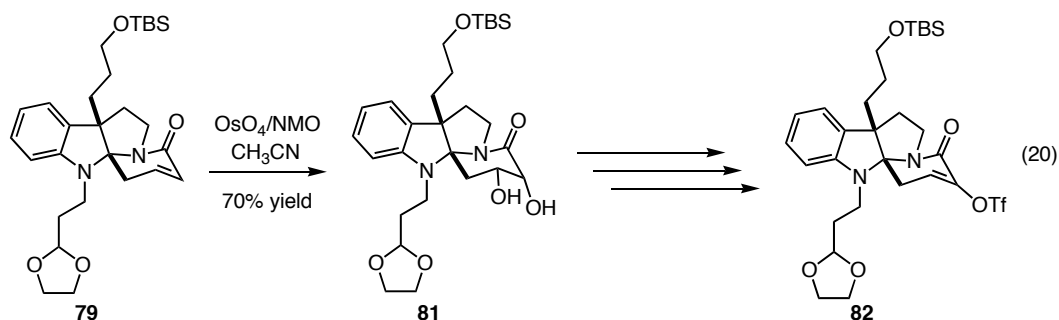
allylsilane needed for the SOMO cyclization. Attempts to access the vinyl bromide coupling intermediate were met with regiochemical issues (eq. 19). In the event, after protection of alcohol **77** as the silyl ether **79**, halogenation only provided the brominated 4-position of the aniline ring **80**. The use of alternative bromine sources led to the same electrophilic aromatic substitution product.

■ Halogenation/Dehydrohalogenation brominated the aniline ring



The need for a chemoselective reaction was met by utilizing a dihydroxylation sequence (eq. 20). The resulting diol **81** should lend itself to further manipulation into a bis-triflate intermediate that should undergo manipulation into vinyltriflate **82**.

■ Dihydroxylation worked well

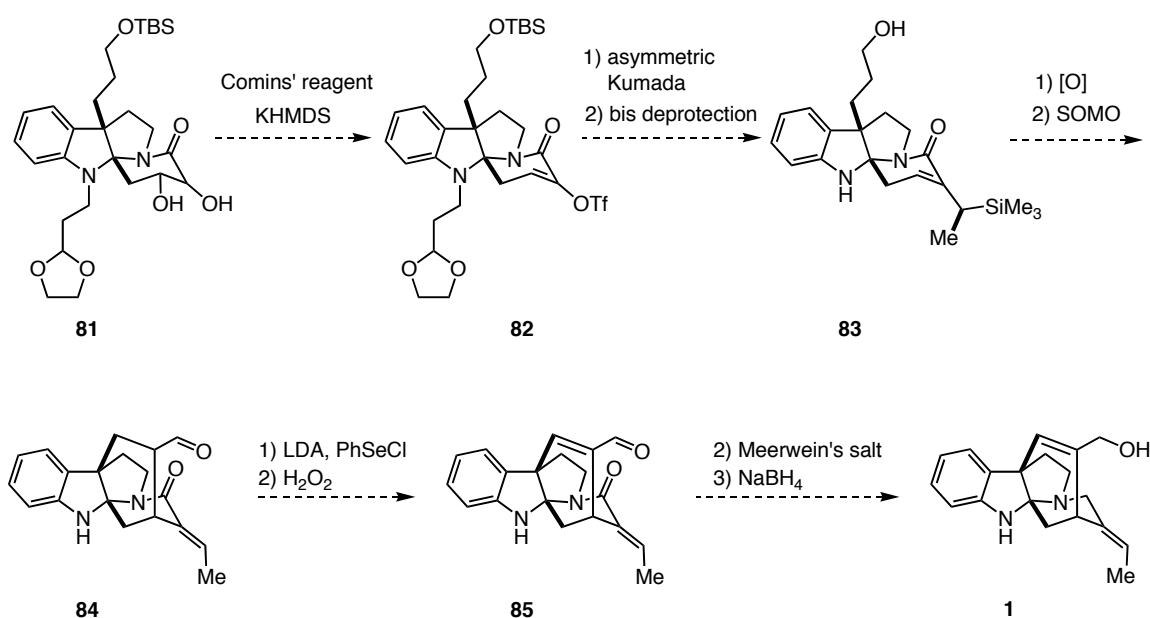


### Future Directions

Diol **81** will be transformed into the bis-triflate that should undergo regioselective elimination of the β-amide triflate to provide intermediate **82**. This intermediate will be subjected to Kumada conditions utilizing the commercially available Grignard of the

desired trimethylsilane. If the methyl stereocenter is not set via substrate-controlled diastereoselective addition, asymmetric conditions will be pursued. Bis-deprotection of the resulting silyl ether produces allylsilane **83**. Subsequent oxidation and then SOMO catalysis will create the final C-C bond to furnish the final ring in **84**. Finally, installation of the alkene, imide formation of the amide, and subsequent NaBH<sub>4</sub> reduction should provide (+)-minfiensine **1** (Fig. 19).

**Figure 19. Plans to Complete the Synthesis**



## Conclusion

In summary, an efficient entry into the ring framework of (+)-minfiensine has been described. We have further established iminium catalysis as a valuable mode of activation to access complex architectures found in natural products. This rapid access to the pyrroloindoline core, followed by a SOMO mediated alkylation event, should rapidly assemble the tetracyclic core bearing functionality that can be manipulated to the desired natural product.



## Supporting Information

**General Information.** Commercial reagents were purified prior to use following the guidelines of Perrin and Armarego.<sup>1</sup> Non-aqueous reagents were transferred under nitrogen via syringe or cannula and purified according to the method of Grubbs.<sup>2</sup> Organic solutions were concentrated under reduced pressure on a Büchi rotary evaporator. Chromatographic purification of products was accomplished using forced-flow chromatography on ICN 60 32-64 mesh silica gel and Iatrobeads<sup>®</sup> according to the method of Still.<sup>3</sup> Thin-layer chromatography (TLC) was performed on EM Reagents 0.25 mm silica gel 60-F plates. Chromatograms were visualized by fluorescence quenching or by staining using either potassium permanganate or anisaldehyde stain.

<sup>1</sup>H and <sup>13</sup>C NMR spectra were recorded on a Varian Mercury 300 Spectrometer, and are internally referenced to residual solvent signals. Data for <sup>1</sup>H NMR are reported as follows: chemical shift (δ ppm), multiplicity (s = singlet, d = doublet, t = triplet, q = quartet, m = multiplet), integration, coupling constant (Hz), and assignment. Data for <sup>13</sup>C NMR are reported in terms of chemical shift. IR spectra were recorded on a Perkin Elmer Paragon 1000 spectrometer and are reported in terms of frequency of absorption (cm<sup>-1</sup>). Mass spectra were obtained from the Caltech Mass Spectrometry Facility and the Princeton Mass Spectrometry Facility by electron ionization, chemical ionization, or fast atom/ion bombardment techniques. Gas liquid chromatography (GLC) was performed on Hewlett-Packard 6850 and 6890 Series gas chromatographs equipped with a split-mode capillary injection system and flame ionization detectors using a Bodman Chiraldex b-

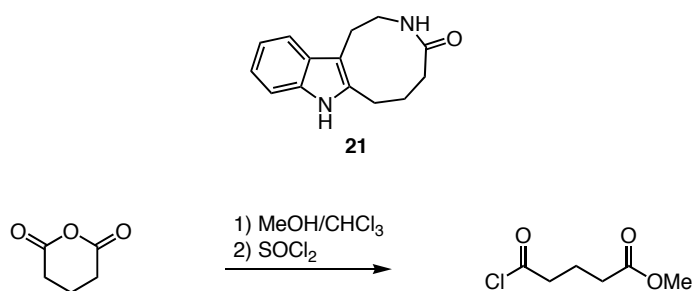
---

(1) Perrin, D. D.; Armarego, W. L. F. *Purification of Laboratory Chemicals*; 3rd ed., Pergamon Press, Oxford, 1988.

(2) Pangborn, A. B.; Giardello, M. A.; Grubbs, R. H.; Rosen, R. K.; Timmers, F. J. *Organometallics* **1996**, *15*, 1518.

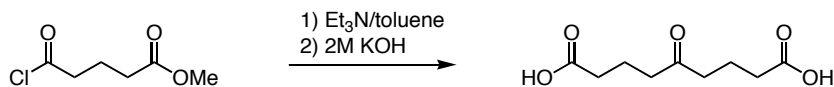
(3) Still, W. C.; Kahn, M.; Mitra, A. J. *J. Org. Chem.* **1978**, *43*, 2923.

DM (30 m × 0.25 mm), a Bodman Chiraldex Γ-TA (30 m × 0.25 mm), or a Hydrodex-B-TBDAC (50 m × 0.25 mm) column, as noted. Optical rotations were measured on a Jasco P-1010 polarimeter, and  $[\alpha]_D$  values are reported in  $10^{-1} \text{ dg cm}^2 \text{ g}^{-1}$ ; concentration (c) is in g/100 mL. Supercritical fluid chromatography was performed on a Berger Minigram equipped with a diode array UV detector ( $\lambda = 214\text{--}258 \text{ nm}$ ) using a chiral column (25 cm) and guard column (5 cm) as noted for each compound.



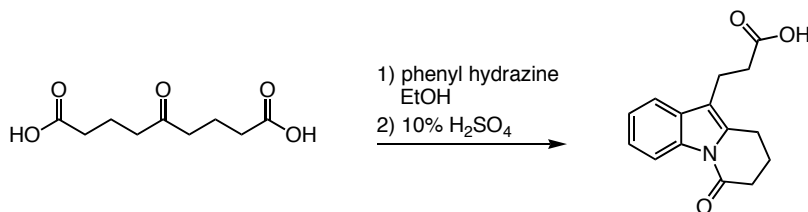
**Methyl-4-(chlorocarbonyl)butanoate.** Dihydro-3*H*-pyran-2,6-dione (49 g, 429 mmol) was suspended in a solution of dry MeOH (17.4 mL, 429 mmol) in  $\text{CHCl}_3$  (390 mL) and refluxed for 5 hours. The resulting solution was cooled to room temperature and  $\text{SOCl}_2$  (62.6 mL, 858 mmol) was added dropwise via addition funnel over 3 hours. After complete addition, excess  $\text{SOCl}_2$  was removed via rotary evaporation and the crude material was distilled at  $67^\circ\text{C}$ , 2.5 mm Hg to provide the desired product as a clear oil (76.1 g, 76% yield). Spectroscopic data were identical to that reported by Oda *et al.*<sup>4</sup>

(4)Oda, H.; Kobayashi, T.; Kosugi, M.; Migita, T. *Tetrahedron* **1995**, *51*, 695-702.

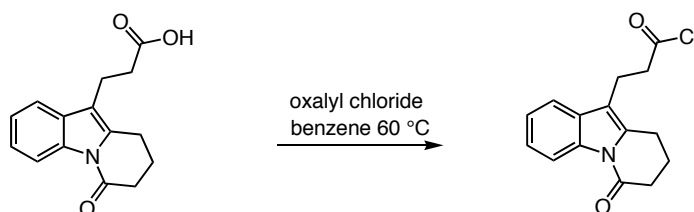


**5-Oxononanedioic acid.** To a clear solution of methyl-4-(chlorocarbonyl)butanoate (130 g, 790 mmol) in benzene (790 mL) cooled to 0 °C was added freshly distilled triethylamine (80 g, 110 mL, 790 mmol) dropwise in order to keep the reaction temperature below 25 °C. The resulting cloudy white solution stirred at 0 °C for 5 minutes and then carefully warmed to 35 °C over 15 minutes. The resulting light yellow oil was stirred at room temperature for 30 minutes and then passed through a filter to remove the triethylamine HCl salts. This solid was washed with benzene (3 × 200 mL) and the resulting elute was concentrated to an orange oil. To this oil was added 2M KOH (680 mL) and the resulting suspension was refluxed for 5 hours. The homogeneous solution was acidified with concentrated HCl (138 mL) and the aqueous solution was concentrated to a solid. These salts were extracted with hot acetone (5 × 100 mL) and the solution was dried over Na<sub>2</sub>SO<sub>4</sub>, filtered, and concentrated. After dissolving the resulting material in hot H<sub>2</sub>O, the product recrystallized overnight at 0 °C. The first batch was harvested and the mother liquor was concentrated. The resulting residue was recrystallized as before. The product was isolated as an amorphous solid (48% average yields). The spectroscopic data were identical to that reported by the Ban Group.<sup>5</sup>

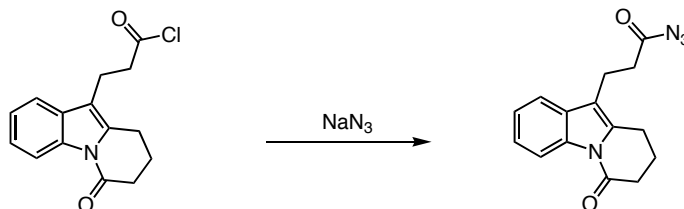
(5) Ban, Y.; Yoshida, K.; Goto, J.; Oishi, T.; Takeda, E. *Tetrahedron* **1983**, *39*, 3657-3668.



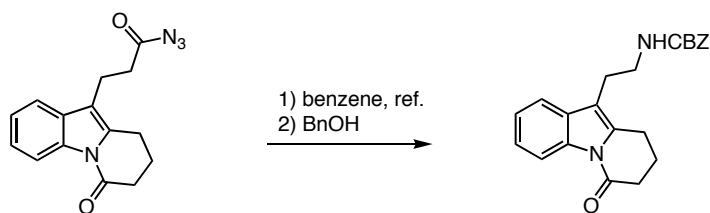
**3-(6,7,8,9-tetrahydro-6-oxopyrido[1,2-*a*]indol-10-yl)propanoic acid.** To a clear solution of 5-oxononanedioic acid (21.8 g, 108 mmol) in EtOH (220 mL) was added phenyl hydrazine (11.7 g, 10.7 mL, 108 mmol). The resulting light yellow solution was stirred at room temperature for 30 minutes and then concentrated to produce an orange solid. To this solid was added 10% H<sub>2</sub>SO<sub>4</sub> (700 mL) and the suspension was refluxed for 1 hour. Upon cooling a brown solid precipitated and was subsequently filtered. The solid was recrystallized from ethanol to afford the product as a white solid (14.4 g, 52% yield). The spectroscopic data were identical to that reported by the Ban Group.<sup>5</sup>



**3-(6,7,8,9-tetrahydro-6-oxopyrido[1,2-*a*]indol-10-yl)propanoyl chloride.** To a suspension of 3-(6,7,8,9-tetrahydro-6-oxopyrido[1,2-*a*]indol-10-yl)propanoic acid (15.2 g, 75.2 mmol) in benzene (20 mL) was added oxalyl chloride (11.45 mL, 129 mmol). The resulting cloudy orange solution was heated to 60 °C for 30 minutes. The resulting homogeneous solution was concentrated to an orange solid and used crude in the next step. The IR data were identical to that reported by the Ban Group.<sup>5</sup>

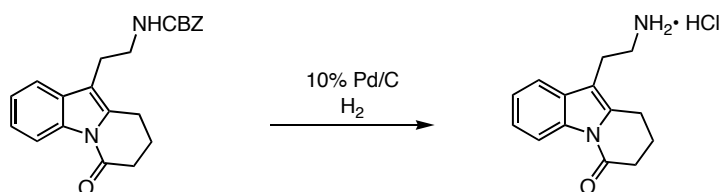


**10-(3-azido-3-oxopropyl)-8,9-dihydropyrido[1,2-*a*]indol-6(7*H*)-one.** To a clear solution of sodium azide (4.36 g, 67.2 mmol) in H<sub>2</sub>O (11 ml) cooled to 0 °C was added a light yellow solution of 3-(6,7,8,9-tetrahydro-6-oxopyrido[1,2-*a*]indol-10-yl)propanoyl chloride in dry acetone (140 ml) dropwise via addition funnel. The resulting cloudy yellow solution was stirred at 0 °C for 10 minutes and room temperature for 30 minutes after which it was diluted with H<sub>2</sub>O (230 mL). The solution sat for 30 minutes to ensure complete precipitation of solid. The product was collected by filtration and dried on high vacuum to afford a white solid (13 g, 82% yield) that was used as is in the next step. The IR data were identical to that reported by the Ban Group.<sup>5</sup>

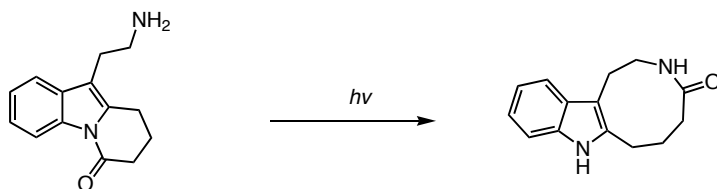


**Benzyl-2-(6,7,8,9-tetrahydro-6-oxopyrido[1,2-*a*]indol-10-yl)ethylcarbamate.** A suspension of 10-(3-azido-3-oxopropyl)-8,9-dihydropyrido[1,2-*a*]indol-6(7*H*)-one was refluxed for 1.5 hours and vigorously evolved nitrogen gas. After cooling to room temperature, freshly distilled benzyl alcohol (5.51 g, 5.30 mL, 51 mmol) was added and the resulting solution was refluxed for 2.5 hours. The reaction was cooled to room

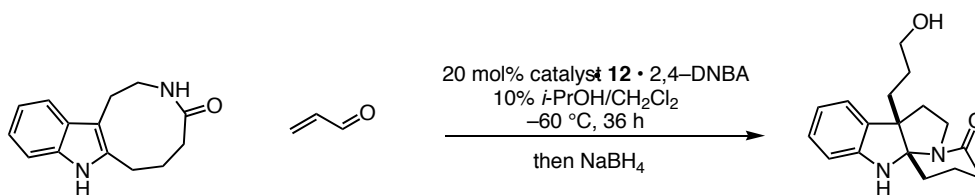
temperature and concentrated to a crude solid. Recrystallization from EtOAc afforded the product as a white solid (12.6 g, 82% yield). The spectroscopic data were identical to that reported by the Ban Group.<sup>5</sup>



**10-(2-aminoethyl)-8,9-dihydropyrido[1,2-a]indol-6(7H)-one HCl salt.** To a suspension of benzyl-2-(6,7,8,9-tetrahydro-6-oxopyrido[1,2-a]indol-10-yl)ethylcarbamate (20.6 g, 56.8 mmol) in MeOH (290 mL) and H<sub>2</sub>O (34 mL) was added AcOH (70 mL) and then 10% Pd/C (2.67 g). The suspension was stirred under 1 atm of H<sub>2</sub> gas. After 2.5 hours the reaction was judged complete by TLC analysis and passed through a plug of celite with the aid of MeOH and then concentrated to an amorphous solid. After dissolving this material into 100 mL of EtOH, HCl (14 mL) was added as a solution in EtOH (50 mL). The precipitate was filtered and washed with EtOH (150 mL) to provide the desired compound as a white solid (12.4 g, 83% yield). The spectroscopic data were identical to that reported by the Ban Group.<sup>5</sup>



**2,3,6,7-tetrahydroazonino[5,4-*b*]indol-4(1*H*,5*H*,8*H*)-one (21).** The intermediate 10-(2-aminoethyl)-8,9-dihydropyrido[1,2-*a*]indol-6(7*H*)-one HCl salt was basified in 10% NaOH (20 mL), then extracted with CH<sub>2</sub>Cl<sub>2</sub> (3 × 20 mL), dried over Na<sub>2</sub>SO<sub>4</sub>, filtered, and concentrated to an amorphous clear solid. This material was dissolved with MeOH (15 mL) and then added to a dry 1 L photo-immersion reactor under Ar. The solution was diluted with 890 mL dry Et<sub>2</sub>O and irradiated with 300 W Hg Lamp. The reaction was judged complete after 25 hours by TLC analysis and concentrated to an oily solid. Purification on silica gel using EtOAc/Acetone (3:2) provided the desired product as a white foamy solid (2.27 g, 69% yield). The spectroscopic data were identical to that reported by the Ban Group.<sup>5</sup>

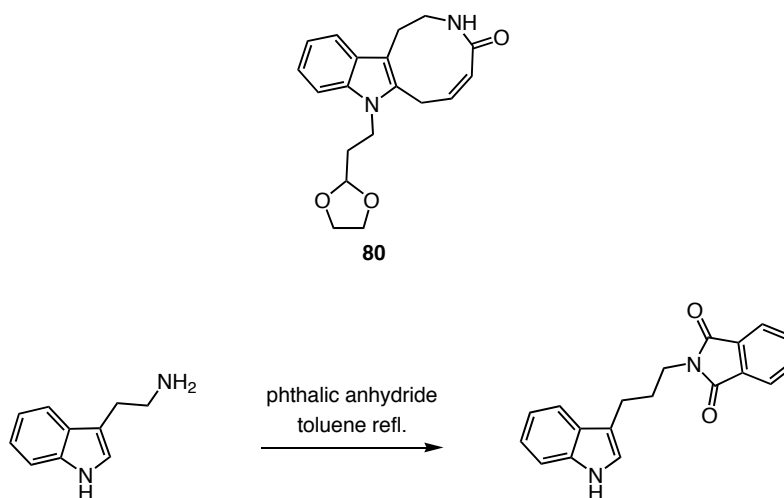


**Dihydro-9a,4a-(iminoethano)-9*H*-carbazole derivative (29).** To a solution of 2,3,6,7-tetrahydroazonino[5,4-*b*]indol-4(1*H*,5*H*,8*H*)-one (30 mg, 0.131 mmol) in 10% *i*-PrOH/CH<sub>2</sub>Cl<sub>2</sub> (1.1 mL) cooled to -60 °C was added the 2,4-dinitrobenzoic acid salt of (2*R*,5*R*)-2-*tert*-butyl-5-benzyl-3-methylimidazolidin-4-one (12 mg, 0.062 mmol) and then

acrolein (11 mg, 0.197 mmol). The resulting solution was stirred for 32 hours until the reaction was judged complete by TLC analysis. To this light yellow solution was added EtOH (1:1 v/v, 1.1 mL). The resulting solution was then transferred to an ice bath. Treatment with NaBH<sub>4</sub> (25 mg, 0.655 mmol) for 30 minutes induced vigorous bubbling and the light yellow solution turned clear. Quenching the excess NaBH<sub>4</sub> was performed by dropwise addition of 5% HCl (0.1 mL). The layers were separated and the aqueous phase was extracted with CH<sub>2</sub>Cl<sub>2</sub> (3 × 1 mL), dried over Na<sub>2</sub>SO<sub>4</sub>, filtered, and concentrated. The crude material was purified on a Gilson-215 Liquid Handler by preparatory high-pressure liquid chromatography to afford the desired product as a foamy white solid (12 mg, 32% yield, 32% ee). Enantiomeric excess was determined by SFC analysis using an ADH column in a 5-50% gradient of MeOH (major t<sub>r</sub> = 5.83 min., minor t<sub>r</sub> = 7.43 min.) IR (film) 3302, 2944, 1624, 1607, 1466, 1408, 1322, 1263, 1182, 1058, 995, 937, 744 cm<sup>-1</sup>; <sup>1</sup>H NMR (500 MHz, CDCl<sub>3</sub>) δ 7.08 – 7.03 (m, 2H, 2 × ArH), 6.77 (t, 1H, J = 7.8 Hz, ArH), 6.58 (d, 1H, J = 7.8 Hz, ArH), 4.56 (bs, 1H, NH), 4.10, (ddd, 1H, J = 7.3, 4.3, 1.4 Hz, NCHH), 3.6 (t, 2H, J = 5.8 Hz, CH<sub>2</sub>OH), 2.94 – 2.88 (m, 1H, NCHH), 2.5 (dd, 1H, J = 7.3 Hz, CHC=O), 2.43 – 2.36 (m, 1H, CHC=O), 2.15 – 1.95 (m, 4H, CHHCH<sub>2</sub>CH<sub>2</sub>C=O, NCH<sub>2</sub>CHH) 1.88 – 1.70 (m, 5H, CH<sub>2</sub>CHHCH<sub>2</sub>OH, NCH<sub>2</sub>CHH, CHHCH<sub>2</sub>CH<sub>2</sub>C=O), 1.53 – 1.47 (m, 1H, CHHCH<sub>2</sub>CH<sub>2</sub>OH; <sup>13</sup>C NMR (75 MHz, CDCl<sub>3</sub>) δ 168.1, 147.9, 132.0, 128.3, 123.6, 119.2, 108.9, 87.6, 63.0, 59.3, 44.1, 37.2, 31.4, 29.9, 29.7, 28.0, 16.9; HRMS (EI<sup>+</sup>) exact mass calculated for [M]<sup>+</sup> (C<sub>17</sub>H<sub>23</sub>N<sub>2</sub>O<sub>2</sub>) requires *m/z* 286.1681, found *m/z* 286.1682.

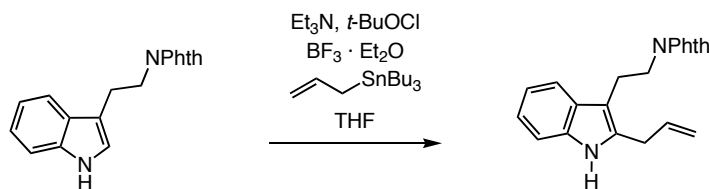
[α]<sub>D</sub><sup>22</sup> = -21.4 ° (c = 10.3, CHCl<sub>3</sub>).





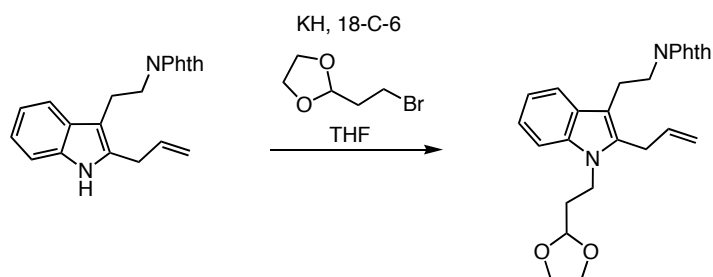
**2-(2-(1*H*-indol-3-yl)ethyl)isoindoline-1,3-dione (69).** A suspension of tryptamine (10 g, 62.4 mmol) and phthalic anhydride (10.15 g, 68.6 mmol) in toluene (390 mL) was refluxed for 16 hours until the reaction was judged complete by TLC analysis. The resulting red solution was concentrated to a pink solid. This crude material was triturated with 3:1 hexanes/CH<sub>2</sub>Cl<sub>2</sub> (6 × 100 mL) to afford a light pink solid that was used as is in the next step. The spectroscopic data were identical to that reported by the Hsung Group.<sup>6</sup>

(6) Luo, S. J.; Zifcsak, C. A.; Hsung, R. P. *Org Lett* **2003**, 5, 4709-4712.



**2-(2-(2-allyl-1*H*-indol-3-yl)ethyl)isoindoline-1,3-dione.** To a red solution of 2-(3-(1*H*-indol-3-yl)propyl)isoindoline-1,3-dione (15 g, 51.7 mmol) in dry toluene (170 mL), under Ar, in the dark, and cooled to  $-78\text{ }^{\circ}\text{C}$ , was added dry triethylamine (8.6 mL, 62 mmol) then *t*-butyl hypochlorite (7.53 mL, 62 mmol) dropwise. The resulting solution was stirred at  $-78\text{ }^{\circ}\text{C}$  for 30 minutes and then, in order, was added allyl tri-*n*-butyl stannane (32 mL, 103.4 mmol) and boron trifluoride etherate (13 mL, 103.4 mmol). This solution was allowed to slowly warm to room temperature over 12 hours until the reaction was judged complete by TLC analysis. A saturated solution of K<sub>2</sub>CO<sub>3</sub> (250 mL) was added and the reaction stirred at room temperature for 30 minutes. The layers were separated and the aqueous phase was extracted with EtOAc ( $3 \times 200\text{ mL}$ ), dried over Na<sub>2</sub>SO<sub>4</sub>, filtered, and concentrated. The crude material was purified by SiO<sub>2</sub> chromatography (20–40% EtOAc/Hexanes) to provide a light yellow solid. Excess tin impurities were removed by suspending the solid in hexanes and stirring with diethylazodicarboxylate (0.5 eq.) for 1 hour followed by filtration and hexane washes ( $3 \times 150\text{ mL}$ ). The product was isolated as a light yellow solid (14 g, 82% yield). IR (film) 3394, 1768, 1702, 1462, 1437, 1395, 1358, 1339, 1243, 1187, 1171, 1121, 1099, 1088, 1021, 912, 735, 715 cm<sup>-1</sup>; <sup>1</sup>H NMR (500 MHz, CDCl<sub>3</sub>)  $\delta$  7.88 (bs, 1H, ind. NH), 7.85 – 7.84 (m, 2H, ArH), 7.73 – 7.70 (m, 3H, ArH), 7.30 – 7.28 (m, 1H, ArH), 7.14 (t, 1H,  $J = 7.06\text{ Hz}$ , ArH), 7.10 (t, 1H,

$J = 7.16$  Hz, ArH), 6.01 – 5.93 (m, 1H,  $\text{CH}_2\text{CH}=\text{CH}_2$ ), 5.21 (dd, 1H,  $J = 18.7, 1.62$  Hz,  $\text{CH}=\text{CH}$  *trans*), 5.16 (dd, 1H  $J = 10.0, 1.44$  Hz  $\text{CH}=\text{CH}$  *cis*), 3.92 (t, 2H,  $J = 7.90$  Hz,  $\text{CH}_2\text{NPhth}$ ), 3.58 (d, 2H,  $\text{CH}_2\text{CH}=\text{CH}_2$ ), 3.10 (t, 2H,  $J = 7.91$  Hz  $\text{CH}_2\text{CH}_2\text{NPhth}$ );  $^{13}\text{C}$  NMR (75 MHz,  $\text{CDCl}_3$ )  $\delta$  168.4, 135.3, 134.8, 133.8, 133.3, 132.2, 128.5, 121.4, 119.5, 118.3, 117.3, 110.4, 108.1; HRMS ( $\text{EI}^+$ ) exact mass calculated for  $[\text{M}]^+$  ( $\text{C}_{21}\text{H}_{18}\text{N}_2\text{O}_2$ ) requires  $m/z$  330.1368, found  $m/z$  330.1370.

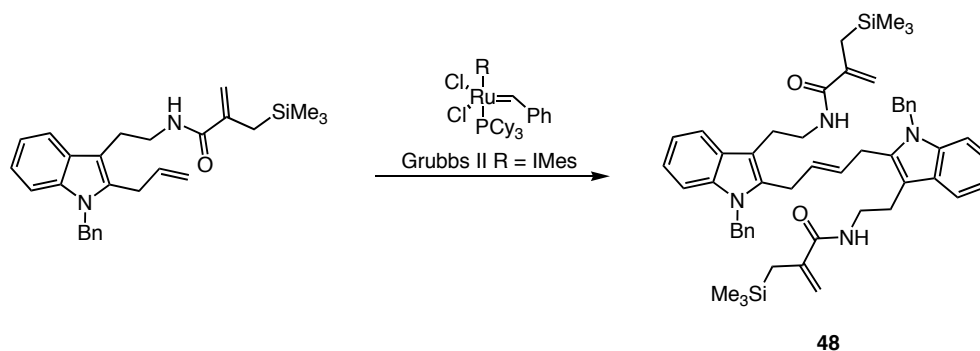


**2-(2-(1-(2-(1,3-dioxolan-2-yl)ethyl)-2-allyl-1H-indol-3-yl)ethyl)isoindoline-1,3-dione**

**(79)** A suspension of KH (30% dispersion in mineral oil, 3.42 g, 25.6 mmol) was added to a flame-dried 250 mL round bottom flask and purged with argon. To this was added anhydrous THF (40 mL) and the resulting suspension was cooled to  $-78$  °C using a dry ice/acetone bath. In another flame-dried 100 mL RBF, under argon, was placed the starting indole (6.54 g, 19.7 mmol) and recrystallized, dried 18-crown-6 (7.8 g, 29.6 mmol). These solids were dissolved in 25 mL dry THF and added in a rapid drop-wise fashion to the KH suspension, stirred at  $-78$  °C for 1 hour and then warmed to  $0$  °C for 40 minutes to ensure complete hydrogen gas evolution. After cooling to  $-78$  °C, the dioxolane reagent (3.3 mL, 27.6 mmol) was added immediately after passing it through a small plug of silica gel and the resulting solution was allowed to slowly warm to room

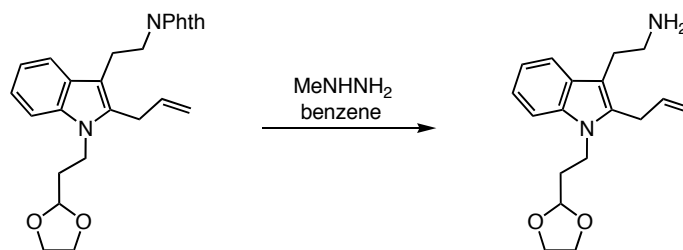
temperature over 6 hours. After stirring for an additional hour at room temperature, the reaction was judged complete by TLC analysis. The reaction was quenched with 200 mL pH 7 buffer solution and the aqueous layer was extracted 3 times with EtOAc (150 mL), dried over Na<sub>2</sub>SO<sub>4</sub>, filtered, and concentrated to a red oil. The product was applied to a silica gel column in toluene and eluted in 20% EtOAc/Hexanes then 40% EtOAc/Hexanes to isolate the protected indole as a light yellow oil (5.26 g, 62% yield).

IR (film) 1770.3, 1708.8, 1467.4, 1533.5, 1395.4, 1363.8, 1179.6, 1136.8, 1021.8, 916.2, 717.5 cm<sup>-1</sup>; <sup>1</sup>H NMR (300 MHz, CDCl<sub>3</sub>)  $\delta$  7.82 – 7.81 (m, 2H, ArH), 7.69 – 7.68 (m, 2H, ArH), 7.31 (d, 1H J = 8.1 Hz, ArH), 7.15 (t, 1H, J = 7.1 Hz, ArH), 7.08 (t, 1H, J = 7.8 Hz, ArH), 5.95 (ddt, 1H, J = 17.7, 10.2, 5.62 Hz, CH=CH<sub>2</sub>), 5.05 (d, 1H, J = 10.1 Hz, CH=CH *cis*), 4.98 (d, 1H, J = 17.1 Hz, CH=CH *trans*), 4.84 (t, 1H, J = 4.37 Hz, OCHO), 4.19 (t, 2H, J = 7.59 Hz, CH<sub>2</sub>NPhth), 4.00 (t, 2H, J = 7.1 Hz, indNCH<sub>2</sub>), 3.87 – 3.83 (m, 4H, OCH<sub>2</sub>CH<sub>2</sub>O), 3.59 (d, 2H, J = 5.6 Hz, CH<sub>2</sub>CH=CH<sub>2</sub>), 3.05 (t, 2H, J = 8.23 Hz, CH<sub>2</sub>CH<sub>2</sub>NPhth), 2.09 – 2.05 (m, 2H, ind.NCH<sub>2</sub>CH<sub>2</sub>); <sup>13</sup>C NMR (75 MHz, CDCl<sub>3</sub>)  $\delta$  168.3, 136.0, 135.2, 134.4, 133.8, 132.2, 127.8, 123.1, 121.1, 119.2, 118.3, 116.4, 109.1, 108.4, 102.2, 38.6, 34.0, 28.5, 23.8; HRMS (EI<sup>+</sup>) exact mass calculated for [M]<sup>+</sup> (C<sub>25</sub>H<sub>26</sub>N<sub>2</sub>O<sub>4</sub>) requires *m/z* 430.1892, found *m/z* 430.1891.

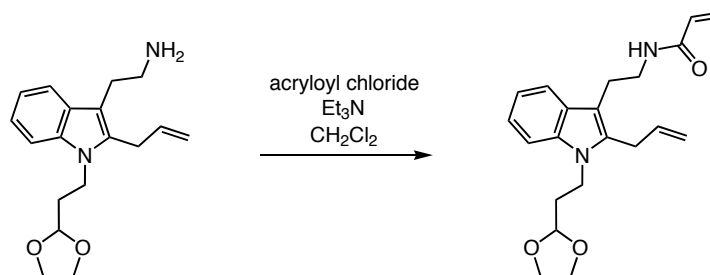


**Indole dimer (48)** To a clear solution of the diene (100 mg, 0.232 mmol) in  $\text{CH}_2\text{Cl}_2$  (50 mL) was added Grubbs II catalyst (19 mg, 0.023 mmol). The resulting brown solution was refluxed for 21 hours until judged complete by TLC analysis. The reaction was concentrated and then passed through a plug of florisil with the aid of EtOAc. The crude material was applied to a silica gel column and eluted in 25% EtOAc/hexanes to provide the dimer as a white solid (35 mg, 36% yield).

IR (film) 3425, 2931, 1611, 1512, 1496, 1465, 1453, 1418, 1356, 1302, 1246, 1175, 1109, 1032, 916, 818, 741, 697  $\text{cm}^{-1}$ ;  $^1\text{H}$  NMR (300 MHz,  $\text{CDCl}_3$ )  $\delta$  7.59 – 7.56 (m, 1H, ArH), 7.16 – 7.06 (m, 2H, ArH), 6.84 – 7.89 (d, 1H, ArH), 6.0 (t, 1H, C=CH), 5.26 (bt, 1H, O=C=CH), 5.17 – 5.14 (m, 2H,  $\text{CH}_2\text{CH}=\text{CH}$ ), 4.91 (bt, 1H, O=C=CH), 3.45 (dt, 1H, 17.1  $\text{NHCH}_2$ ), 3.25 (s, 2H,  $\text{NCH}_2\text{Ph}$ ), 2.89 (t, 2H,  $\text{CH}_2\text{CH}_2\text{NH}$ ), 1.73 (s, 2H,  $\text{CH}_2\text{SiMe}_3$ );  $^{13}\text{C}$  NMR (75 MHz,  $\text{CDCl}_3$ )  $\delta$  170.8, 145.3, 139.6, 138.4, 136.5, 130.4, 130.1, 129.5, 128.9, 127.5, 123.1, 121.1, 119.9, 115.9, 111.2, 111.1, 48.2, 42.2, 29.0, 26.0, 24.5, 0.0; HRMS ( $\text{EI}^+$ ) exact mass calculated for  $[\text{M}-2\times \text{CH}_2\text{SiMe}_3]^{2+}$  ( $\text{C}_{44}\text{H}_{44}\text{N}_2\text{O}_2$ ) requires  $m/z$  632.3531, found  $m/z$  632.3589.

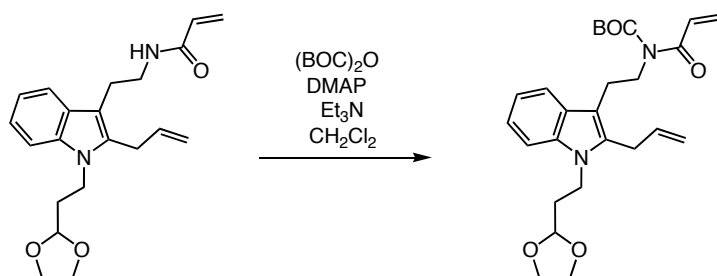


**2-(1-(2-(1,3-diololan-2-yl)ethyl)-2-allyl-1*H*-indol-3-yl)ethanamine** To a solution of 2-(2-(1-(2-(1,3-dioxolan-2-yl)ethyl)-2-allyl-1*H*-indol-3-yl)ethyl)isoindoline-1,3-dione (5.26 g, 12.2 mmol) in benzene (4.8 mL) was added methylhydrazine (6.49 mL, 122 mmol). The reaction proceeded for 16 hours at room temperature until judged complete by TLC analysis. Filtration of the precipitate followed by rotary evaporation of benzene provided the desired material as a crude light yellow solid that was used as is in the next step. IR (film) 2931, 2886, 1737, 1637, 1562, 1468, 1417, 1364, 1314, 1228, 1216, 1178, 1136, 1055, 1016, 942, 915, 869, 744, 734, 701  $\text{cm}^{-1}$ ;  $^1\text{H}$  NMR (500 MHz,  $\text{CDCl}_3$ )  $\delta$  7.58 (d, 1H,  $J = 6.5$  Hz, ArH), 7.38 – 7.36, (bm, 1H, ArH), 7.19 (t, 1H,  $J = 6.67$  Hz, ArH), 7.10 (t, 1H,  $J = 6.5$  Hz), 5.99 – 5.90 (m, 1H,  $\text{CH}_2=\text{CH}$ ), 5.10 (bd, 1H,  $J = 8.58$  Hz,  $\text{CH}=\text{CH}_2$ ), 4.99 – 4.06 (bm, 1H,  $\text{CH}=\text{CH}_2$ ), 4.89 (t, 1H,  $J = 9.97$  Hz, OCHO), 4.24 – 4.22 (bm, 2H,  $\text{CH}_2\text{NH}_2$ ), 4.05 – 4.01 (m, 2H,  $\text{OCH}_2\text{CH}_2\text{O}$ ), 3.92 – 3.87 (m, 2H,  $\text{OCH}_2\text{CH}_2\text{O}$ ), 3.63 – 3.58 (bm, 2H, IndNCH<sub>2</sub>), 2.91 – 2.89 (bm, 2H,  $\text{CH}_2\text{CH}_2\text{NH}_2$ ), 2.15 – 2.09 (bm, 2H, ind.NCH<sub>2</sub>CH<sub>2</sub>);  $^{13}\text{C}$  NMR (75 MHz,  $\text{CDCl}_3$ )  $\delta$  136.0, 135.5, 134.2, 128.0, 121.0, 118.9, 118.4, 109.3, 102.2, 65.0, 42.8, 38.1, 34.0, 28.6, 28.4; HRMS ( $\text{EI}^+$ ) exact mass calculated for  $[\text{M}]^+$  ( $\text{C}_{18}\text{H}_{24}\text{N}_2\text{O}_2$ ) requires  $m/z$  300.1837, found  $m/z$  300.1842.



***N*-(2-(1-(2-(1,3-dioxolan-2-yl)ethyl)-2-allyl-1*H*-indol-3-yl)ethyl)acrylamide** To a light yellow solution of crude 2-(1-(2-(1,3-diololan-2-yl)ethyl)-2-allyl-1*H*-indol-3-yl)ethanamine (12.2 mmol) in dry CH<sub>2</sub>Cl<sub>2</sub> (24 mL) under Ar and cooled to 0 °C was added triethylamine (1.78 mL, 12.8 mmol). Next, acryloyl chloride (1.04 mL, 12.8 mmol) was slowly added dropwise and the reaction stirred for 8 hours until judged complete by TLC analysis. The reaction was concentrated, applied to a silica gel column in toluene, and eluted in 60% EtOAc/Hexanes (2 ×) to provide the product as a clear oil (2.8 g, 65% yield, 2 steps). IR (film) 3273, 2970, 1738, 1657, 1625, 1545, 1469, 1409, 1366, 1229, 1217, 1138, 1055, 1016, 987, 943, 745 cm<sup>-1</sup>; <sup>1</sup>H NMR (500 MHz, CDCl<sub>3</sub>)  $\delta$  7.59 (d, 1H, *J* = 7.82 Hz, ArH), 7.39 (d, 1H, *J* = 8.1Hz, ArH), 7.22 (t, 1H, *J* = 7.05 Hz, ArH), 7.13 (t, 1H, *J* = 7.01 Hz, ArH), 6.27 (dd, 1H, *J* = 16.9, 1.4 Hz, O=CH=CH), 6.03 (m, 1H, O=CH), 5.65 (bt, 1H, NH), 5.61 (dd, 1H, *J* = 10.3, 1.4 Hz, O=CH=CH), 5.13 (dd, 1H, *J* = 10.1, 1.5 Hz, CH<sub>2</sub>CH=CH), 4.97 (dd, 1H, *J* = 18.7, 1.6 Hz, CH<sub>2</sub>CH=CH), 4.90 (t, 1H, *J* = 4.36 Hz, OCHO), 4.25 (t, 2H, *J* = 7.59 Hz, CH<sub>2</sub>NH), 4.02 – 4.03 (m, 2H, OCH<sub>2</sub>CH<sub>2</sub>O), 3.92 – 3.90 (m, 2H, OCH<sub>2</sub>CH<sub>2</sub>O), 3.58 (dt, 2H, *J* = 3.65, 1.68 Hz, ind.CH<sub>2</sub>CH<sub>2</sub>NH), 2.15 – 2.11 (m, 2H, NCH<sub>2</sub>CH<sub>2</sub>CH); <sup>13</sup>C NMR (75 MHz, CDCl<sub>3</sub>)  $\delta$  165.4, 136.1, 135.6, 130.9, 127.8, 126.2, 121.3, 119.7, 119.2, 118.2, 116.4, 109.3, 108.9,

102.2, 65.1, 65.0, 40.0, 38.2, 33.9, 28.4, 24.5; HRMS (EI<sup>+</sup>) exact mass calculated for [M]<sup>+</sup> (C<sub>21</sub>H<sub>26</sub>N<sub>2</sub>O<sub>3</sub>) requires *m/z* 354.1943, found *m/z* 354.1944.

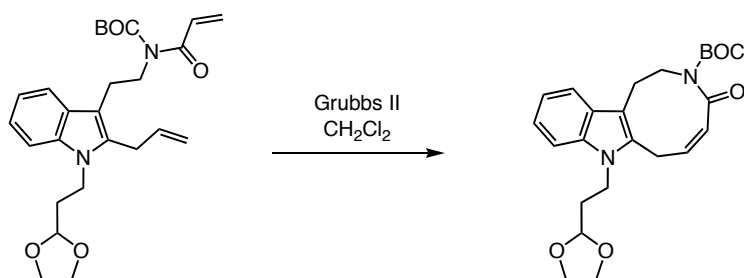


***t*-butyl-2-(1-(2-(1,3-dioxolan-2-yl)ethyl)-2-allyl-1*H*-indol-3-yl)ethylacryloylcarbamate**

To a light yellow solution of *N*-(2-(1-(2-(1,3-dioxolan-2-yl)ethyl)-2-allyl-1*H*-indol-3-yl)ethyl)acrylamide (2.7 g, 7.62 mmol) in dry CH<sub>2</sub>Cl<sub>2</sub> (7.7 mL), under Ar and cooled to 0 °C, was added DMAP (971 mg, 7.62 mmol), triethylamine (1.06 mL, 7.62 mmol), then (BOC)<sub>2</sub>O (1.75 mL, 7.62 mmol). The resulting mixture was warmed to room temperature and stirred for 12 hours. In order to drive the reaction more of each reagent (0.5 eq.) was added at room temperature and the reaction stirred for 10 hours until judged complete by TLC analysis. After concentrating, the crude solid was applied to a silica gel column in toluene and eluted in 30% EtOAc/Hexanes to provide the desired product as a light yellow oil (2.5 g, 72% yield). IR (film) 2977, 2886, 1727, 1678, 1469, 1405, 1368, 1351, 1293, 1250, 1205, 1178, 1145, 1058, 979, 944, 854, 745 cm<sup>-1</sup>; <sup>1</sup>H NMR (500 MHz, CDCl<sub>3</sub>) δ 7.67 (d, 1H, *J* = 7.72 Hz, ArH), 7.31 (d, 1H, *J* = 8.09 Hz, ArH), 7.15 (t, 1H, *J* = 7.03 Hz, ArH), 7.10 (t, 1H, *J* = 7.81 Hz, ArH), 7.0 (d, 1H, *J* = 10.4 Hz, ArH), 6.97 (d, 1H, *J* = 10.4 Hz, O=CH=CH<sub>2</sub>), 6.31 (dd, 1H, *J* = 16.8, 1.7 Hz, O=CCH=CH

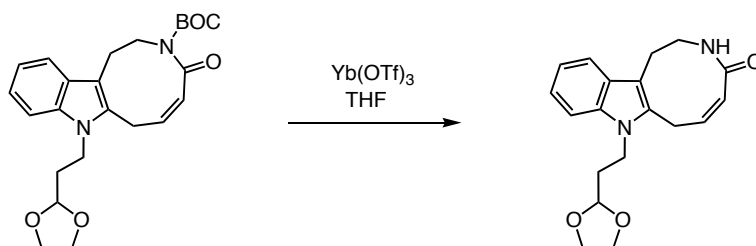


*trans*), 5.93 (ddt, 1H,  $J = 17.6, 10.2, 5.5$  Hz,  $\text{CH}_2\text{CH}=\text{CH}_2$ ), 5.66 (dd, 1H,  $J = 10.4, 1.7$ ,  $\text{O}=\text{C}=\text{CHCH}$  *cis*), 5.06, (dd, 1H,  $J = 10.1, 1.5$  Hz,  $\text{CH}_2\text{CH}=\text{CH}$  *cis*) 4.94 (dd, 1H,  $J = 17.0, 1.5$  Hz,  $\text{CH}_2\text{CH}=\text{CH}$  *trans*), 4.85 (t, 1H,  $J = 4.37$  Hz,  $\text{OCHO}$ ), 4.18 (t, 2H,  $J = 7.65$  Hz  $\text{CH}_2\text{CH}_2\text{NC}=\text{O}$ ), 3.99 – 3.96 (m, 2H,  $\text{OCH}_2\text{CH}_2\text{O}$ ), 3.86 (m, 2H,  $\text{OCH}_2\text{CH}_2\text{O}$ ), 3.57 (d, 2H,  $J = 5.6$  Hz,  $\text{CH}_2\text{CH}=\text{CH}_2$ ), 2.96 (t, 2H,  $J = 7.75$  Hz,  $\text{CH}_2\text{CH}_2\text{NC}=\text{O}$ ), 2.09 – 2.05 (m, 2H, ind. $\text{NCH}_2\text{CH}_2$ ), 1.45 (s, 9H, BOC);  $^{13}\text{C}$  NMR (75 MHz,  $\text{CDCl}_3$ )  $\delta$  168.8, 153.3, 136.0, 135.4, 134.4, 127.9, 127.2, 121.06, 119.0, 118.4, 116.3, 109.1, 108.8, 102.2, 83.2, 65.0, 45.6, 38.1, 33.9, 28.5, 27.9, 23.7; HRMS ( $\text{EI}^+$ ) exact mass calculated for  $[\text{M}]^+$  ( $\text{C}_{28}\text{H}_{35}\text{N}_2\text{O}_5$ ) requires  $m/z$  454.2467, found  $m/z$  454.2469



**(*Z*)-*tert*-butyl-8-(2-(1,3-dioxolan-2-yl)ethyl)-1,2-dihydro-4-oxoazonino[5,4-*b*]indole-3(4*H*,7*H*,8*H*)-carboxylate** To a solution of *tert*-butyl-2-(1-(2-(1,3-dioxolan-2-yl)ethyl)-2-allyl-1*H*-indol-3-yl)ethylacryloylcarbamate (500 mg, 1.09 mmol) in dry  $\text{CH}_2\text{Cl}_2$  (1090 mL), under Ar, was added Grubbs II catalyst (278 mg, 0.327 mmol). The resulting brown mixture was refluxed for 12 hours and was judged complete by TLC analysis. After concentrating, the crude material was passed through a plug of florisil with the aid of EtOAc. The brown residue was applied to a silica gel column in toluene and eluted

with 30% EtOAc/hexanes (2 ×). The resulting material was passed through another plug of florisil with the aid of EtOAc and concentrated to provide the desired material as a foamy light brown solid (311 mg, 67% yield, average is about 60%). IR (film) 1724, 1682, 1470, 1444, 1415, 1366, 1323, 1230, 1146, 1085, 1024, 857, 770, 740  $\text{cm}^{-1}$ ;  $^1\text{H}$  NMR (500 MHz,  $\text{CDCl}_3$ )  $\delta$  7.52 (d, 1H,  $J = 7.76$  Hz, ArH), 7.28 (d, 1H, ArH), 7.17 (t, 1H,  $J = 7.02$  Hz, ArH), 7.11 (t, 1H,  $J = 7.89$  Hz, ArH), 6.31 – 6.29 (m, 1H, HC=CHC=O), 6.22 – 6.29 (m, 1H, HC=CHC=O), 4.89 (t, 1H,  $J = 4.12$  Hz, OCHO), 4.23–4.14 (m, 2H, indNCH<sub>2</sub>), 4.06 – 4.02 (m, 2H, OCH<sub>2</sub>CH<sub>2</sub>O), 3.96 – 3.91 (m, 2H, OCH<sub>2</sub>CH<sub>2</sub>O), 3.86 – 3.84 (bm, 2H, (BOC)NCH<sub>2</sub>), 3.54 (bd, 2H,  $J = 5.89$  Hz CH<sub>2</sub>CH=CH), 3.13 (bt, 2H,  $J = 5.63$  Hz, CH<sub>2</sub>CH<sub>2</sub>N(BOC)), 2.18 – 2.09 (m, 2H, ind.NCH<sub>2</sub>CH<sub>2</sub>), 1.49 (bs, 9H, BOC);  $^{13}\text{C}$  NMR (75 MHz,  $\text{CDCl}_3$ )  $\delta$  172.4, 153.5, 136.8, 135.9, 131.6, 127.1, 121.7, 119.1, 118.2, 109.1, 108.7, 102.1, 82.8, 65.1, 45.4, 38.5, 33.5, 28.0, 23.4, 22.8, 21.1; HRMS ( $\text{EI}^+$ ) exact mass calculated for  $[\text{M}]^+$  ( $\text{C}_{24}\text{H}_{31}\text{N}_2\text{O}_5$ ) requires  $m/z$  426.2154, found  $m/z$  426.2154.

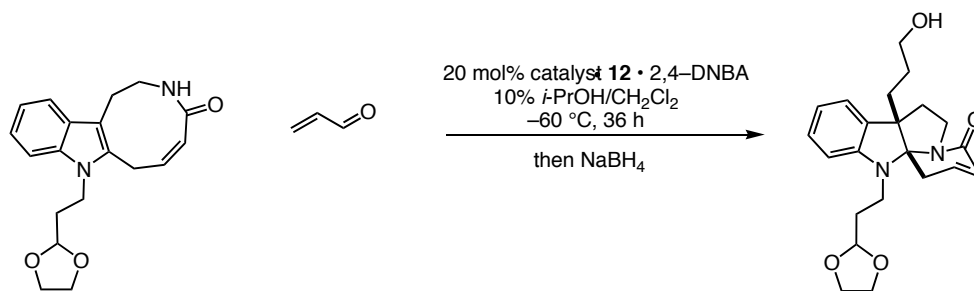


**(Z)-8-(2-(1,3-dioxolan-2-yl)ethyl)-2,3-dihydroazonino[5,4-*b*]indol-4-(1*H*,7*H*,8*H*)-one**

**(80)** A light brown solution of (*Z*)-*tert*-butyl-8-(2-(1,3-dioxolan-2-yl)ethyl)-1,2-dihydro-

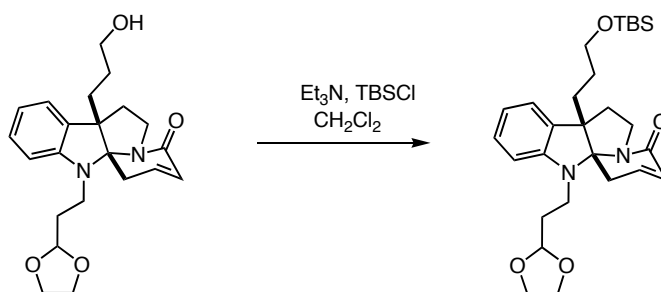
4-oxoazonino[5,4-*b*]indole-3(4*H*,7*H*,8*H*)-carboxylate (311 mg, 0.729 mmol) and (271 mg, 0.437 mmol) in THF (14.6 mL) was stirred at room temperature for 12 hours until judged complete by TLC analysis. The mixture was concentrated to a brown residue and filtered through a plug of celite with the aid of CH<sub>2</sub>Cl<sub>2</sub>. After concentrating, the crude material was purified by silica gel chromatography with 1:1 EtOAc/acetone (2 ×). The resulting material was passed through a plug of florisil with the aid of EtOAc to afford the desired material as a white solid (233 mg 98% yield, typical yields are > 90%). IR (film) 3405, 2954, 2887, 1648, 1604, 1557, 1525, 1467, 1417, 1277, 1256, 1224, 1144, 1030, 945, 891, 816, 792, 746, 709 cm<sup>-1</sup>; Amide ring flip<sup>7</sup> occurs and complicates the NMR, tried DMSO, THF-D<sub>8</sub>, CDCl<sub>3</sub>, obtained in CD<sub>2</sub>Cl<sub>2</sub> as the spectra is the cleanest. It seems to be a 2:1 mixture of *trans/cis* isomers (500 MHz, CDCl<sub>3</sub>)  $\delta$  7.5 (d, 1H, ArH), 7.33 (d, 1H, ArH), 7.17 (t, 1H, ArH), 7.08 (m, 1H, ArH), 6.44 – 6.42 (m, 1H, HC=CHC=O), 6.07 – 6.00 (m, 1H, HC=CHC=O), 5.39 (bs, 1H, NH), 4.86 – 4.82 (m, 1H, OCHO), 4.27 – 4.21 (m, 2H, indNCH<sub>2</sub>), 4.00 – 3.97 (m, 2H, OCH<sub>2</sub>CH<sub>2</sub>O), 3.87 – 3.82 (m, 2H, OCH<sub>2</sub>CH<sub>2</sub>O), 3.62 – 3.61 (bm, 2H, O=CHNCH<sub>2</sub>), 3.56 – 3.54 (m, 2H, CH<sub>2</sub>CH=CH), 3.17 – 3.02 (m, 2H, CH<sub>2</sub>CH<sub>2</sub>NHC=O), 2.07 – 2.05 (m, 2H, ind.NCH<sub>2</sub>CH<sub>2</sub>); <sup>13</sup>C NMR (75 MHz, CDCl<sub>3</sub>)  $\delta$  171.6, 136.7, 136.2, 132.4, 128.8, 124.1, 121.9, 119.5, 118.4, 109.7, 43.3, 39.1, 34.6, 34.3, 33.3, 32.2, 26.9, 25.4; HRMS (EI<sup>+</sup>) exact mass calculated for [M]<sup>+</sup> (C<sub>19</sub>H<sub>23</sub>N<sub>2</sub>O<sub>3</sub>) requires *m/z* 326.1630, found *m/z* 326.1634.

(7) Borgen, G. *Mag. Res. Chem.* **1991**, 29, 805.



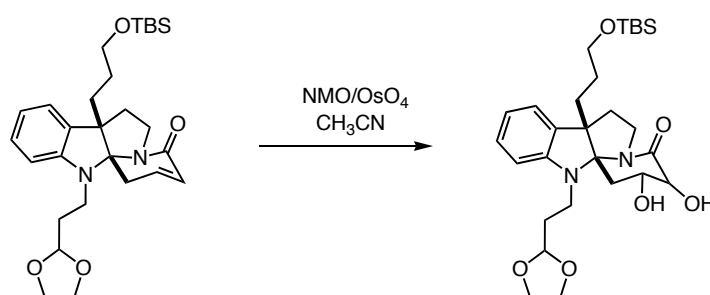
**Dihydro-9a,4a-(iminoethano)-9*H*-carbazole derivative (81)** To a solution of 2,3,6,7-tetrahydroazonino[5,4-*b*]indol-4(1*H*,5*H*,8*H*)-one (30 mg, 0.131 mmol) in 10% *i*-PrOH/CH<sub>2</sub>Cl<sub>2</sub> (1.1 mL) cooled to -60 °C was added the 2,4-dinitrobenzoic acid salt of (2*R*,5*R*)-2-*tert*-butyl-5-benzyl-3-methylimidazolidin-4-one (**12**, 0.062 mmol) and then acrolein (11 mg, 0.197 mmol). The resulting solution was stirred for 32 hours until the reaction was judged complete by TLC analysis. To this light yellow solution was added EtOH (1:1 v/v, 1.1 mL). The resulting solution was transferred to an ice bath. Treatment with NaBH<sub>4</sub> (25 mg, 0.655 mmol) for 30 minutes induced vigorous bubbling and the light yellow solution turned clear. Quenching the excess NaBH<sub>4</sub> was performed by the dropwise addition of 5% HCl (0.1 mL). The layers were separated and the aqueous phase was extracted with CH<sub>2</sub>Cl<sub>2</sub> (3 × 1 mL), dried over Na<sub>2</sub>SO<sub>4</sub>, filtered, and concentrated. The crude material was purified on a Gilson-215 Liquid Handler by preparatory high-pressure liquid chromatography to afford the desired product as a foamy solid (12 mg, 32% yield, 32% ee). Enantiomeric excess was determined by SFC analysis using an ADH column in a 5-50% gradient of MeOH (major *t<sub>r</sub>* = 5.83 min., minor *t<sub>r</sub>* = 7.43 min.) IR (film) 3407, 2947, 2878, 1658, 1599, 1491, 1453, 1436, 1387, 1322, 1261, 1218, 1137, 1055, 874, 817, 744 cm<sup>-1</sup>; <sup>1</sup>H NMR (500 MHz, CDCl<sub>3</sub>) δ 7.04 (t, 1H, *J* = 7.5

Hz, ArH), 6.95 (d, 1H,  $J = 7.79$  Hz, ArH), 6.63 – 6.59 (m, 2H, ArH, CH=CHCO), 6.35 (d, 1H,  $J = 7.79$  Hz, ArH), 6.02 (dd, 1H,  $J = 9.84$  Hz, 2.84 Hz, ArH), 4.78 (t, 1H,  $J = 4.30$  Hz, OCHO), 4.06 – 4.00 (m, 1H, NCH), 3.81 – 3.76 (m, 2H, OCH<sub>2</sub>CH<sub>2</sub>O), 3.54 – 3.51 (m, 2H, OCH<sub>2</sub>CH<sub>2</sub>O), 3.52 (t, 2H,  $J = 6.21$  Hz, CH<sub>2</sub>OH), 3.30 – 3.21 (m, 2H, NCH<sub>2</sub>), 2.86 – 2.21 (m, 2H, CHCH=CH, NCH), 2.56 – 2.51 (m, 1H, CHCH=CH), 2.11 – 2.04 (m, 1H, NCH<sub>2</sub>CH), 1.79 – 1.74 (m, 5H, CH<sub>2</sub>CH<sub>2</sub>CH<sub>2</sub>OH, NCH<sub>2</sub>CH<sub>2</sub>CHO(O), NCH<sub>2</sub>CCH), 1.52 – 1.50 (m, 1H, CHCH<sub>2</sub>OH), 1.32 – 1.29 (m, 1H, CHCH<sub>2</sub>OH); <sup>13</sup>C NMR (75 MHz, CDCl<sub>3</sub>)  $\delta$  161.9, 148.8, 136.6, 130.8, 128.6, 124.0, 122.8, 117.5, 105.0, 102.8, 88.9, 65.0, 63.0, 60.0, 43.4, 38.9, 32.3, 31.1, 31.0, 27.8; HRMS (EI<sup>+</sup>) exact mass calculated for [M]<sup>+</sup> (C<sub>22</sub>H<sub>29</sub>N<sub>2</sub>O<sub>4</sub>) requires  $m/z$  384.2049, found  $m/z$  384.2044;  $[\alpha]_D^{22} = -5.47^\circ$  ( $c = 0.37$ , CHCl<sub>3</sub>).



**Carbazole silyl ether (82)** To an ice-cold solution of dihydro-9a,4a-(iminoethano)-9*H*-carbazole derivative 29 (116 mg, 0.302 mmol) in dry CH<sub>2</sub>Cl<sub>2</sub> (1.5 mL, 0.2 M), under Ar, was added DMAP (15 mg, 0.121 mmol), triethylamine (88  $\mu$ L, 0.634 mmol), and then TBSCl (91 mg, 0.604) dropwise as a solution in CH<sub>2</sub>Cl<sub>2</sub> (100  $\mu$ L). The resulting solution was stirred at 0 °C for 3.5 hours until judged complete by TLC analysis. The title compound was isolated as a light yellow oil (134 mg, 89% yield) after purification by

flash chromatography on silica gel (100% EtOAc). IR (film) 2952, 2929, 2856, 1663, 1603, 1490, 1426, 1387, 1359, 1251, 1218, 1135, 1093, 1045, 940, 835, 814, 776, 740  $\text{cm}^{-1}$ ;  $^1\text{H}$  NMR (500 MHz,  $\text{CDCl}_3$ )  $\delta$  7.08 (t, 1H,  $J = 7.61$  Hz, ArH), 6.99 (d, 1H,  $J = 7.21$  Hz, ArH), 6.69 – 6.63 (m, 2H, ArH,  $\text{CH}_2\text{CH}=\text{CH}$ ), 6.39 (d, 1H,  $J = 7.84$  Hz, ArH), 6.08 (d, 1H,  $J = 9.84$  Hz, ArH), 4.85 – 4.82 (m, 1H, OCHO), 4.08 – 4.04 (m, 1H, NCNCH), 3.97 – 3.94 (m, 2H,  $\text{OCH}_2\text{CH}_2\text{O}$ ), 3.85 – 3.82 (m, 2H,  $\text{OCH}_2\text{CH}_2\text{O}$ ), 3.52 – 3.49 (m, 2H,  $\text{CH}_2\text{OTBS}$ ), 3.38 – 3.27 (m, 2H, indNCH<sub>2</sub>), 2.96 – 2.87 (m, 2H, NCNCH,  $\text{CHCH}=\text{CH}$ ), 2.58 – 2.54 (m, 1H,  $\text{CHCH}=\text{CH}$ ), 2.10 – 2.07 (m, 1H,  $\text{NCH}_2\text{CH}$ ), 1.87 – 1.79 (m, 5H,  $\text{CH}_2\text{CH}_2\text{CH}_2\text{OTBS}$ ,  $\text{NCH}_2\text{CH}$ , ind.NCH<sub>2</sub>CH<sub>2</sub>), 1.53 – 1.47 (m, 1H,  $\text{CHCH}_2\text{OTBS}$ ), 1.34 – 1.28 (m, 1H,  $\text{CHCH}_2\text{OTBS}$ );  $^{13}\text{C}$  NMR (75 MHz,  $\text{CDCl}_3$ )  $\delta$  161.9, 148.6, 136.6, 131.2, 128.5, 124.0, 122.7, 117.4, 104.9, 102.8, 89.1, 64.9, 63.0, 59.2, 43.3, 39.1, 38.9, 32.3, 31.1, 31.0, 27.9, 25.9, -5.3; HRMS ( $\text{EI}^+$ ) exact mass calculated for  $[\text{M}-\text{CH}_2]^+$  ( $\text{C}_{28}\text{H}_{42}\text{O}_4\text{Si}$ ) requires  $m/z$  498.2913, found  $m/z$  498.2911.



**Carbazole silyl ether diol (83)** To a solution of carbazole silyl ether (300 mg, 0.60 mmol) in  $\text{CH}_3\text{CN}$  (8.6 mL) was added NMO (156 mg, 1.2 mmol) and  $\text{OsO}_4$  (76  $\mu\text{L}$ , 0.012 mmol, 4% w/v solution in  $\text{H}_2\text{O}$ ), and the resulting black reaction was stirred at room

temperature. After 21 hours, additional NMO (156 mg, 1.2 mmol) and OsO<sub>4</sub> (76  $\mu$ l, 0.012 mmol) were added to drive the reaction that had stalled by LCMS analysis. After 24 hours, the reaction was complete by LCMS and was then concentrated. The title compound was isolated as a light orange oil (200 mg, 63% yield) after purification by flash chromatography on silica gel (1:1 EtOAc/acetone). IR (film) 3437, 2953, 2929, 2886, 2857, 1651, 1603, 1493, 1462, 1373, 1250, 1229, 1129, 1049, 945, 894, 837, 777, 739 cm<sup>-1</sup>; <sup>1</sup>H NMR (500 MHz, CDCl<sub>3</sub>)  $\delta$  7.07 (t, 1H, J = 7.7 Hz, ArH), 7.21 (d, 1H, J = 7.29 Hz, ArH), 6.65 (t, 1H, J = 7.4 Hz, ArH), 6.36 (d, 1H, J = 7.79 Hz, ArH), 4.78 (t, 1H, J = 4.24 Hz, OCHO), 4.33 – 4.32 (m, 2H, HOCHCHOHC=O), 4.23 (dd, 1H, J = 13.95, 2.54 Hz, NHCH<sub>2</sub>), 3.96 – 3.92 (m, 2H, OCH<sub>2</sub>CH<sub>2</sub>O), 3.85 – 3.84 (m, 2H, OCH<sub>2</sub>CH<sub>2</sub>O), 3.59 – 3.45 (m, 2H, CH<sub>2</sub>OTBS), 3.29 – 3.15 (m, 1H, ind.NCH), 2.80 (dd, 1H, J = 11.5, 5.13 Hz, HOCHCH), 2.61 (dt, 1H, J = 11.5, 6.29 Hz, NCHCH<sub>2</sub>), 2.11 – 2.07 (m, 1H, HOCHCH), 1.97 – 1.81 (m, 6H, NCH<sub>2</sub>CH<sub>2</sub>, CH<sub>2</sub>CH<sub>2</sub>CH<sub>2</sub>OTBS, ind.NCH<sub>2</sub>CH<sub>2</sub>), 1.16 – 1.15 (m, 1H, CH<sub>2</sub>CH<sub>2</sub>OTBS), 1.43 – 1.38 (m, 1H, CH<sub>2</sub>CH<sub>2</sub>OTBS), 0.86 (s, 9H, OTBS), 0.0 (s, 6H, OTBS); <sup>13</sup>C NMR (75 MHz, CDCl<sub>3</sub>)  $\delta$  169.8, 148.7, 131.7, 128.3, 123.5, 117.7, 105.2, 102.5, 91.4, 69.8, 67.7, 65.12, 65.10, 63.1, 60.1, 43.4, 39.4, 37.8, 32.6, 31.7, 31.5, 28.3, 25.9, 18.4, –5.0; HRMS (EI<sup>+</sup>) exact mass calculated for [M–CH<sub>2</sub>]<sup>+</sup> (C<sub>28</sub>H<sub>44</sub>N<sub>2</sub>O<sub>6</sub>Si) requires *m/z* 166.1358, found *m/z* 166.1359.